Lab-Scale Cable Shovel Model with Potential for Fault Detection Applications

by

Zhounan Li

A thesis submitted in partial fulfillment of the requirements for the degree of

Master of Science

Department of Mechanical Engineering
University of Alberta

Abstract

Cable shovels are mostly used as primary equipment in large-scale surface mining operations. A single unexpected component failure could cause unforeseen costly shutdowns, reduced productivity and may even pose a great danger to on-site personnel. The ideal maintenance strategy is to reveal incipient faults in advance that the repair schedule and equipment have enough time to get prepared. Many challenges will occur if conducting the fault detection experiments on the real mining shovels. In this research, a lab-scale shovel model with the potential for fault detection is proposed.

With the knowledge of the benefits of physical modelling and full-size cable shovel structures and fundamental functions, a lab-scale shovel model is designed and fabricated based on the Komatsu P & H 4100XPC cable shovel with a scaled-down factor 15. The shovel model is validated that the model has a similar working mechanism and performance as the full-size mining shovel. Besides, the shovel model is able to simulate the fundamental operation processes by a robust control system based on EtherCAT technology.

Vibration analysis is an effective method for fault detection based on the fact that the vibration patterns under normal and abnormal conditions are different and the variation is the indicator of the presence of faults. A PC-based data acquisition system is designed to obtain the vibration signal of the mechanical systems. Two artificial failure modes with different time-varying behaviours are seeded to the shovel model. In order to extract the fault signatures from the signal, various signal processing techniques in time, frequency and time-frequency domains are used to distinguish the

faulty components from the healthy ones and some techniques are also able to predict the scale of faulty conditions.

A lab-scale cable shovel model with time-varying behaviours provides a platform for fault detection that can be also applied to other areas such as soil-tool interaction, equipment health monitoring and autonomous excavation.

This journey is hard and the pandemic makes it even harder. I dedicate my work to my beloved grandpa, Mingsheng Zhou, who provided me with unconditional love, endless support, and encouragement throughout my life.

Acknowledgements

Table of Contents

List of Tables

List of Figures

Chapter 1

Introduction

Among various loading units in large-scale surface mining operations, cable shovels are used as primary equipment for overburden removal and ore material collection[1, 2]. Roughly speaking, the basic operating cycle can be categorized into two parts: the digging process and the dumping process. The digging process is a stage where a ground engaging tool interacting with the environment[2]. The dumping process is a stage where the shovel carries the ore material and swings to the dump position, dumps into a truck and swings back for the next digging process[2, 3]. Structural components failure mostly occurs and grows during the digging process. Due to variable conditions in the terrain, repetitive and interaction loads may damage the structural components and elements in the power transmission[4, 5]. Even though maintenance personnel visually checks the components that tend to be worn out or broken based on the history maintenance records, some faults at an early stage are not easy to be found but it can slowly change the dynamics and kinematics of the shovel without notice. A single component fault may lead to sequential failure to other parts of the machine[6, 7] (failure is the difference from the expected results while the fault is the cause of that failure), which can cause unforeseen costly shutdowns, reduced availability, and high cost of maintenance spending and lost production[2, 7, 8].

1.1 Motivation

Maintenance departments in the mining industry used to conduct repairs when the machine failed. However, as time goes by, it has been proved that this strategy is not ideal for machines with complex systems such as mining equipment. As mentioned, even a single worn-out component may lead to a failure of the whole system which will result in unnecessary shutdowns, high maintenance costs and lost production. With half a year of mining experience in Teck's cardinal river operation, maintenance for heavy machines was conducted based on the manufacturer's predetermined intervals which are estimated from the failure rate distribution from historical data. On one hand, this age-based strategy can help reduce unplanned downtime; on the other hand, planners tend to make conservative maintenance decisions, which is to say that the remaining useful life of the machine may be wasted and unnecessary maintenance cost is added. Overall, the ideal maintenance strategy should take the component's condition into account: it can reveal incipient failures in advance that planners have enough time to plan the next maintenance schedule.

In order to have a good knowledge of components' condition, extra transducers and sensors may need to be installed; besides, a new data acquisition system could also be required. Those system-level installations would require equipment shutdowns and reduce production. In addition, for a great amount of time, shovels may not be in the operating cycle: cleaning the bank, travelling from one face to another, etc. Finally, the shovel is subject to high variability in operation and the challenge of getting access to a machine in the field makes the use of a scale model shovel for evaluation of faults the most practical first step.

1.2 Objectives of the Study

The ideal maintenance strategy is to make repair plans based on the condition of components. It can not only push the usage limit to a great extent but also avoid

unexpected shutdowns. Fault detection analysis plays an important role in the implementation of the ideal maintenance program. With the help of fault detection, incipient component failure can be identified so that repair plans can be made in advance; preventing an unplanned failure that could have more severe consequences in terms of downtime and cost.

Vibration analysis is one of the most effective methods used in condition-monitoring to detect faults in machine systems. It identifies component conditions by measuring the vibration levels and frequencies of the machinery[9]. Based on the fact that vibration levels in healthy and faulty conditions are different[10], vibration analysis can identify machines with abnormal vibration signals which is regarded as an indicator of a fault[2].

Vibration analysis may require extra transducers or sensors for condition monitoring on actual mining equipment. This extra work could reduce the availability of equipment and increase the production cost. In addition, data collection is not efficient on an actual mining shovel when the shovel is not in operation mode where faults can be easily revealed. On the contrary, a lab-scale shovel model is easier and cost-efficient to be manipulated; also, the data collection and filtering is more focused on the process where faults are expected to occur.

Consequently, this research will investigate the ability of vibration analysis to identify faults in a shovel using a lab-scale model shovel. Specific objectives include:

1. *Design, development and fabrication of a lab-scale shovel model with an inherent time-varying behaviour.* The model will perform functions used in the operation mode, which are hoist, crowd and swing. The working mechanism of each system will be similar to an actual mining shovels. It will also provide a platform to introduce mechanical faults and sensors at various locations;

2. *Access the observability of the presence of faults through vibration analysis during the operation mode.* This will be achieved by developing a baseline for health

3

conditions and monitoring the signal change for various seeded structural faults. Signal processing techniques in the time, frequency and time-frequency domains will be considered for fault detection.

1.3   Thesis Outline

To have a better understanding of the background of the relevant topics involved in the present study, Chapter 2 is divided into three sections and provides additional information about cable shovel structural analysis, condition monitoring techniques and vibration analysis. Cable shovel modelling is broken down in section 2.1. First, an overview of the resistance forces that shovel encounter during the excavation process is presented in section 2.1.1. For a better design of the lab-scale shovel model, it is essential to have an insight into the behaviour of the whole system. Classical dynamical modelling of a cable shovel developed by S. Frimpong is discussed in section 2.1.2. Additionally, a comprehensive understanding of dynamics and kinematics is included in section 2.1.3. It is then followed by the review of the literature on model validation, which is an important connection between the actual equipment and the model. Several validation methods including fractional analysis, similitude theory, distortion analysis are well discussed in section 2.1.4.

The second part of the literature review (section 2.2) focuses on three common maintenance strategies in the modern mining industry: reactive maintenance, preventive maintenance and predictive maintenance. It presents an overview of those three maintenance philosophies and applications. It is then followed by the review of the literature on condition monitoring technique which is one of the most effective maintenance strategies in the mining industry. Reliability-centred maintenance (RCB) and condition-based maintenance (CBM) are well discussed in section 2.2.1. This chapter will be concluded with a review of the state of the art in mining equipment condition monitoring.

The third part of the literature review is dedicated to the review of vibration

analysis in section 2.3. As one of the most effective condition-monitoring strategies, the benefits of vibration analysis and the mechanical vibration process are included in this section. In section 2.3.1, common failure modes on mining equipment are well summarized and studied. Later, digital signal processing techniques covering time, frequency and time-frequency domains are presented in section 2.3.2.

Chapter 3 summarizes the methodology used for fault detection on the lab-scale cable shovel investigation. A research roadmap is included, which covers the research stages from preliminary study to the method implementation. Section 3.2 outlines the experimental platform requirements and design. In addition, section 3.3 explains the techniques for analyzing the data for equipment monitoring.

Chapter 4 presents the approach used for the design and construction of the lab-scale shovel. Generally speaking, experimental design can be divided into two parts: first, philosophy of solid modelling and physical model design; second, solid model validation and motion control. In the first part, the benefits of physical modelling and the study of cable shovel essential structures and functions are discussed in section 4.1 and 4.2, respectively. Critical functions and structure design are included in section 4.3. In the second half, the similarity analysis is presented in section 4.4 since the lab-scale cable shovel model needs to be verified before using the scale model shovel for any experiments. It is then followed by the full description of the control system as shown in section 4.5.

Chapter 5 shows the cable shovel's potential for faults seeding and sensors' implementation. Also, in this chapter, vibration analysis techniques are performed to monitor the structural integrity of the shovel model. To explain the model's potential for fault detection, the design of the data acquisition system and failure modes' selection and implementation are discussed in section 5.1 and 5.2, respectively. It is then followed by the vibration analysis for fault detection. First, time-domain analysis based on statistical features of the signals is applied to disclose the existence of faults and presented in section 5.3.1. Following the time-domain analysis, frequency

and time-frequency domains analysis is discussed in section 5.3.2. As common signal processing techniques, power spectrum analysis and short-time Fourier transform are applied on the signal and their effectiveness and limitations are discussed.

Chapter 6 summarizes the main results of the work and discusses the limitations of the proposed methods and plans for future work.

Chapter 2

Literature Review

Cable shovels play a critical role in large-scale surface mining operations. Keeping mining equipment in good condition is always challenging in the mining industry. The objectives of the research can be summarized into two categories: first, design and develop a shovel model with time-varying behaviours; second, access the observability of the existence of artificial faults. In order to achieve those objectives, this chapter provides insights into the preliminary studies in three parts: firstly, comprehensive studies for full-size cable shovels will be reviewed that include kinematic and dynamic modelling of shovels. It is then followed by the review of the validation of physical model techniques; secondly, maintenance strategies commonly used in the mining industry will be reviewed and modern condition monitoring solutions are also studied; last but not least, common failure modes and vibration signatures will be studied and it is then followed by a review of digital signal processing techniques in vibration analysis.

2.1 Cable Shovel Modelling

2.1.1 Shovel Resistance Forces

In order to understand the health condition of the earth moving machines, it is necessary to have a good knowledge of their working mechanism and performance behavior. The dipper excavation process consists of penetration, cutting and scooping[11]. Pen-

etration is the insertion of the digging tool (e.g.dipper tooth) into the material, cutting is the lateral movement of the digging tool and scooping is the combination of the rotation and retreat of the dipper. In the digging process, the dipper teeth apply the cutting force acting on the lip of the dipper teeth and have to overcome resistance forces from the dug material. The resistance forces combine the cutting forces at the dipper teeth and lip and the excavation forces due to material movement along, ahead and inside the dipper body[1, 12]. The shovel resistance force model proposed by Hemanmi [13] includes six forces that must be overcome during the excavation process, as shown in Figure 2.1. The six resistance forces acting on the dipper are
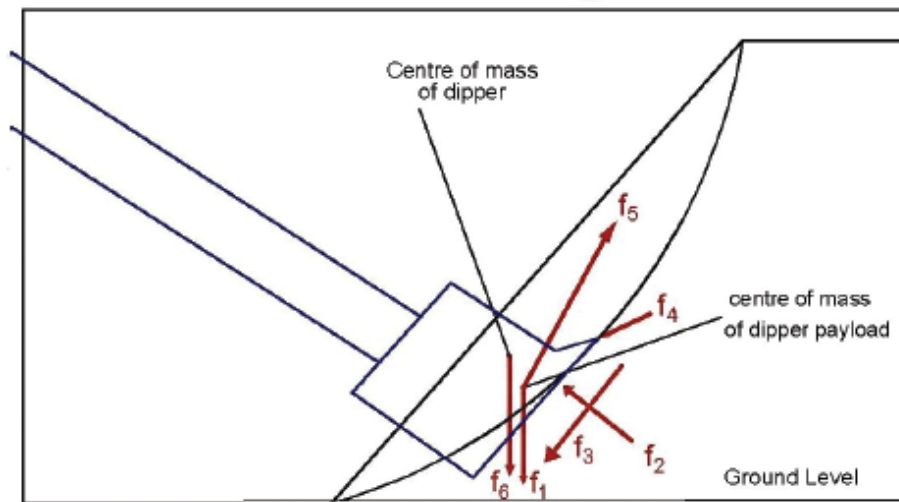
Figure 2.1: Resistance Forces During Excavation[1]

denoted by f_1 to f_6 in Figure 2.1 are as follows[1, 12, 13]:

- f_1: the force required to overcome the weight of the loaded material inside and above the dipper;

- f_2: the resistance force coming from the bucket's compacting action on the material in front of the bucket on the muck pile;

- f_3: the friction force between the dipper wall and the dug material;

- f_4: the force required to compensate for the cutting resistance of the material;

- f_5: the inertia force of the material inside and above the dipper;

- f_6: the force to move the empty bucket.

From f_1 to f_5 are dynamic forces. Those five forces vary in both magnitude and direction due to the material to be loaded, bucket geometry and size and, the bucket motion and the environment effects[13]. Specifically, f_1 is highly affected by the bucket motion and the magnitude and force acting point vary during the excavation process. f_2 can be zero if the bucket motion does not have pushing and compacting action on the material. Compared with f_2, the friction force f_3 always exists and its direction is the same as the bucket moving direction. f_5 is depending on the acceleration of the bucket motion[13]. f_3 and f_4 are the cutting forces and can be combined as one single force by using Zekenin et al's empirical model[14] which is expressed in Equation 2.1.

$$P = 10C_0d^{135}(1 + 2.6w)(1 + 0.0075\beta')z \tag{2.1}$$

where C_0 is a measure of the compactness and density of soil.From the standard referred by Zekenin et al, the C_0 is the number of impacts to penetrate a flat cylindrical tip with a cross-section of 1 cm^2 to a depth of $10cm$ when a 2.5 kg mass falls from a height of 0.4 m. d here is the depth of cutting, w is the bucket width in meters and β' is the cutting angle in degrees. z is the coefficient of blade impact on cutting force, which depends on w and d.

2.1.2 Dynamic Modelling of Cable Shovel

Dynamic modelling is another factor showing the shovel's work mechanism and performance behavior. The dynamic equations of cable shovels can be obtained by using either the Lagrange method or iterative Newton-Euler method; while the iterative Newton-Euler method is commonly applied because of the efficiency in software implementation, which is significant to real-time simulation and parameter estimation[15, 16]. Besides, the use of Lagrange formulation requires the designer to have

an insight into the behaviour of the whole system. On the contrary, the iterative Newton-Euler method treats each link and joint in the system as a free body, which can be used recursively for a link involving variables of the adjacent links[17]. The Newton-Euler dynamic algorithm for the crowd force and hoist torque calculation includes two parts: firstly, the Euler-Newton equations can be applied recursively to each link from the dipper handle to dipper; secondly, the forces and torques can be iteratively computed from dipper back to the dipper handle[18]. The Newton-Euler formulation yields forces and torques at connecting joints, which is useful for design and diagnostics.

The dynamic modelling of cable shovel developed by S. Frimpong[19] is by far the most comprehensive model. The dynamics equation for the cable shovel is expressed as Equation A.1.

$$D(\boldsymbol{\Theta})\ddot{\boldsymbol{\Theta}} + C(\boldsymbol{\Theta}, \dot{\boldsymbol{\Theta}})\dot{\boldsymbol{\Theta}} + G(\boldsymbol{\Theta}) = F - F_{\text{load}}\left(F_{\text{t}}, F_{\text{n}}\right) \tag{2.2}$$

where $D(\boldsymbol{\Theta})$,$C(\boldsymbol{\Theta}, \dot{\boldsymbol{\Theta}})$ and $G(\boldsymbol{\Theta})$ represents the generalized inertia matrix, Coriolisand centripetal torque, and gravity torque respectively. $\boldsymbol{\Theta}$ is the vector of generalized variables. F is the cable shovel's breakout force and $F_{\text{load}}\left(F_{\text{t}}, F_{\text{n}}\right)$ represents the resistive force during the dipper-soil digging process. A detailed explanation about the dynamic modelling is included in Appendix A.

In Equation A.1, the force F, provided by the crowd and hoist motors, is mainly to overcome external effects. The external effects consists of two parts: the first part comes from the dynamics effects including the inertia effect, Coriolis and centripetal effects, and gravity; the other part is the interaction between the dipper and soil. Meanwhile, $D(\boldsymbol{\Theta})$ and $G(\boldsymbol{\Theta})$ describe the effect of the dipper and dipper handle's geometrical and material properties. $C(\boldsymbol{\Theta}, \dot{\boldsymbol{\Theta}})$ represents the kinematics and dynamics of the digging strategies such as digging profile and cycle time while $F_{\text{load}}\left(F_{\text{t}}, F_{\text{n}}\right)$ is related to the physical and mechanical property of the soil[19]. Other effects are not considered in the dynamic modelling here, which includes the friction effects during

the transmission process.

Overall, the dynamic modelling developed by Frimpong in Equation A.1 mainly contributes to the digging process, which is restricted to dipper, boom and dipper handle. Based on this assumption, the crowd system, including the dipper handle and dipper assembly, only moves in the vertical plane and the rotation of the upper structure (swing function) is not considered in the dynamic modelling here. According to the variables in the Equation A.1, it can tell that dynamic modelling considers the geometrical and material properties of the dipper and dipper handle, physical and mechanical properties of the soil being excavated, and the crowd and hoist forces. Besides, the dynamic modelling also requires a comprehensive understanding of kinematics and dynamics of cable shovels, which will be discussed in the following sections.

2.1.3   Cable Shove Kinematics and Dynamics

A good understanding of cable shovel's kinematics and dynamics is crucial to improve the cable shovel's digging efficiency and reliability. According to the dynamic modelling mentioned above, a good knowledge of the kinematics and dynamics of cable shovels is necessary during the digging process. Based on the assumption of dynamic modelling, crowd arm and dipper assembly only moves in the vertical plane and swing motion is not considered. Frimpong proposed a coordinate system to make the analysis of the kinematics and dynamics of the cable shovel consistent and unified[18].

In Figure 2.2, the global coordinate $X_w Y_w Z_w$ represents the coordinate for the base and upper structures of the shovel (swing function is not considered) while the local coordinates $O_0 X_0 Y_0 Z_0$, $O_1 X_1 Y_1 Z_1$ and $O_2 X_2 Y_2 Z_2$ indicate the coordinates for the boom, dipper handle and dipper respectively. The kinematics and dynamics of cable shovels mainly concentrate on the crowd arm and dipper assembly since the upper structure is assumed to be fixed when digging[20, 21]. A detailed analysis of

11
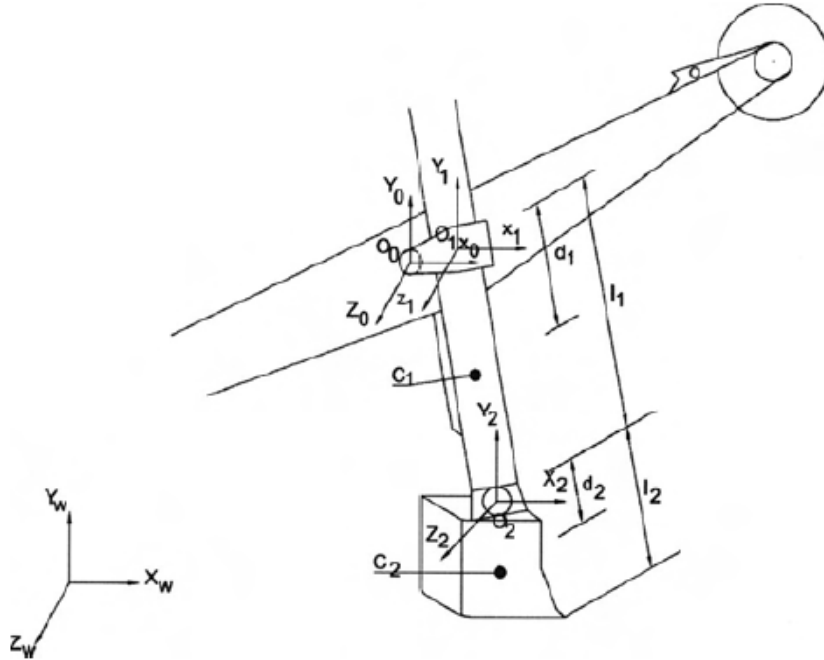
Figure 2.2: Coordinate System for the Upper Structure Components[18]

the cable shovel's kinematics and dynamics will be discussed as follows based on the coordinate system in Figure 2.2 and the assumption mentioned above.

Cable Shovel Kinematics

During the digging process, the crowd arm extends the dipper to extract the soil and when the dipper is full the dipper is retracted after the excavation. It is of importance to understand the linear velocity, linear acceleration, angular velocity and angular acceleration of the components involved in the digging process. Therefore, a good knowledge of cable shovel kinematics models for the front-end assembly is necessary for the analysis of the digging process. Frimpong proposed a complete kinematic model[18] for cable shovel by using Newton-Euler formulations. According to the proposed kinematics modelling, the outward iterations describe the motion of the front-end parts during the excavation process; the inward iterations, on the other hand, describe the motion of the front-end assembly as it is being extracted

after the digging process. As the bucket is empty, based on the outward iterations, the motion has higher angular and linear displacements and velocities, and smaller moments about the centers of rotations; while the bucket is loaded, the kinematics of the retracting motion is opposite, which has slower angular and linear displacements and velocities, and higher moments about the center of rotations.

Cable Shovel Dynamics

Cable shovel dynamics model determines the inertia forces, moments and resistive force during the excavation process. The dynamic models are derived for the front-end part of the shovel which is shown in Figure 2.2 and the interaction between dipper and soil is represented in Figure 2.3. The results from the kinematic model of cable
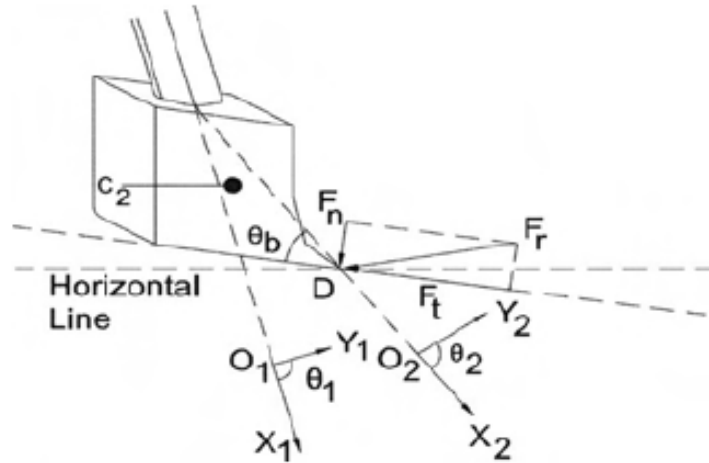
Figure 2.3: Interaction Between Dipper and Soil[18]

shovel are required to simulate the dynamic model[18]. The action forces are used to yield the breakout force which needs to be greater than the resistive force during the excavation. The resistive forces, produced by the digging materials, are the resultant of the tangential and normal forces incident on the plane of excavation[18] illustrated in Figure 2.3. The moments from the active forces, resistive forces, and the centers of rotation about joints are critical in the shovel performance[18, 22]. Similar to the

13

deduction of the kinematics, the dynamic models are also exploited using the outward and inward iteration to study the dynamics of the excavation process in the extension and retraction phases[22].

2.1.4   Cable Shovel Model Validation

When analyzing the performance or fault detection of the earth-moving machines, the best object would be the shovel itself. However, considering the cost of the experiment and the capability to repeat tests in a controlled environment, using the actual shovel is not practical[23, 24]. It is easy to think that a scaled cable shovel might be a good for evaluating faults in the lab due to its smaller size and easy-to-control ability in a limited controlled space. Then, if a relationship can be derived from the developed data that connects the structure and performance parameters between the lab model and actual machine, this will greatly improve the credibility of scaled cable shovel[24]. In other words, if the main structure is scaled down from the actual size of the shovel, the performance of the lab-scale shovel is similar to the full-size shovel and the digging scheme is the same as the full-size shovel, then it can be concluded that the behaviour of the scaled shovel during the experimental lab tests would be similar to the behaviour of the shovel in the field[24]. Hence, modelling is a useful tool that mimics rather than studying the actual entity or phenomenon[24, 25].

Modelling has been widely applied to various engineering applications and can be categorized as follows[25]:

- Physical: respecting to the main structural characteristic of the examined phenomenon;

- Computer: established from mathematical equations or learning base;

- Analog: where electrical systems are employed to create a time series of a governing equation implemented using analogous circuits;;

- Limited: where the model is restricted to certain features of the phenomenon;

- Distorted: when various scaling parameters comply with various rules.

The development of the model experiment consists of three stages[25]: first, identify the characteristics of the phenomenon and filter the features needed to be examined in the prototype which refers to "an idealization of the field problem in which only those factors considered essential and relevant have been retained"[26], and then construct the model; second, design experiments to test the model under different working conditions; third, adapt the results from the model to the prototype. In the transition from the model to prototype, modification and manipulation of the model are necessary to conduct to make the prototype applicable to investigated field processes[25]. The development of the model allows researchers to simplify the complicated machines and only focus on the critical components or systems for the study.

Fractional Analysis

The fractional analysis is any procedure for obtaining some information about the answer to a problem in the absence of methods or time for finding a complete solution[27]. The purpose of the fractional analysis is to find as much information as possible even though the complete and exact solution cannot be found or is hard to find. The most common techniques for fractional analysis include dimensional analysis and the method of similitude[25].

Dimensional analysis is using dimensionally homogeneous equations to deduce information about an event so that the form of the equations is independent of the fundamental units of measurement[25, 28]. The contribution of the dimensional analysis is to reduce the number of terms when predicting the equation by using the number of dimensions needed to describe the phenomena[25]. Dimensional analysis can provide insight into the fundamental aspects of a generalized analysis; however,

it cannot describe the mechanism of the physical processes. In a word, dimensional analysis can be utilized when information is not sufficient on the governing equation of the phenomenon[25].

The theory of similitude is another common technique of the fractional analysis and a method to simplify the complexity of the phenomenon, which has been applied to various areas including structural engineering, vibration and impact problems[29]. Similitude theory can be utilized to accurately predict the behaviour of the phenomenon through the scaling laws applied to the experimental results from the scaled models under similarity conditions[29–31] The prediction of the phenomenon by using the similitude theory can be summarized in Figure 2.4
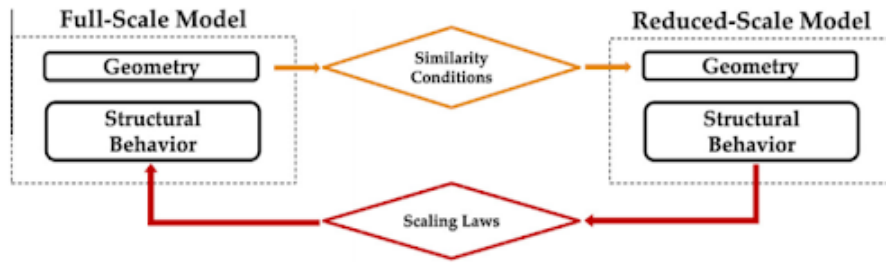
Figure 2.4: Similitude Theory for the Phenomenon Behaviour Prediction[29]

Overall, the similitude theory is applied to the equations of the process and the understanding of the physical concepts is necessary before using the theory of similitude. Therefore, compared with dimensional analysis, the theory of similitude requires a list of important and pertinent parameters, which may have less accurate and complete solutions[25].

The Theory of Modelling

The theory of modelling is based on the similarity of processes and dealing with the methods of model designing[14]. Modelling without changing the physical nature of the phenomenon is called physical modelling; modelling according to the use of electronic computers is called mathematical modelling[14]. When modelling earth-moving machines it is possible to use geometric, physical and physico-mathematical

16

modelling[14]. Zelenin et. al. summarized the following conditions if two phenomena (processes) or objects (machines) are similar[14]:

- Geometric Similarity: represents the proportionality of the linear dimensions of the prototype and the model $(l, x, y, z$ etc):

$$\frac{l_m}{l_p} = \frac{x_m}{x_p} = \frac{y_m}{y_p} = \frac{z_m}{z_p} = l_c \tag{2.3}$$

$$\alpha_m = \alpha_p; \beta_m = \beta_p; \gamma_m = \gamma_p \tag{2.4}$$

where l_c is the coefficient of similitude with respect to linear dimensions and subscript p and m represent the prototype (original) and model respectively;

- Physical similarity: represents the similarity of the kinematic and dynamic parameters of the processes:

Velocity:

$$\frac{v_m}{v_p} = \frac{l_m}{t_m} = \frac{l_p}{t_p} = \frac{l_c}{t_c} \tag{2.5}$$

Force:

$$\frac{P_{\mathrm{m}}}{P_{\mathrm{p}}} = \frac{m_{\mathrm{m}} a_{\mathrm{m}}}{m_{\mathrm{p}} a_{\mathrm{p}}} = m_{\mathrm{c}} \frac{l_{\mathrm{c}}}{t_{\mathrm{c}}^2} = \rho_{\mathrm{c}} l_{\mathrm{c}}^2 v_{\mathrm{c}}^2 \tag{2.6}$$

Work:

$$\frac{A_{\mathrm{m}}}{A_{\mathrm{p}}} = \frac{P_{\mathrm{m}} l_{\mathrm{m}}}{P_{\mathrm{p}} l_{\mathrm{p}}} = m_{\mathrm{c}} v_{\mathrm{c}}^2 = \rho_{\mathrm{c}} l_{\mathrm{c}}^3 v_{\mathrm{c}^2} \tag{2.7}$$

Power:

$$\frac{N_{\mathrm{m}}}{N_{\mathrm{p}}} = \frac{P_{\mathrm{m}} v_{\mathrm{m}}}{P_{\mathrm{p}} v_{\mathrm{p}}} = \frac{m_{\mathrm{c}} v_{\mathrm{c}}^2}{t_{\mathrm{o}}} = \rho_{\mathrm{c}} l^2 v_{\mathrm{c}}^3 \tag{2.8}$$

where v_c and t_c are the coefficients of similitude with respect to velocity and time respectively. $m, a, \rho_{\mathrm{c}}, m_{\mathrm{c}}$ represent the mass, acceleration, density ratio and mass ratio respectively.

Based on the completeness and exactness of simulation being studied, modelling can be categorized into complete, incomplete and approximate[14]. The complete modelling is the similarity of motion of the material is maintained both in space and

17

in time; while the incomplete modelling investigated the process that is similar to the prototype either in time only or in space only. The approximate modelling is where the non-dominant parameters have a known influence but not causing significant change to the investigated processes[14].

2.2 Maintenance Strategies

Reliability is defined as the ability of a component or system to perform the required functions under the desired conditions of operation within a given time frame[2]. It is critical to keep good reliability of machines especially in the industries involving production. Nowadays, modern industries have designed reliability-centred maintenance strategies for their production equipment in order to increase reliability and productive capacity[32]. With good maintenance on the equipment, unplanned reliability-related accidents can be reduced; in other words, good maintenance strategies can improve equipment reliability, lower the downtime and increase productivity to its maximum extent.

Many types of research have been conducted to analyze the maintenance strategies of productive equipment[2, 33, 34]. Kothamasu et al[33] summarized the commonly used maintenance strategies which are shown in Figure 2.5. In the past, personnel in maintenance departments performed the reactive maintenance strategy to maintain the equipment; here machines were used to its limit and repair would not be conducted until the machine failed. However, it has been proved that this scheme is not ideal for machines with complex systems such as electric mining shovels. The company cannot risk running it to failure since it will be costly to repair highly damaged parts and also pose safety risks to operators. Today, industries are mostly using preventive maintenance strategies. This maintenance strategy is age-based at predetermined intervals to reduce the probability of failure or performance degradation[33]. Manufacturers usually provide predetermined intervals which are estimated from the failure rate distribution that is constructed from the historical data extracted from
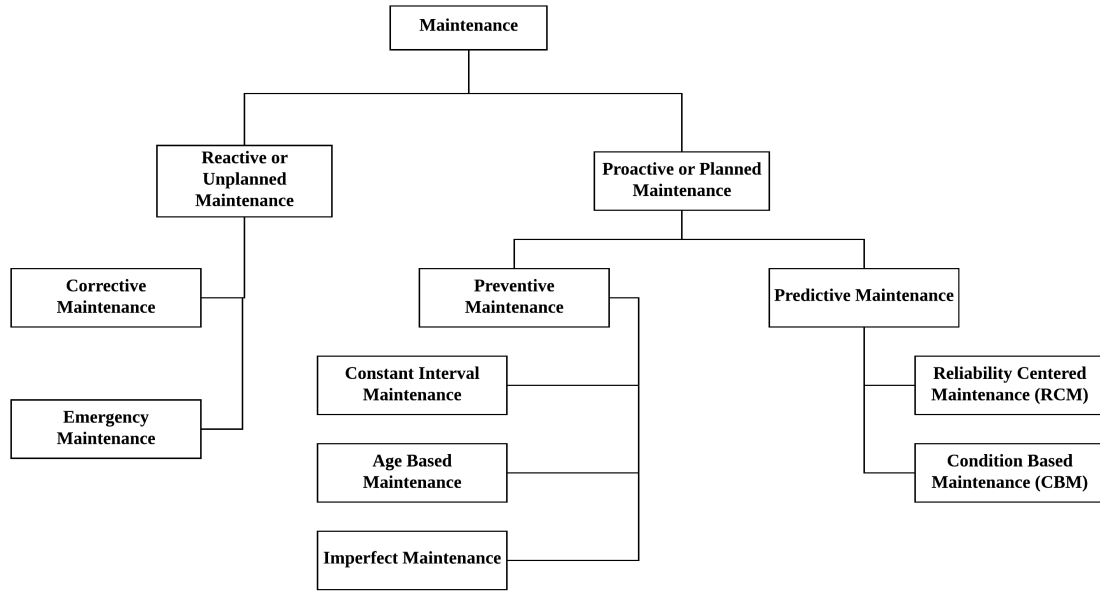
Figure 2.5: Taxonomy of Maintenance Philosophies[33]

the system[33]. Although the age-based preventive maintenance help to reduce unplanned downtime, planners tend to make conservative maintenance schedules. As a result, some remaining useful life of machines is wasted and unnecessary maintenance cost is added.

Compared with the preventive maintenance (fixed schedule), the planned downtime schedule in the predictive maintenance scheme is adaptively determined[33]. Predictive maintenance can help to estimate the time-to-failure of a machine and find the optimal time to schedule maintenance for the equipment[35]. The characteristics of the three common maintenance strategies: reactive, preventive and predictive maintenance are summarized graphically in Figure 2.6.

2.2.1 Condition Monitoring

Among the three common maintenance strategies mentioned above, it is apparent to see that the most efficient maintenance strategy is predictive maintenance, which consists of reliability-centred maintenance (RCM) and condition-based maintenance (CBM). RCM is an approach to utilize the reliability estimates of the system to draft a
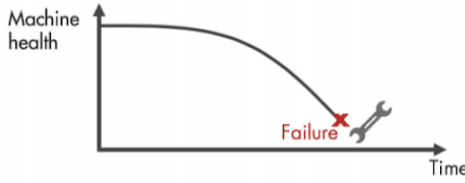
(a) Reactive Maintenance
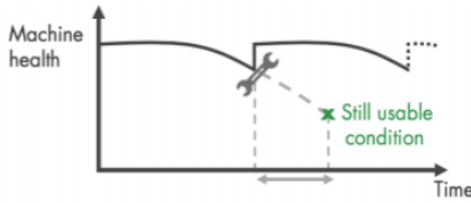
(b) Preventive Maintenance
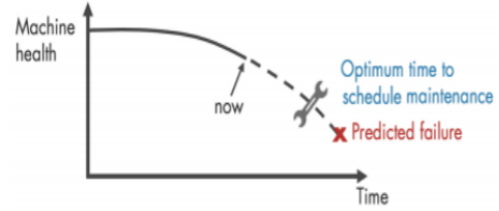
(c) Predictive Maintenance

Figure 2.6: Characteristics of Reactive, Preventive and Predictive Maintenance[35]

schedule for maintenance[33]. An RCM maintenance interval is predetermined by the failure rate distribution of the system, which is similar to preventive maintenance, but condition monitoring techniques are increasingly used to find the optimal maintenance intervals[36, 37]. Condition-based maintenance is to make a downtime maintenance schedule by observing equipment's condition which is usually represented by condition parameters such as vibration characteristics[33]. CBM relies on incipient failures and the resultant changes in the monitored parameters[10, 33] to diagnose and prognoses the equipment issues[38]. Condition monitoring has the potential to predict incipient failure weeks or months in advance, so planners can be able to plan maintenance to use the minimum disruption of production to order replacement parts and fix them[10], as shown in Figure 2.7.

Fault detection is the first step in condition-based maintenance. Any fault detection system consists of data collection, feature extraction and feature assessment[2]. There are two main categories in fault detection methods including model-based and pattern recognition-based methods. The major difference between these two methods comes from the understanding of the machine model: model-based method re-
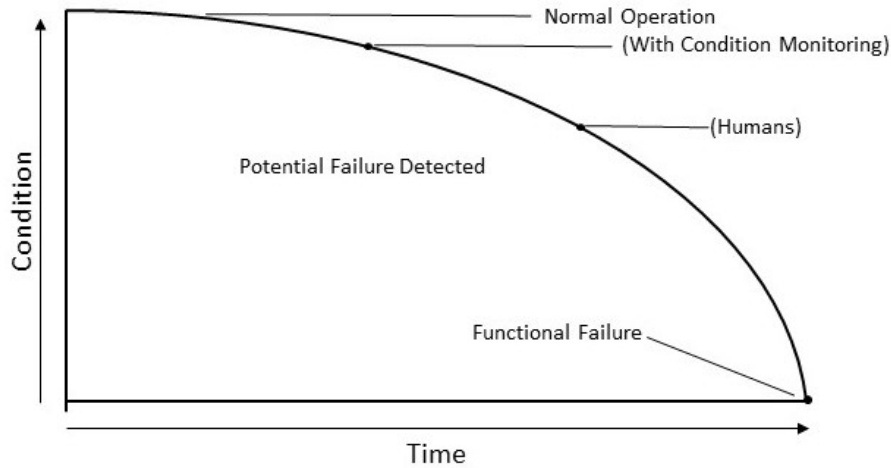
Figure 2.7: Incipient Fault Detection Feature of Condition Monitoring[32]

quires the physics specific, the explicit mathematical model of the monitored machine and model-based approach can be effective if a correct and accurate model is built; sometimes, explicit mathematical modelling may be hard to obtain for complex systems[38]; the pattern recognition-based model is purely data-driven with the use of artificial intelligence. A well-trained pattern recognition-based model can effectively detect a fault as it learns from the fault-free and fault datasets[39]. A drawback of this approach is that it needs a large dataset. Condition monitoring is to use the information obtained externally about internal effects[10], and common techniques to analyze the internal conditions vary from vibration analysis, lubricant analysis, noise, thermography and so on.

2.2.2 Modern Condition Monitoring Solutions on Earthmoving Equipment

As mentioned previously, with good maintenance on the earthmoving equipment, unplanned reliability-related accidents can be reduced. Good maintenance strategies will improve equipment reliability, lower downtime and increase productivity. Condition monitoring allows early incipient failure prediction, which can be used by planners to

schedule downtime and make work orders. Various technology companies and manufacturers are implementing cutting-edge tools and technological devices to monitor the working condition and performance of complicated earthmoving equipment.

Damage Monitor-MS, developed by CADETECH for damage monitoring on mining shovels, is a real-time operational condition supervisory system for electromechanical shovels, which detect the structure damage by fatigue due to fluctuating load[40]. For each crack-prone zone (CPZ), a Damage Monitor node is installed, which calculates damage by fatigue in real-time based on measured strain and a finite element model. As the stress magnitude and/or damage accumulation rate exceed the user-defined limits, the Damage Monitor-MS will generate an alert indicating the severity of the detected condition. This structure integrity management tool allows structure inspection and fault severity evaluation[40]. The flowchart of the Damage Monitor-MS working mechanism is shown in Figure 2.8.
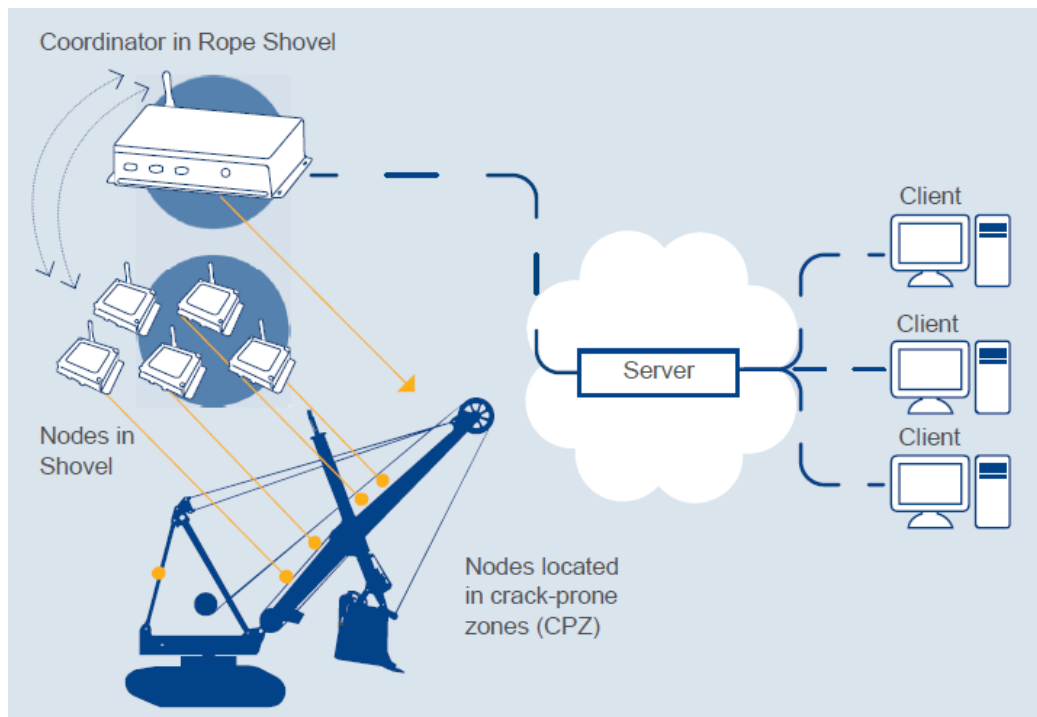
Figure 2.8: Working Mechanism of Damage Monitor-MS Developed by CADE-TECH[40]

SiAMFlex-MS, another high-end condition monitoring tool developed by CADE-

TECH for mining shovels, is a vibration monitoring system for hoist, crowd and swing transmissions of electromechanical shovels[41]. Compared with conventional equipment, which is based on Fast Fourier Transform, the spectral analysis of SiAMFlex uses a tailor-made spectral algorithm to monitor the mechanical condition of the transmission components in electromechanical mining shovels[41]. Data acquisition and processing hardware on board on the monitored mining shovels receives the vibration signals from a series of sensors that are installed on the components of interest. SiAMFlex is capable of self-selecting and storing the most appropriate vibration data for further analysis by specialists. The flowchart of the SiAMFlex working mechanism is summarized in Figure 2.9.
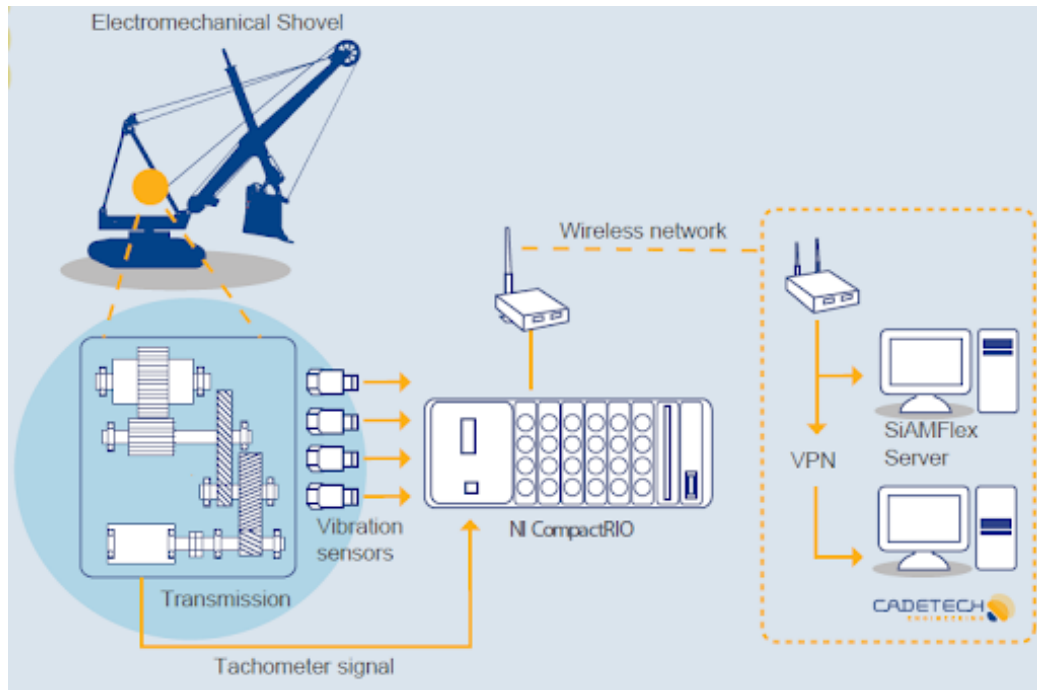
Figure 2.9: Working Mechanism of SiAMFlex-MS Developed by CADETECH[41]

P&H was the first mining equipment manufacturer to utilize predictive technology on earthmoving machines. Also, P&H uses a portable vibration analyzer to detect mechanical defects in the mechanical components of the machine[2, 42]. P&H expanded the line of products to include modern health monitoring and diagnostic features; for continuous monitoring, P&H has implemented a system based on the PreVail

23

platform[2, 42]. PreVail Remote Health Management (RHM) technology along with Vibration Monitoring systems address health monitoring, production and machine performance. The PreVail system includes a data-collection module mounted in a compartment and connected to the control system module onboard the machine. Through a wireless network or a satellite channel, PreVail has the ability to transmit trend data and event files for maintenance and operations personnel. In order to identify and provide early warning of faults, PreVail RHM provides condition-based equipment monitoring (CBEB) models that use algorithms to detect certain data trends that deviate from normal control limits. As the collected real-time data and analysis reveals a system data anomaly by CBEB models, the first-snapshot notification (FSN) function will be triggered that the P&H support office can receive the warning notice[43].

Although, the real-time condition monitoring tools developed by technology companies or manufacturers mentioned above can predict incipient failures successfully, they still have some limitations: measurements are only conducted when shovels make particular movements at particular speeds. The key step to acquire the proper data is when the shovel is in operation with no loading and waiting for a truck[42]. Hence, obtaining proper data for further analysis is still challenging due to various operation modes (variable loads or speed).

Recent studies have been conducted to overcome the constant load/speed limitations. Timusk, Lipsett and Mechefske have investigated the application of the vibration analysis for machinery in transient operating modes[44]. A laboratory apparatus with variable speed and loading capacity to replicate the duty cycle of the excavator has been developed. Rather than using the characteristics of the normal operating condition as prior information, a novelty detection scheme for fault detection was adopted. The novelty detection algorithm includes a training period, where it will be considered as the baseline for the normal operating condition, and any condition with a significance deviation will receive a novelty score. Realizing the effect of the

24

operating modes on the physical response of the system and diagnostic parameters, Timusk et al. compared a number of classification methods to obtain real-time information regarding the shovel operating modes[45]. It is been proved that there is a strong relationship between speed changes and vibration response acquired by accelerometers[46]. McBain and Timusk also proposed that segmentation of the vibration signal based on speed segments can improve the accuracy of classification methods[46] adopted in the novelty detection algorithm[45].

Except for the operation modes, highly variable load/speed's effects on vibration monitoring have been recently studied[47–49]. Those experiments proved that time-frequency methods can successfully improve the detection of the local damage for such systems under time-varying cyclic load. During excavation with variable loads and rotational speeds, it is concluded that the influence of the load in the physical response can be significant at lower rotational speeds[49].

2.3   Vibration Analysis

Vibration analysis is one of the most effective condition-monitoring strategies to detect faults in machine systems, which can be defined as a process for measuring the vibration levels and frequencies of machinery and using that information to analyze how healthy the machine and its components are[9]. The vibration signature of a machine is the characteristics pattern of vibration it generates when it is in operation[50]. Vibration signatures in the standard condition and faulty condition of the machine are different[10]; in other words, vibration analysis focuses on the circumstances that defects in a machine change the normal vibration signature which can be considered as an indicator of the fault[2].

Vibration analysis is by far the most prevalent method for machine condition monitoring because of its distinctive advantages compared with other methods. The benefits of the vibration analysis[10] are summarized as follows:

- *Immediate Reaction to Change*: the vibration analysis can sense the change of the vibration change of the machine components as soon as the deflects show up and develop. With the oil analysis, for example, several days can be taken to collect oil sample and analysis;

- *Accurately Point to the Faulty Component*: vibration analysis can locate the faulty components that exhibit increased vibration. On the contrary, taking oil analysis as an example, the faulty component may not be detected since many metal parts have the same chemical compositions;

- *High Sensitivity*: with advanced signal processing techniques, weak fault indications can be extracted in the vibration signals.

Vibration monitoring uses signals generated by component defects as the source to indicate a deficiency. As defects grow in magnitude and deterioration, the vibration increases in amplitude and frequency[32]. Vibration monitoring can uncover issues in machines involving mechanical or electrical imbalance, misalignment, or looseness. Therefore, vibration monitoring or vibration analysis can reveal and track the appearance or development of deficiencies in machine components[32].

The mechanical vibration process can be categorized into four main stages as summarized in Figure 2.10. First, the mechanism generates vibration; then the generated

Generation → Transmission → Propagation → Radiation

Figure 2.10: Mechanical Vibration Process[51]

oscillatory energy transfers from the mechanism of the generation to a structure; third, the energy is propagated throughout the structure system; at last, any structure part will impart power to its surroundings[51].

2.3.1 Common Failure Modes on Mining Equipment

As mentioned above, vibration analysis can utilize the signal generated by the mechanical or electric failure and different failure modes may have their distinctive vibration signatures. Change in vibration signals is attributed to the change in condition[2], it is important to find the relation between the failure modes and vibration signatures. Common transducers for vibration analysis include accelerometers, proximity probes and encoders. With a good knowledge of the vibration signatures, it is necessary to choose proper transducers to collect the vibration signals: radial vibration in the plane perpendicular to the rotation axial can be detected by radial vibration transducers such as proximity probes and accelerometers; torsional vibration, variations in angular velocity of the shaft, can be detected through shaft encoders[2, 10]. Figure 2.11 summarizes the commonly witnessed machinery faults diagnosed by vibration analysis. Among those common vibration-analyzed failure modes, excessive clear-

Unbalance	**Gear Defects**	**Cavitation**
Bent Shaft	**Misalignment**	**Bearing Defects**
Eccentricity	**Shaft Cracks**	**Oil Whip/Whirl**
Looseness	**Rotor Rubs**	**Belt Drive Problems**

Figure 2.11: Common Witnessed Machinery Faults Diagnosed by Vibration Analysis[34]

ance in joints and gear misalignment happen frequently in earth moving machines, which then will be studied further as follows.

Joint Clearance/Looseness

Joints exist frequently in modern machines. The functionality of a joint allows the relative motion between the connected components. Due to the inevitable clearance between the mating parts, it can lead to surface contact, shock transmission and the development of friction and wear. Even though the clearance is small, it can cause vibration and fatigue phenomenon, lack of precision or abnormal behaviours[52]. Mechanical looseness is a common maintenance downtime for rotating equipment, which will mostly occur at three locations: internal assembly looseness, looseness at the machine, and structure looseness[2]. This fault could arise between a bearing linear in its cap, a sleeve or rolling element bearing or an impeller on a shaft[2]. Proximity probes and accelerometers can be used to detect the loss of contact due to joint clearance[53, 54].

In the analysis of a revolute joint, the journal and bearing centers coincide, which represents the ideal or perfect working situation for a revolute joint. However, in reality, the inclusion of the clearance may separate two centers so that two extra degree-of-freedoms are added to the system[52]. Figure 2.12a depicts the classical
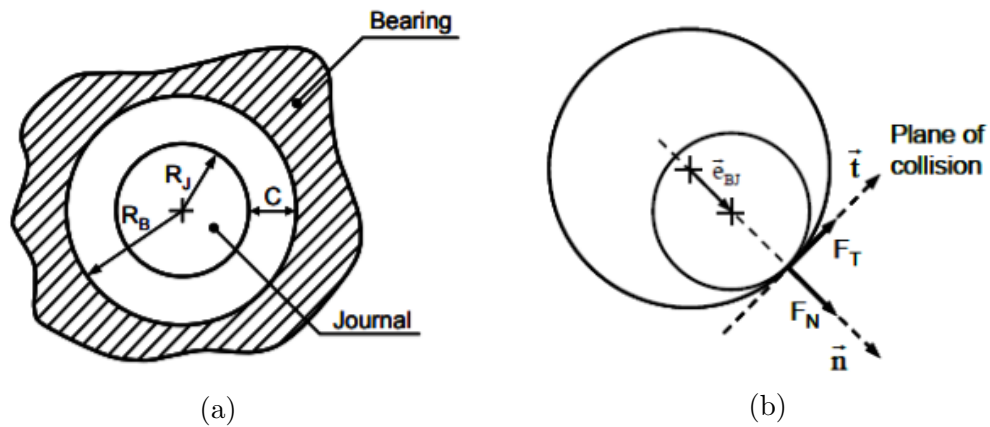
Figure 2.12: (a)Revolute Joint with Clearance; (b)Normal and Tangential Forces Due to Bearing and Journal Impact[52]

revolute joint consisting of journal-bearing assembly and clearance, where R_B, R_J and C denote the radius of bearing, the radius of journal and clearance distancing

respectively. In a dry condition, the journal can freely move within the bearing until the journal hits the bearing wall. During the collision, a normal contact force along with the friction force is evaluated to determine the dynamics of the revolute joint. Figure 2.12b illustrates the normal and tangential forces due to the journal-bearing impact. The impact can be treated as an eccentric oblique collision with two bodies[52], and the corresponding impulse can be transmitted throughout the mechanical system[55].

In the revolute joint with clearance, three different modes of motion between the journal and bearing can be considered: continuous contact mode, free-flight mode, and impact mode[52, 56], which are illustrated in Figure 2.13. In the continuous contact mode, the journal and bearing are in contact and a sliding motion is assumed to exist. During this mode, the penetration depth varies along the circumference of the journal. This mode ends at the instant when the journal and bearing separate and the journal enters the free-flight mode. In the free-flight mode, the journal moves freely inside the bearing; in other words, there is no contact between the journal and bearing. After the free-flight mode, the journal enters the impact mode, where the impact forces applied and removed. This mode is characterized by a discontinuity in the kinematic and dynamic response, and a significant exchange of momentum occurs between the impacting bodies. At the termination of the impact mode, the journal can enter either free-flight or continuous contact mode. When analyzing the dynamics of a revolute joint with clearance, if the path of the journal center is plotted for the discrete instant of time, the types of motion modes of the journal inside the bearing can be easily detected[52].

Gear Misalignment

Failure in gears, transmission shafts and drive trains is common in gearboxes of earth-moving machines. Those components are very flexible, even if a perfect alignment is achieved as shown in Figure 2.14, random dynamics forces can make shafts to bend
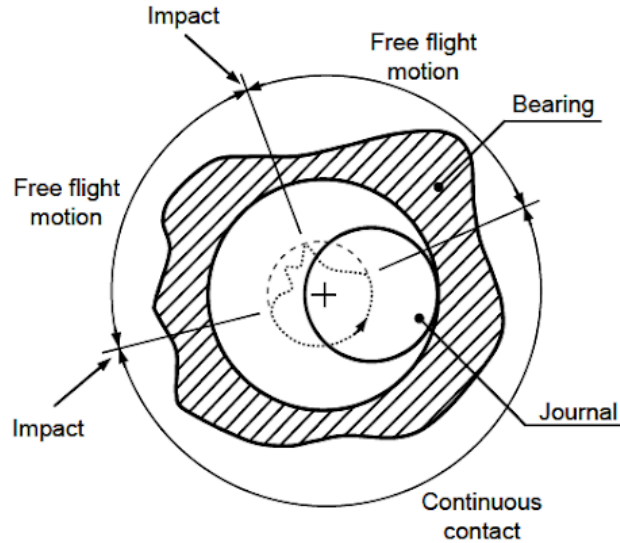
Figure 2.13: Three Types of Journal Motion Inside the Bearing[52]

causing gear misalignment[57]. Various reasons can lead to gear misalignment such as failing lubrication quality, wear of shaft bearings, losses of shaft eccentricity or shaft bend and deforms[57].
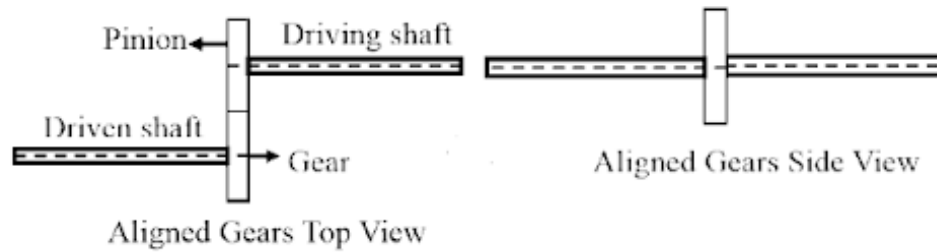
Figure 2.14: Perfect Gear Alignment[57]

The fault of gear misalignment can be grouped into two categories: lateral misalignment and angular misalignment. Specifically speaking, lateral misalignment consists of radial and axial misalignment and angular misalignment consists of yaw and pitch misalignment which are illustrated in Figure 2.15 and 2.16 respectively.

Gears are said to be radial misalignment, as shown in Figure 2.15a, when gear teeth are brought away from each other by increasing the center-to-center distance while shafts remain parallel. Because of the reduction of the contact area of the teeth under the mesh, the teeth meshing stiffness reduces, backlash and tooth bending

30

(a) Radial Misalignment

(b) Axial Misalignment
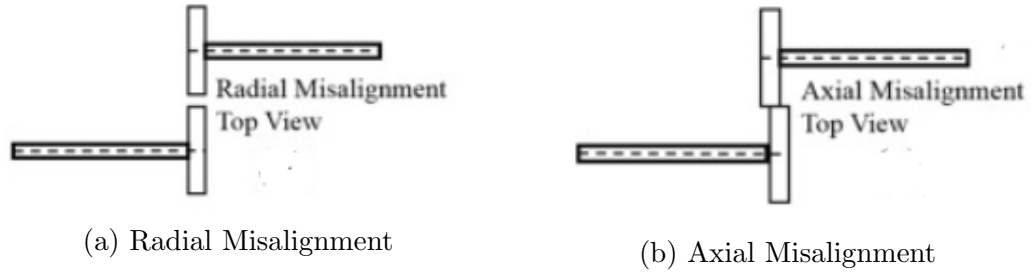
Figure 2.15: Two Type of Lateral Gear Misalignment[57]

(a) Yaw Misalignment

(b) Pitch Misalignment
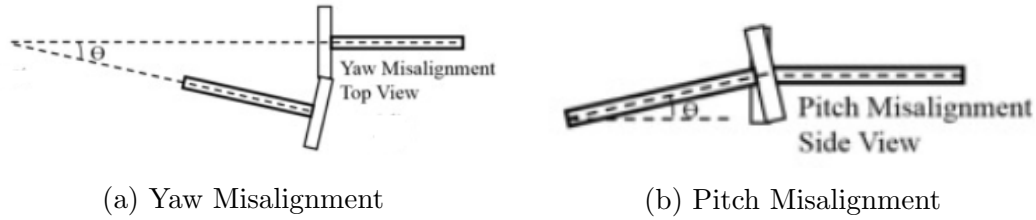
Figure 2.16: Two Type of Angular Gear Misalignment[57]

increase as the contact ratio decreases gear noise reduces[57]. Axial misalignment is the other lateral gear misalignment as shown in Figure 2.15b. When subjected to axial misalignment, the center-to-center distance remains the same but one gear is moving forward or backward along its axis leading to the reduction of contact area along its face width. In addition, as the contact area decreases, contact stresses and deformation will increase which causes a reduction in meshing stiffness[57, 58].

Yaw misalignment is one of the angular misalignment illustrated in Figure 2.16a. When subjected to yaw misalignment, the gear shafts are positioned at an angle on the horizontal plane. In this case, the contact area between gears is subjected to increase or decrease depending on whether the pinion shaft is moving towards or away from the gear shaft. If the pinion shaft is displaced towards the gear shaft, the pinion teeth move further into the gear resulting in the increase of the contact ratio which would then cause more gear noise. On the contrary, as the pinion shaft is moving away from the gear shaft the contact ratio would decrease and result in lower noise[57]. Pitch misalignment is the other angular gear misalignment fault illustrated in Figure 2.16b. Compared to the yaw misalignment, the gear shafts are positioned at

31

an angle at a vertical plane. Since the pinion teeth are tilted, more edge region comes in contact with the meshing region which causes the increase of the deformation and decrease in mesh stiffness[57]. Among the gear misalignment, the pitch misalignment causes more contact stresses[58].

2.3.2   Digital Signal Processing Techniques

With the help of the appropriate signal processing techniques, signals collected from the machine can reveal the machine's health condition. Mostly, signals collected from sensors are contaminated by some noise and thus may not be able to directly diagnose the machine faults. Features of collected signals can be detected with the assistance of certain techniques. Feature extraction techniques come with two main functionalities: first, increase the signal to noise ratio; second, locate certain components in signals to assist detection in machine faults. Numerous digital processing signal techniques have been applied to the fault diagnosis analysis, which are varying from statistical to model-based techniques, and from comprising various signal processing algorithms to extracting useful diagnostic information from collected signals[59]. The success in the detection of change depends on the significance of the deviation and effectiveness of the algorithm that is used for the interpretation of the data[2, 10, 60]. Digital signal processing techniques are grouped into three categories: time domain, frequency domain and time-frequency domain.

Time Domain

Most of the signals are initially obtained as a series of digital values representing proximity, velocity, or acceleration in the time domain. Time-domain feature extraction includes four main categories: statistical parameters, time-synchronous averaged signal-based methods, filter-based methods, and stochastic/advanced methods[59], which is shown in Figure 2.17.

The use of statistical parameters is one of the common digital signal processing
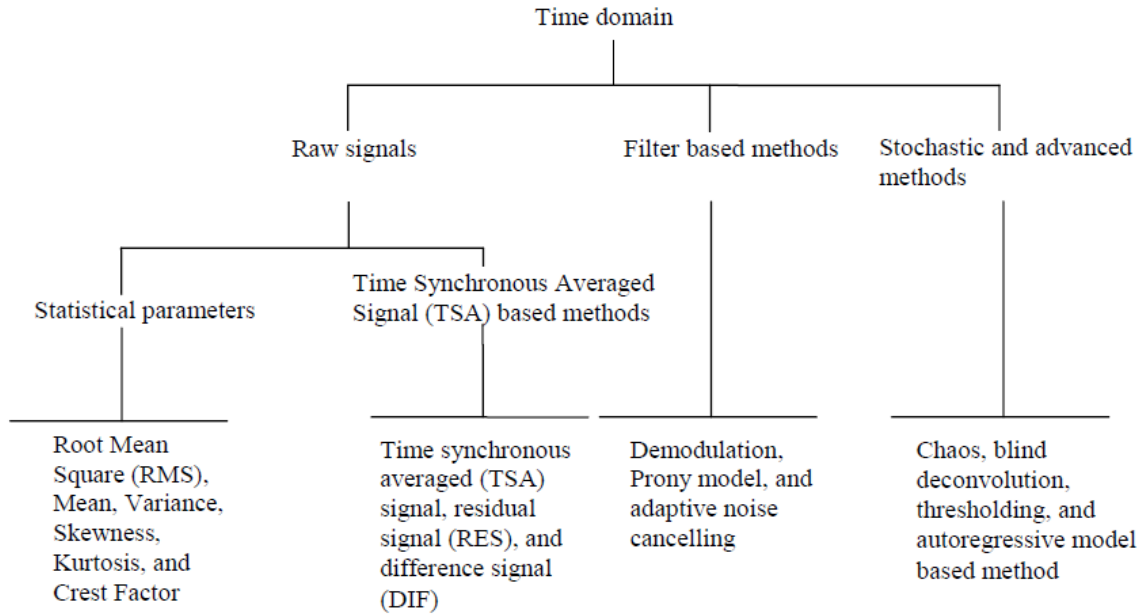
Figure 2.17: Overview of Time-Domain Vibration Feature Extraction Techniques[59]

techniques in the time domain. Statistical parameters include Root Mean Square (RMS), Mean, Variance, Skewness, Kurtosis, and crest factor. RMS is a time analysis feature that measures the power content in the vibration signals and a basic approach that can manage to measure defects in rotating machinery but often not sensitive to detecting incipient faults. Mean, Variance, Skewness and Kurtosis are the four statistical moments of distributions (such as non-Gaussian distribution and cumulative density distribution) to simplify vibration analysis. Kurtosis measures the relative peakedness or flatness of the distribution and can be used as an indicator of major peaks in a data segment. The crest factor is the ratio of peak level to the RMS level of the input signal. Because of the high sensitivity to the signal peak, the crest factor can be used to detect the signal pattern change due to impulse vibration sources, e.g., tooth breakage on the gear and defect on the outer race of a bearing[59]. The expressions of statistical parameters along with other statistical features are summarized in Appendix B.

The second approach for the time domain is time-synchronous averaging-based methods consisting of time-synchronous average (TSA) signal, residual signal (RES)

and difference signal (DIFS). TSA is defined as a periodicity feature of the vibration signal[61]. TSA signal is obtained by time-synchronous averaging of the initial data and reducing redundant noise by removing any periodic events that are not synchronous with the specific sampling frequency[61]. RES is defined as the signal that results from subtracting the TSA from the synchronized vibration signal, i.e., RES consists of the time-synchronous averaged signal with the primary meshing and shaft components along with their harmonics removed. DIFS is defined as the signal that results from removing the regular meshing, i.e., shaft frequency and harmonics, primary frequency and harmonics, from TSA signals[59].

The third technique for the time domain is filter-based methods including demodulation, Prony model and adaptive noise cancellation (ANC). These techniques mainly focus on the noise removal and signal to isolate from raw signals. The demodulation process is the inverse of the modulation process and can be categorized into amplitude and phase demodulation. The amplitude demodulation, also known as high-frequency resonance, resonance demodulation or envelop analysis, separates low-level frequency from high-frequency background noise[62]. The Prony analysis estimates the model parameters (e.g., amplitude, frequency, damping, and phase shift) by fitting the summation of the damped sinusoidal components to the equally spaced sample. This technique can be utilized in fault diagnosis and original data recovery[61]. An adaptive filter can effectively model the relationship between two signals in an iterative active manner. Based on that characteristic, ANC can especially remove the background noise from time wave[61].

The last technique for analyzing the time series signals is stochastic methods such as chaos, blind deconvolution, and thresholding. Blind source separation (BSS), also known as blind deconvolution, is a signal processing technique that removes the unobserved signals from a set of observations of numerous signal combinations[63]. This technique is effective in some cases where there is a lack of knowledge about the different combinations of signals received by each sensor[61].

Frequency Domain

Similar to the time domain, the frequency domain is another approach to understand a machine's condition with received signals. In the frequency domain, each sine wave will be presented as a spectral component, which is shown in Figure 2.18. Frequency
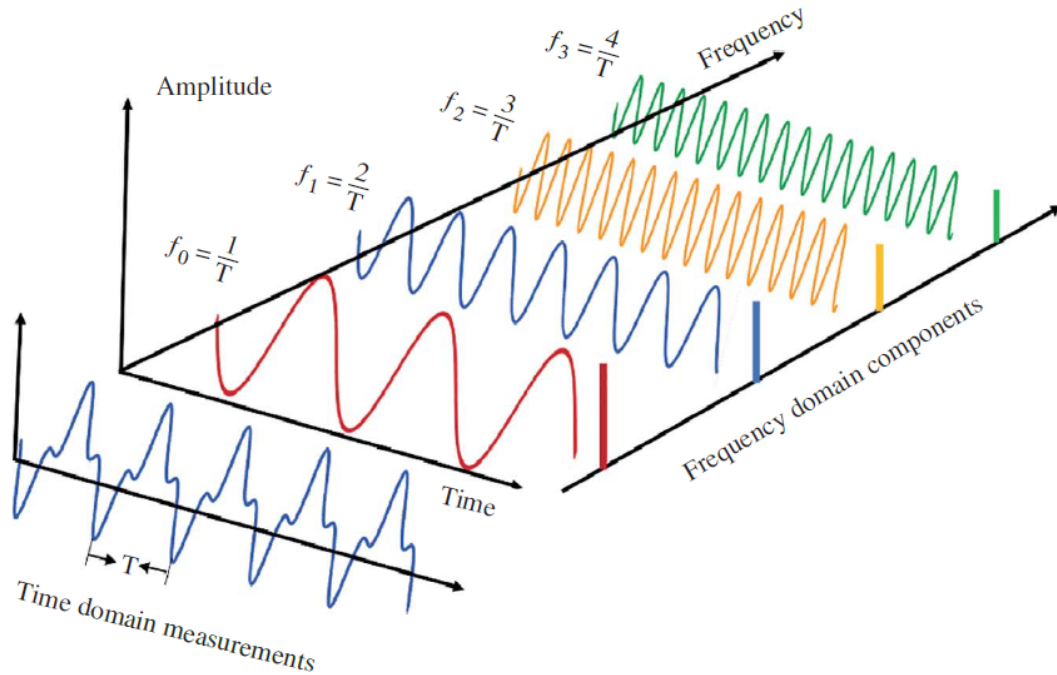
Figure 2.18: Signals on Time Domain and Frequency Domain[64]

domain analysis can extract information based on the frequency characteristics that may not be easily observed in the time domain. In reality, each component on the machine can produce a certain frequency. However, those produced frequencies cannot be seen individually in the measured signal since what is seen is the summation of those signals that sensors measured. Thanks to the frequency domain analysis, the spectrum of the frequency components from the time domain waveforms makes it easier to observe each source of vibration[61].

Fourier analysis, also known as harmonic analysis, is the decomposition of the series into a summation of sinusoidal components, where each sinusoid has a specific amplitude and phase[61]. The Fourier analysis is based on the Fourier Transform (FT)

which can transform a time-series signal from time-domain to frequency domain. The FT can be expressed as:

$$X(\omega) = \int_{-\infty}^{\infty} x(t)e^{-i\omega t}dt \tag{2.9}$$

Fast Fourier transform (FFT) is an efficient algorithm computing the Discrete Fourier transform (DFT) and its inverse for a stationary time series signal with a significant complexity reduction[61]. FFT can reveal the fundamental and harmonic frequencies existing in a signal. Therefore, the failure modes with distinctive repetitive frequencies or the faults that change the frequencies of the normal signal can be identified[2]. There are mainly two techniques including power spectrum analysis and frequency domain statistical features that can extract various frequencies spectrum features representing a machine's condition.

Power spectrum analysis is commonly defined as the Fourier transform of the auto-correlation function[65]. The discrete notion of the power spectrum equation is expressed as:

$$PS(f) = \sum_{n=0}^{N-1} r_{xx}[n]e^{-i2pnfT_s} \quad P = 1, 2, 3 \ldots \tag{2.10}$$

where $r_{xx}[n]$ is the auto-correlation function. Unlike the Fourier transform, the power spectrum does not have phase information, it can then be applied to situations where phase is not considered useful[65]. A common approach to evaluating the power spectrum is called *spectral averaging*. Averaging is achieved by dividing the waveform into a number of possible overlapping segments and calculating the energy density on each of these segments. The final power spectrum is constructed from the ensemble average of the power spectra from each segment[65]. The segmentation in spectral averaging is shown in Figure 2.19.

The second approach to analyze the frequency spectrum information is to use frequency spectrum statistical features. Similar to the amplitude or phase features in the time domain, these frequency spectrum statistical features allow a quick overview of a machine's condition without specific diagnostic capabilities[66]. Common frequency
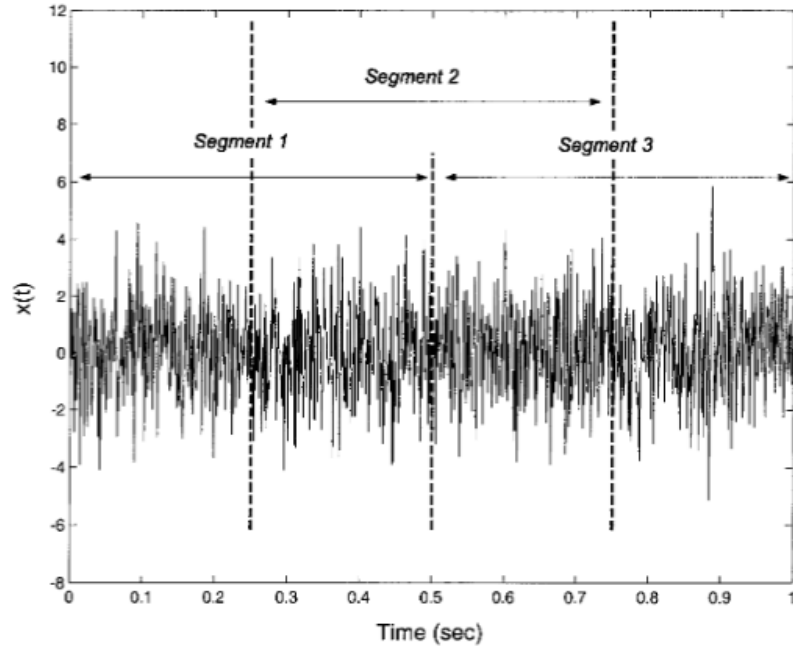
Figure 2.19: Example of Segmentation in Spectral Averaging[65]

spectrum statistical features are summarized in Appendix C.

Time-Frequency Domain

As mentioned above, the Fourier transform provides an effective transformation of a signal from the time domain to the frequency domain. In some cases, valuable time-series information of the spectral components is included in the phase characteristic of the Fourier transform, which is not easy to be used in the frequency domain[61]. Moreover, the Fourier transform is conducted based on the assumption that the signal is stationary; however, most analyses of rotating machines are based on investigating the vibrations during a speed sweep, i.e., machines are either speed up from low to high RPM or slowed down from high to low RPM[64]. This results in non-stationary signals that traditional Fourier transform is not suitable anymore.

On the contrary, the time-frequency domain can be applied to the non-stationary waveform signals, which are very common in failure modes[61]. The time-frequency features of the time-indexed series signals can be extracted through several time-frequency analysis techniques including short-time Fourier transform (STFT), wavelet

37

transform (WT), Hilbert-Huang transform (HHT), empirical mode decomposition (EMD), local mean decomposition (LMD).

Short-time Fourier transform as one of common time-frequency domain analysis can analyze non-stationary signals when compared with the original Fourier transform. STFT is expressed using the following equation:

$$X(\tau, \omega) = \int_{-\infty}^{\infty} x(t)\omega(t - \tau)e^{-i\omega t}dt \tag{2.11}$$

where $x(t)$ is the time-domain vibration signal, τ is the time variable and $\omega(\tau)$ is a window function, commonly a Hann window or Gaussian window centred around zero. Reducing window size can improve accuracy with respect to time resolution, which can also lead to increased computing time. To increase the frequency resolution, a larger time interval is required, but it will invalidate the stationary assumption. The window size is fixed the whole time and has to be chosen in advance. Recent studies have shown that STFT is an effective method for condition monitoring including failure modes classification[67], life cycle estimation[68], and fault feature extraction[69].

Wavelet analysis is another important approach in time-frequency domain analysis, which decomposes the signal based on a family of 'wavelets'[61]. Similar to the window in STFT, the wavelet families have fixed shapes, i.e., Haar, Daubechies, Morlets, etc; the wavelet function is scalable allowing the wavelet transformation to be adaptable to a wide range of frequency and time resolutions. The mother wavelet function can be calculated through the following equation:

$$\psi_{s,\tau}(t) = \frac{1}{\sqrt{s}}\psi\left(\frac{t - \tau}{s}\right) \tag{2.12}$$

where s, τ and t represent the scaling parameter, transformation parameter and time respectively. The wavelet transform is an extension of the Fourier transform, which maps the original signal from the time domain to the time-frequency domain. The wavelet functions transformed from the mother wavelet have the same shape but the different dimensions and places as the mother wavelet[61]. There are three common

transforms in wavelet analysis including the continuous wavelet transform (CWT), discrete wavelet transform (DWT), and wavelet packet transform (WPT)[70].

The next common technique for the time-frequency domain analysis is *Hilbert-Huang transform*. Unlike other time-frequency methods mentioned that use a predetermined structure either through time or frequency[2], HHT is a self-adaptive technique that can extract the instantaneous frequency of non-stationary and nonlinear time-series[71]. The three important terms including empirical mode decomposition, intrinsic mode function and Hilbert spectrum analysis need to be discussed in advance in order to have a better understanding of HHT.

After reviewing the condition monitoring and fault detection literature for common failures in mining equipment, many studies have conducted experiments on a simplified linear model such as slider-crank mechanism but none has created a scaled version of shovel model for machinery diagnostics. As reviewing the literature in the area of similitude theory, a reduced-scale model under similarity conditions can accurately predict the behaviour of the full-size machine. Developing a scaled model with inherent time-varying mechanisms similar to full-size shovel and a platform for condition monitoring can provide more trustworthy and valuable results prior to the field implementation.

Chapter 3

Methodology

Industrial machines are usually operating under either stationary or non-stationary conditions. The stationary condition is used to describe the constant state of loading and invariable rotating speed[2]. The classical equipment operated under the stationary condition includes the conveyor belt mechanism and heat pipe[72]. These machines' behaviours and performance can be easily monitored to detect any anomaly in the normal state due to a change of condition, i.e., the presence of faults[2, 72]. Hence, the maintenance of such machines is relatively easy and the high-cost of unplanned downtime can be minimized or even avoided[2]. Machines under non-stationary conditions, on the other hand, are relatively harder to monitor since they are generally operated in a time-varying manner and undergo changes including external loading and rotational speeds[73, 74]. Due to the difficulties in condition monitoring, the maintenance system on those machines are relatively complex, and often experience high-cost unplanned shutdowns[7, 8]. Typical industrial equipment working under non-stationary conditions includes earthmoving machines[6].

In the mining industry, a great number of phenomenon earthmoving machines encounter unplanned breakdowns which can cause high-cost maintenance and delays in production. As mentioned in section 2.2.1, most unplanned maintenance can be prevented by proper condition monitoring and incipient faults detection[36, 37]. To overcome current industrial challenges, this experiment proposes a solution to detect

common faults in mining electric cable shovels.

3.1 Research Roadmap

A lab-scale cable shovel model is designed and fabricated which has three functions: swing, hoist and crowd. According to the actual cable shovel operation modes, the cable shovel model is programmed to simulate the working cycle: the processes of digging and dumping. For the condition monitoring of the equipment, vibration monitoring and analytical techniques are proposed which have the ability to detect and classify common faults of cable shovels.

The research road map and steps are summarized in Figure 3.1. These steps can be broken into four major phases: a preliminary study, experiment platform design, experiments, and data analysis and processing for fault detection. In the preliminary study, assumptions and constraints are determined. The lab-scale shovel will be designed with three basic mining shovel's functions which are crowd, hoist and swing. The dynamics and kinematics of cable shovel will be studied. Meanwhile, as for condition monitoring, common failure modes of cable shovels along with digital signal processing techniques for vibration analysis are studied. Besides, finite element analysis for common faults is carried out in Solidworks shown in Appendix D.

Findings from the preliminary study provide a foundation for the development of the equipment setup. Parts could be modified based on the results from the model simulation from the preliminary study. Components will either be purchased online or machined in the machine shop in the Department of Mechanical Engineering at the University of Alberta. Meanwhile, failure modes will be determined and manufactured. A data acquisition system for vibration analysis is configured.

Based on the industrial cable shovel's working process, a PLC algorithm is developed and implemented. Before seeding the artificial faults, a validation of the physical modelling of the shovel model needs to be conducted. Fault detection experiments are performed by creating a fault-free baseline first and then injecting selected faults
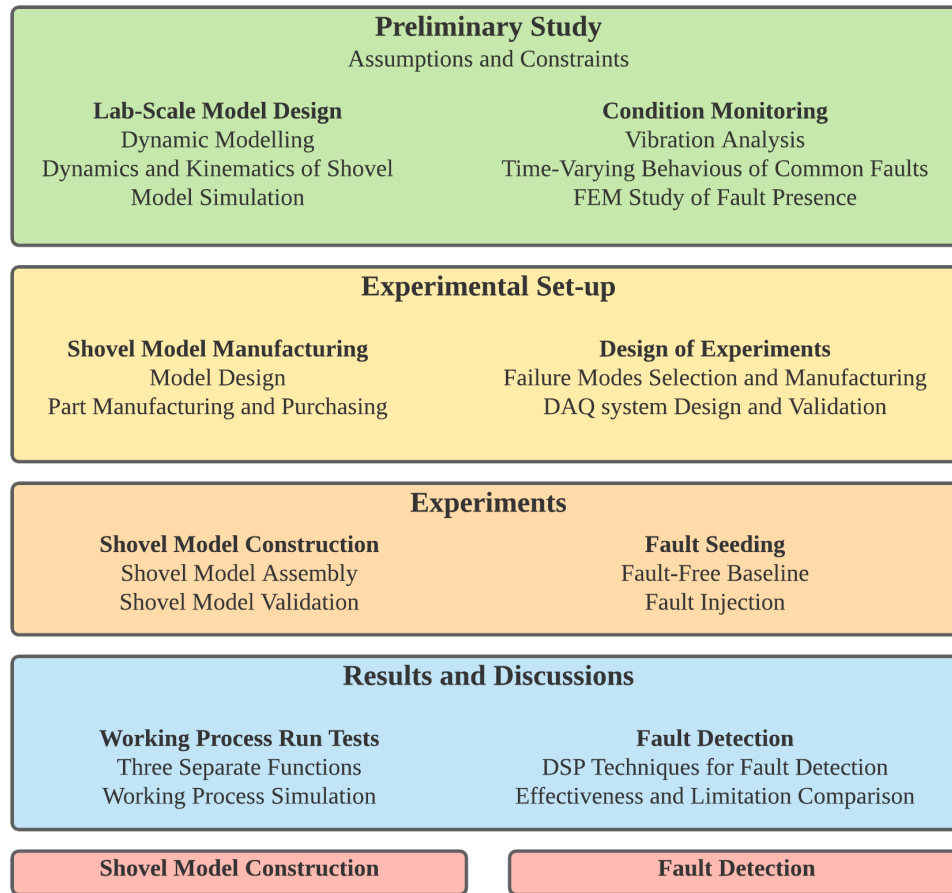
Figure 3.1: Research Roadmap for Lab-Scale Cable Shovel Modelling and Fault Detection

separately. During the iterative operation, vibration-based condition monitoring is adopted. Various signal processing techniques will be utilized to analyze vibration signals and their effectiveness and limitations will be discussed and compared.

3.2 Experimental Platform Design

The experimental platform or cable shovel model was designed to simulate the mining cable shovel's operation process. There were various objectives that shaped the design criteria. The cable shovel model is required to:

- Have three main functions that commonly used in the actual shovel's work

process: hoist, crowd and swing;

- Produce the main systems that have identical or similar working mechanism as the industrial cable shovels do;

- Produce a time-varying behaviour;

- Provide potential for faults seeding and transducers and sensors' implementation.

Accordingly, the designed cable shovel model has three basic functions including crowd, hoist and swing. A study has been conducted to understand the structure and kinetics and dynamics of actual cable shovel by numerous field visits and literature reviews. Each main function has a similar structure and kinematics and dynamics when compared to the real cable shovels. A PLC algorithm has been developed to control the servo motors for those main functions to realize a common operation process. The shovel model has been scaled down for lab use but still has enough space to install transducers and sensors.

3.3   Equipment Monitoring

Since shovels play an essential role in surface mining, it is crucial to have the capability to monitor the health of mining equipment. Vibration analysis is one of the most effective methods for condition-monitoring on machines, which focus on the situation that defects in a machine change the normal vibration signature which then can be considered as an indicator of the fault. Fault detection analysis usually needs help from signal processing techniques as mentioned in section 2.3.2. Digital signal processing techniques can be grouped into three categories: time domain, frequency domain and time-frequency domain. In order to collect the vibration level of the part that is of interest, the accelerometer is introduced which will be discussed in detail in section 5.1.

To investigate the condition monitoring of the equipment, the following methodology is adopted:

1. *Failure modes*: there are various types of mechanical failures that occurred in mining shovels such as unbalance, gear defects, bent shafts and etc. Common failure modes in mining shovels are selected;

2. *Sensor Location*: after the selection of the failure modes, the type of the sensor, the sensor's installation location and installation method should be decided. At the chosen sensor location, an accelerometer can reveal the vibration level of the components or subsystems;

3. *Healthy State Development*: vibration signals were collected during the free motion of the shovel under fault-free conditions to develop a baseline for the healthy state of the components or subsystems;

4. *Faulty State Development*: the selected failure modes were seeded separately. Vibration signals were collected to develop the faulty state for the components or subsystems under each failure mode;

5. *Fault Detection*: fault detection analysis was conducted by comparing the data under healthy and faulty states using various signal processing techniques.

For the failure modes selection, according to past literature and field investigation, looseness is a common failure in mining equipment. In this research, two types of looseness were analyzed: bolt looseness and shaft wear looseness. Moreover, shaft wear looseness can also lead to gear misalignment although it has a minor effect compared to shaft wear looseness. Fault modes will be discussed more in section 5.2. Various signal processing techniques including time, frequency and time-frequency domains were applied to evaluate the changes in the signal caused by the presence of a fault. The effectiveness of those techniques will be discussed in Chapter 5.

Chapter 4

Cable Shovel Model Construction

With the full understanding of earth-moving machines working condition, mining shovels can be well maintained and pushed to the limit of their capabilities. The best way to understand shovel performance and fault characteristics is to run tests on an operating shovel; however, taking into account the cost of these experiments and the challenge in doing repeat tests in the field, performing experiments on a full size shovel is not practical.[24]. In order to overcome the cost of and inconvenience of the testing on the actual cable shovel, a lab-scale shovel model can be created. The scaled-size cable shovel can successfully avoid the challenges from the actual size machines mentioned above as long as the relationship or similarity interaction can be validated between the full-size machine and the scaled model. In other words, if it can be shown that the performance of the scaled cable shovel is the same as the full-size shovel, then it can be concluded that the behaviour and conditions of the scaled cable shovel testing in the lab would be similar to the cable shovels in the field[24].

This chapter is structured as follows. Before designing a lab-scale shovel model, a comprehensive knowledge of physical modelling methodology and a full-size cable shovel structure is necessary. This chapter first introduces the benefits of physical modelling. After that, fundamental cable shovel structures and a complete digging phase are studied. It is then followed by a comprehensive explanation of shovel model structure design. Following a complete design of the shovel model, a validation of the

physical model is conducted. Last but not least, in order to create a model with time-varying behavior, a reliable control system is designed by using common industrial control technology.

4.1 Advantages of Physical Modelling

Scaled modelling not only can make the experiments convenient and cost-effective, but it can also be applied to various applications. One of the primary values of physical modelling is that the elements that need to analyze can only be considered; in other words, it is not necessary to model all aspects of the full-size machine but just need to keep the focus on those which are important for the analysis[25]. The advantages of physical modelling are summarized as follows[25]:

1. Predict the working performance of the phenomenon;

2. Provide an appreciation of the nature, magnitude, and effort of the physical parameters in the system;

3. Provide a solution to predict the performance of the digging equipment if the analytical relation is not found;

4. Provide cost-efficient experiments compared to full-size testing;

5. Can have repeat tests in a controlled environment;

6. Avoid material variability challenge in the field;

7. Minimize the problems associated with operator practice in the field;

8. Concentrate on the parameters that need to be investigated and omit unnecessary data associated with field data.

From the summary mentioned above, it can be seen that various benefits come with physical modelling. In order to have a good knowledge of cable shovel and fault

detection techniques, creating a scaled shovel is an effective approach to achieve the goals.

4.2 Full-Size Cable Shovel Structure and Functions Studies

Cable shovels are designed for excavating and loading materials in the surface mining operations. Figure 4.1 illustrates the common mining cable shovels structure. The
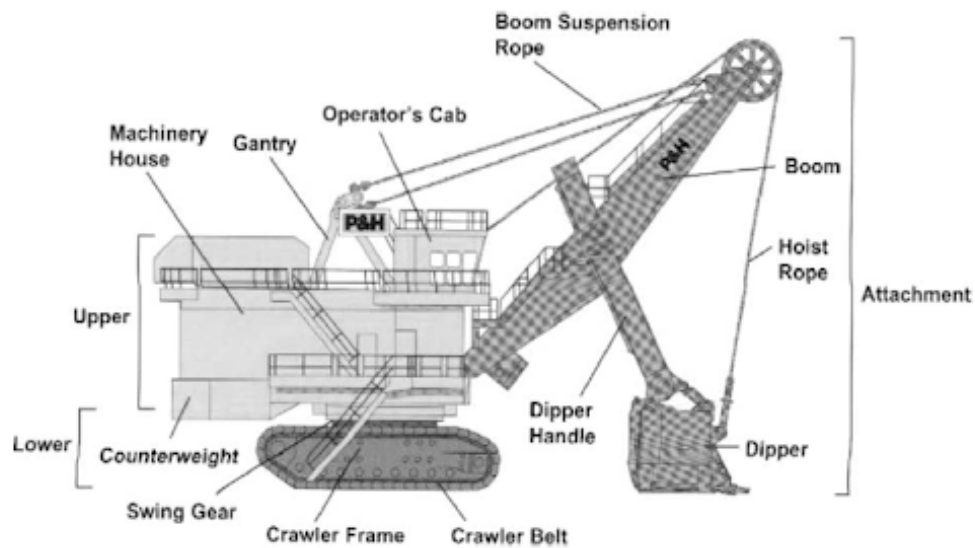
Figure 4.1: Cable Shovel Structure[75]

cable shovel consists of three major assemblies including the lower body, the upper body and the front-end attachment. The lower body provides a stable base for the shovel and includes the propelling system and the swing gear. The propelling system consists of a pair of propelling motors, crawler frames and crawler belts. The upper body provides a platform for the machinery house, electric room, gantry, operator's cabin, swing motor and transmission, hoist system, etc. The deck plan of the common cable shovel is illustrated in Figure 4.2.

The gantry is attached to the upper body and used for holding the boom by using the boom suspension rope. The hoist system mainly consists of hoist motors, drum
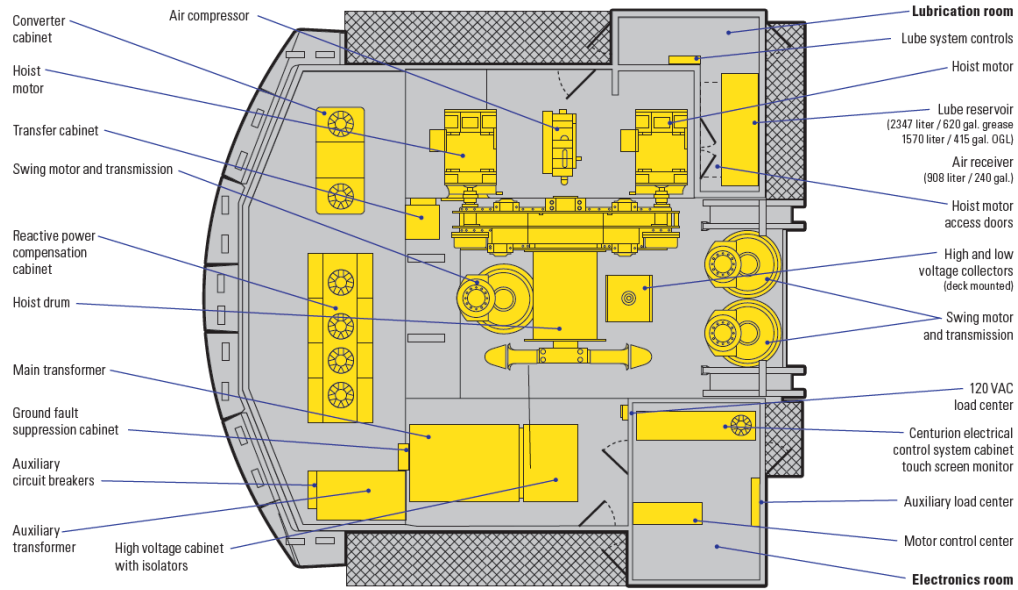
Figure 4.2: P&H 4100 Machinery Desk Plan[76]

and hoist rope. The upper assembly is the roller and center pin mounted on the lower part. The front-end attachment is usually utilized in the digging process. The attachment consists of the boom, crowd motor and transmission, dipper handle and dipper.

The primary dynamic functions for cable shovels include propel, swing, crowd and hoist. The propel system can assist the shovel to crawl steadily from one digging site to another on a rough condition road. Swing motor powers the swing transmission that in turn drives the swing pinion which is meshed with the swing gear. Multiple swing motors and transmissions are commonly used to rotate the upper body from digging face to haulage trucks. Crowd motor drives the crowd pinion engaged with a dipper handle. The reversible electric crowd motor allows the dipper handle to push the dipper forward and also retract the dipper. The rotating hoist drum can extend and pull back the hoist ropes connecting to the dipper. Two hoist motors are typically employed to elevate and lower the dipper. The digging process is accomplished when the dipper handle is crowded and the dipper is lifted through the digging face. A complete digging phase is illustrated in Figure 4.3.
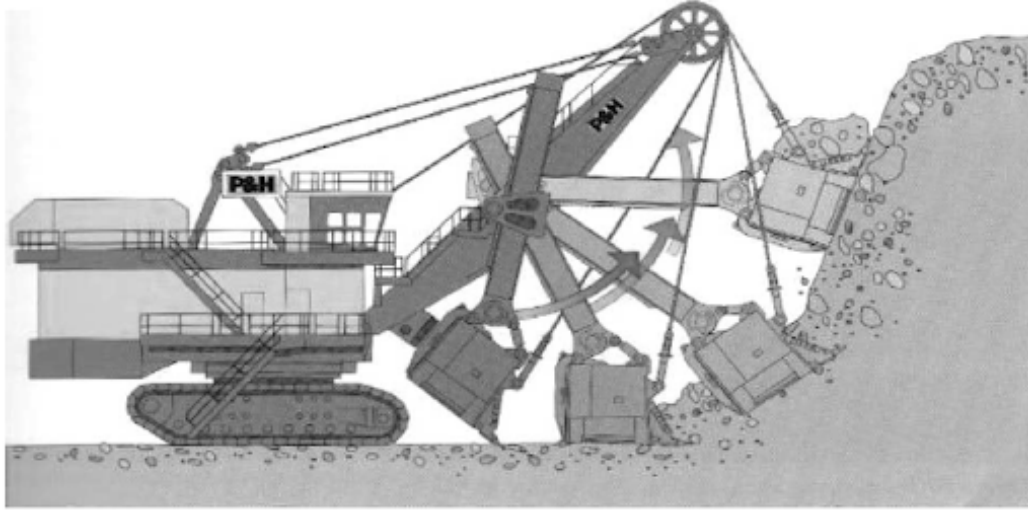
Figure 4.3: Complete Digging Phase of a Cable Shovel[75]

4.3 Shovel Model Structure Design

The lab-scale shovel model replicates the three basic dynamic motions including swing, hoist and crowd of a commercial cable shovel, scaled down by a factor of 15. This choice was based on important considerations: optimum size for laboratory experiments, time and control over material preparations, economics and machining capability[25]. The scaled-down factor provides a baseline for the similarity analysis of the shovel model; in this research, two aspects of similarities are considered: geometric similarity and physical similarity which are studied in section 2.1.4. For the structure design of the shovel model, the geometric similarity is taken into account; in other words, the geometric dimension of the full-size shovel will be linearly scaled down by around 15 (to shrink the size to 15 is optimal but due to the limitation of the machine tools, manufacturing process and parts quantity in stock, the actual scaled-down factor deviates). The physical similarity decides the motor selection and control, which will be discussed in section 4.4. According to the geometric similarity, an overview view of the shovel model with overall dimension is shown in Figure 4.4. An annotated side view of the shovel model is presented in Figure 4.5 illustrating the basic structures and functions of the shovel model. The four fundamental struc-
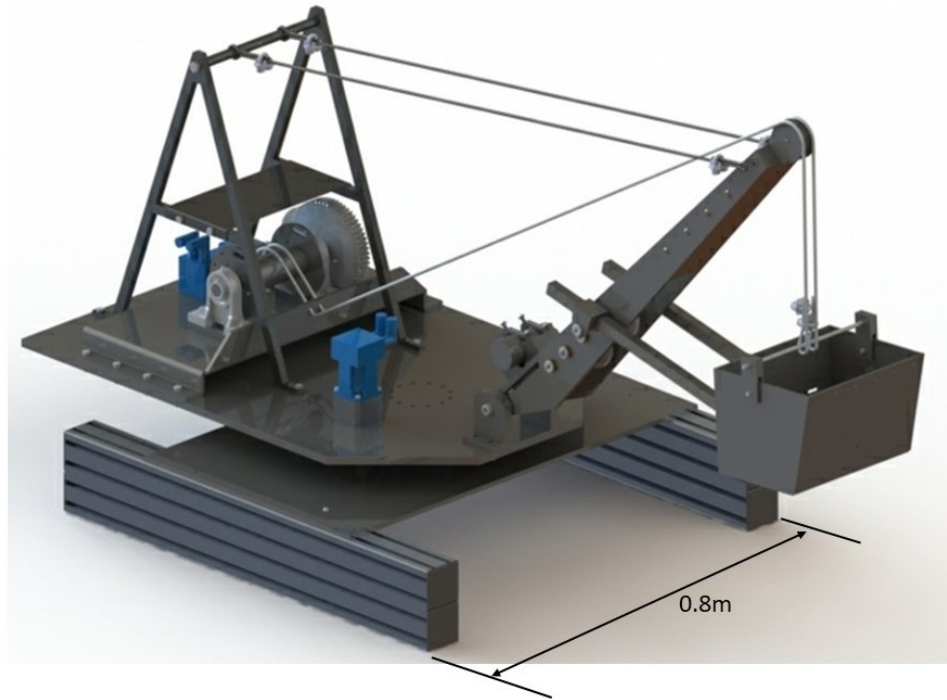
(a)
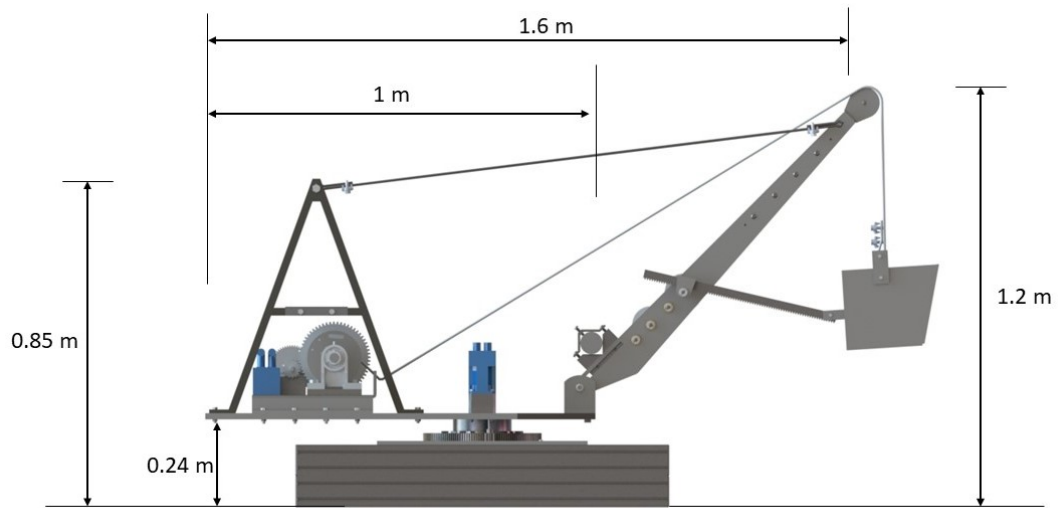
(b)

Figure 4.4: Overview of Lab-Scale Cable Shovel Model

tures in the cable shovel modelling including gantry assembly, swing, hoist and crowd systems will be described.
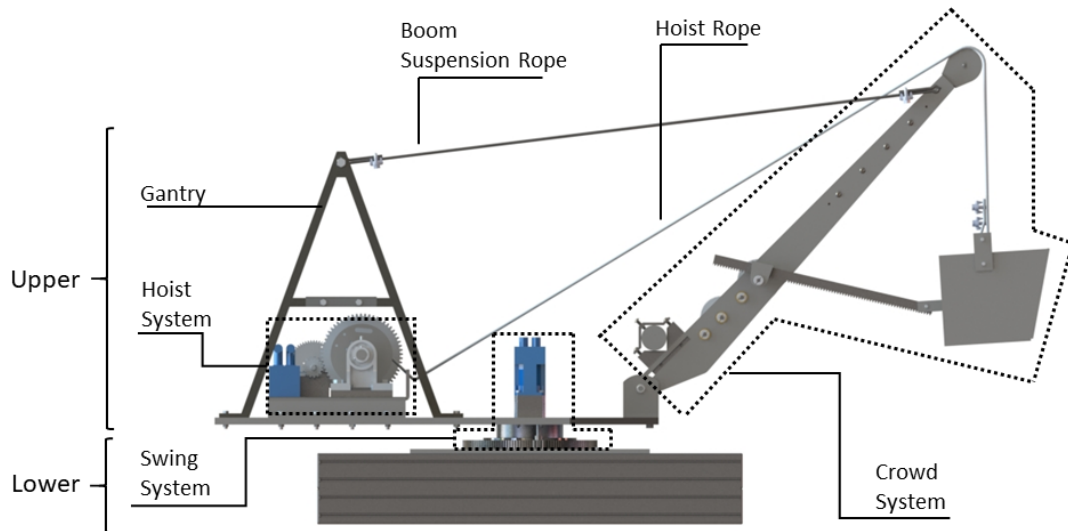
Figure 4.5: Annotated Side View of Cable Shovel Model

4.3.1 Gantry Assembly

It can be seen from Figure 4.6 that the gantry assembly consists of gentry frames, an instrument tray and a gantry crossbeam. The gantry provides a steady platform to support the boom component. The gantry frames are fastened on the top plate and held by an instrument tray and a crossbeam. One end of the gantry ropes is twined around the grooves on the crossbeam and the other end is tied on the hooks bolted at the tip the boom.

4.3.2 Lower Body Assembly

The lower body of the physical modelling provides a base and platform for the rotation from the digging face to the dumping location. The lower works are attached to the top plate with the inside ring of the roller bearing and a spacer. The outside ring of the roller bearing is bolted to the base plate. A 150-tooth swing gear is fixed on the base plate and is meshed with a 12-tooth gear pinion driven by a servo motor mounted on the top plate. Since the propel motion is not considered, the crawlers are replaced with two 80 mm × 160 mm × 900 mm aluminum extrusions which not

51
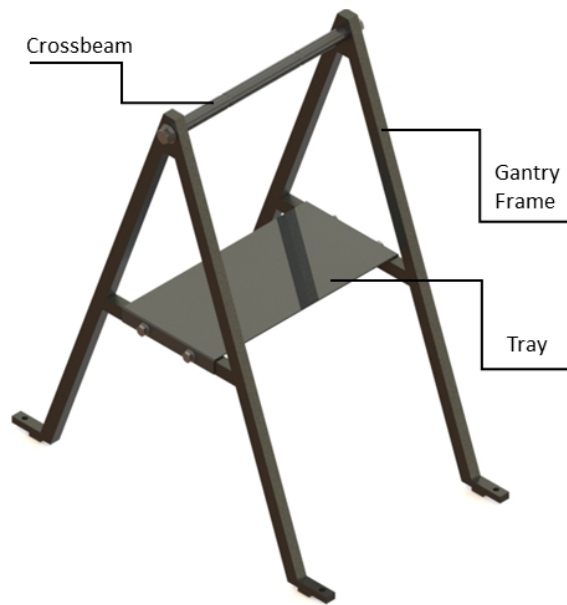
Figure 4.6: Annotated View of Gantry Assembly

only provide a solid base for the shovel model but also offer a potential for installing casters so that the model can be easily moved around. An annotated view of the lower works is shown in Figure 4.7.
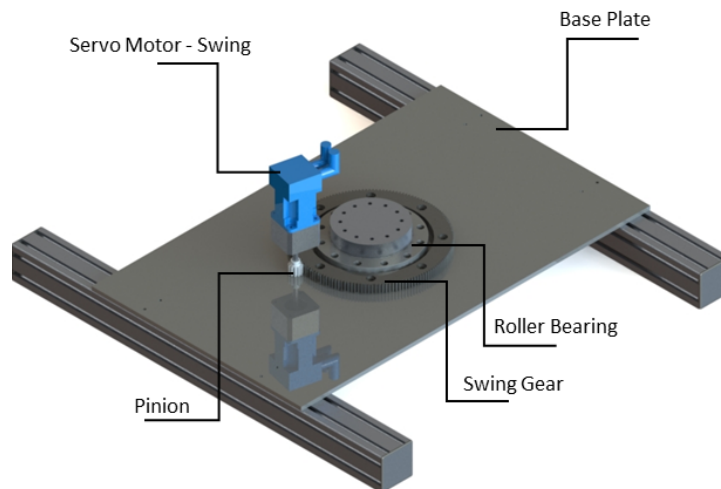
Figure 4.7: Annotated View of Lower Body Assembly

4.3.3 Hoist System Assembly

An annotated view of the hoist system is shown in Figure 4.8. The hoist components including the hoist servo motor, gear train and drum are all bolted on the hoist mount which is then fixed on the top plate. It was designed to separate the hoist system from the rest of the shovel for later assembly and maintenance. The hoist drum rotates to extend and retract the hoist ropes through the smooth rope guide embedded at the front of the hoist mount. The rope guide ensures the hoist ropes move along the crowd arm side planes.
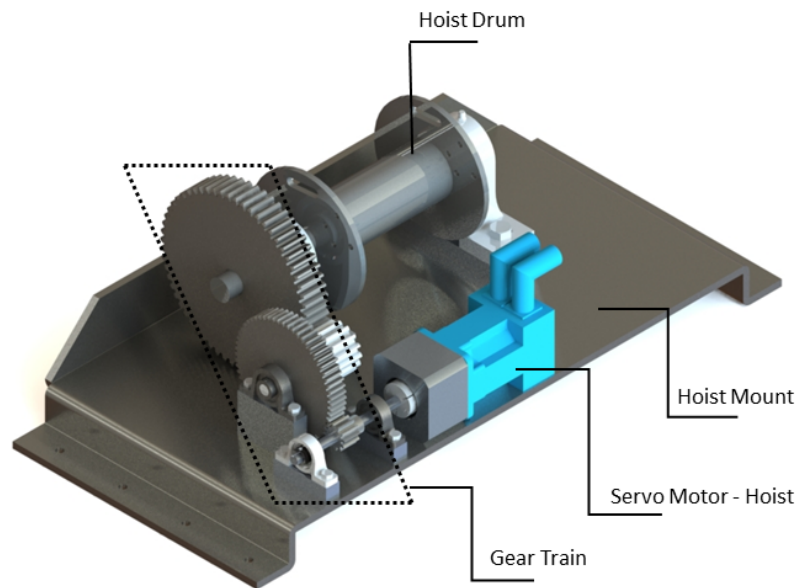
Figure 4.8: Annotated View of the Hoist System

4.3.4 Crowd System Assembly

As shown in Figure 4.9, the crowd system consists of components including boom mount, boom, crowd motor, motor mount, gear train, dipper handle, hoist pulley, suspension rope hook and bucket assembly. The boom mount is bolted on the top plate and crowd ropes connecting the crowd hook and gantry hold the boom at the desired angle. The dipper handle is modified from a gear rack meshed with a gear

pinion driven by a crowd motor. The crowd motor is selected by using similarity analysis with scale factor of 15 and a detailed analysis regarding the motor power required and motor selection can be found in section 4.4.1. The dipper crowd mount (shown in Figure 4.10) is attached with the dipper handle and the bucket can freely rotate around the dipper mount shaft. Hoist ropes connect the dipper rope interface and hoist drum via the hoist pulley bolted on the tip of the boom.
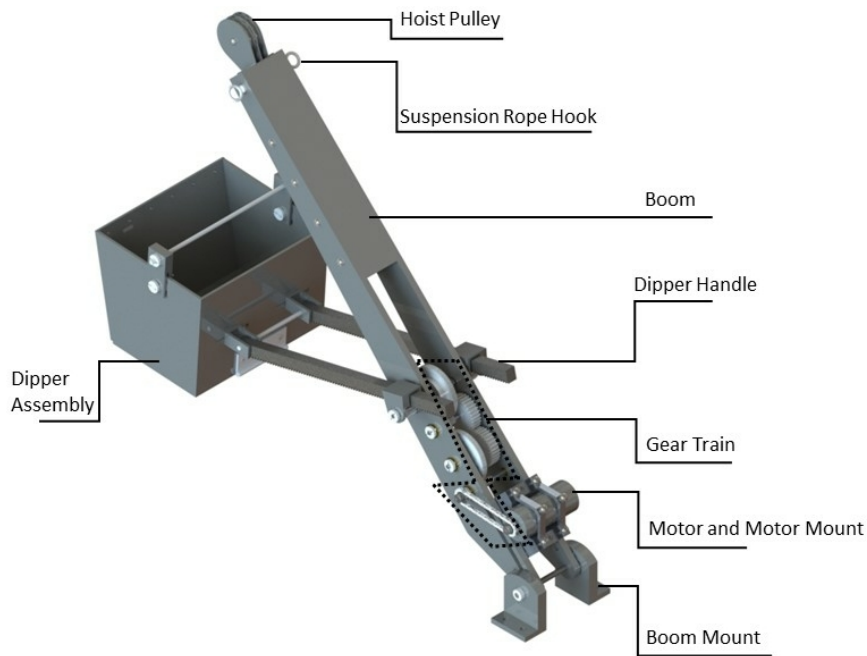
Figure 4.9: Annotated View of the Crowd System

Figure 4.10 presents the annotated view of the dipper assembly. The dipper assembly contains a dipper door, a spring hinge, two dipper crowd mounts, a dipper body and a dipper rope interface (dipper shaft and dipper clips). The dipper door open-close function is achieved manually by a spring door hinge and two hooks located at the dipper door and dipper body.

4.4 Similarity Analysis of Shovel Model

From previous sections, the advantages of physical modelling have been discussed. For this project, the lab-scale model is economical and applicable to laboratory experi-
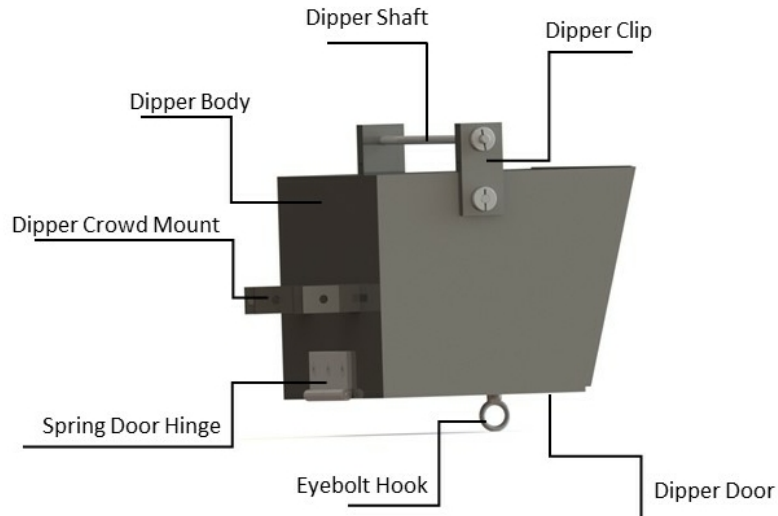
Figure 4.10: Annotated View of Dipper Assembly

ments. A 1 : 15 Komatsu P & H 4100XPC lab-scale cable shovel has been designed, which can simulate three motions including crowd, hoist and swing functions. Before conducting any experiments on the physical model it is necessary to validate the physical model, which is to prove that the model has similar working mechanisms and performance as the actual-size cable shovel. The data then can be used for other research such as fault detection after the lab-scale cable shovel has been validated otherwise the conclusion will not be convincing since the connection between the physical model and full-size cable shovel is not made. Similarity analysis and inertia considerations are considered next.

4.4.1 Similarity Analysis

As has been discussed in section 2.1.4, factional analysis is used to find as much as possible information about the problem whose complete and exact solutions cannot be found or is hard to find. Among various techniques for fractional analysis, similitude analysis is commonly used. It not only can simplify the complexity of the full-scale model but also provides a foundation to predict the behaviour of the full-size machine

from a reduced-scale model. The following parameters are derived for the similarity analysis based on the scale ratio $S = 15$ [25].

Scale Ratio = Prototype Length/Model Length =

$$\frac{l_p}{l_m} = S \tag{4.1}$$

Linear Velocity Ratio =

$$\frac{v_p}{v_m} = \frac{\frac{l_p}{S}}{\frac{l_m}{S}} = \frac{l_p}{l_m} = S \tag{4.2}$$

Rotational Speed Ratio =

$$\frac{\omega_p}{\omega_m} = \frac{v_p/R_p}{v_m/R_m} = \frac{v_p}{v_m} \cdot \frac{R_m}{R_p} = S \cdot \frac{R_m}{R_p} \tag{4.3}$$

Power Ratio =

$$\frac{P_p}{P_m} = \frac{F_p v_p}{F_m v_m} = \frac{(\rho_p V_p g) v_p}{(\rho_m V_m g) v_m} = \frac{\rho_p S^4}{\rho_m} \tag{4.4}$$

where l, v, P, F, ω, R and ρ represent the length, linear velocity, power, force rotational speed, rotation radius and density, respectively; and meanwhile, subscripts p and m represent full-size machine and reduced-scale model, respectively. Before conducting the similarity analysis, it is assumed that the densities of the material of the actual mining shovels and the shovel model are the same. Then the equations for the similarity analysis can be simplified as:

$$\text{Linear Velocity Ratio} = S \tag{4.5}$$

$$\text{Rotational Speed Ratio} = S \cdot \frac{Rm}{Rp} \tag{4.6}$$

$$\text{Power Ratio} = S^4 \tag{4.7}$$

The hoist, crowd and swing systems' velocities of P&H 4100XPC are estimated in Appendix E and the powers of the three systems are also provided[77]. According to the similarity analysis and information about the full-size shovel, the parameters of the shovel model are summarized in Table 4.1.

Table 4.1: Similarity Analysis for Shovel Model Parameters

Parameter	System	P&H 4100 XPC	Reduction Ratio	Shovel Model
Velocity	Hoist	$1.1m/s$	S	$0.073m/s$
	Crowd	$0.53m/s$		$0.035m/s$
	Swing	$1.5RPM$	$S \cdot \frac{Rm}{Rp}$	$2.11RPM$
Power	Hoist	$2300kW$	S^4	$0.045kW$
	Crowd	$545kW$		$0.011kW$
	Swing	$1091kW$		$0.022kW$

In order to satisfy the velocity requirements for the shovel model, the model motors need to be operated at 465 RPM, 1528 RPM and 168 RPM for hoist, crowd and swing systems, respectively. Motor speed calculation along with rotation radius for full-size shovel (R_m) and shovel model (R_p) are discussed in Appendix F. To achieve the necessary output power for three systems shown in Table 4.1, Beckhoff servo motors with rated output power at 0.15 kW were selected with a consideration of 80% to 90% efficiency for common servo motors[78].

4.4.2 Inertia Considerations

Motors are commonly used in common mechanical systems to achieve precise positioning, velocities and torques. To evaluate the motor's ability to effectively control the load, the ratio of the load inertia to the motor inertia plays an important role[79]. The inertia ratio can be expressed as:

$$\text{Inertia Ratio } = \frac{J_L}{J_M} \tag{4.8}$$

where J_L and J_M represent inertia of load reflected to motor and inertia of the motor, respectively. In this analysis, inertia is referred to as the mass moment of inertia and also known as rotational inertia. When designing a mechanical system, the goal is to achieve the inertia ratio of 1:1. It is not always achievable due to

cost-effectiveness, material requirements or component sizing. According to various applications, typical inertia ratio limit values (shown in Table 4.2) are recommended by Beckhoff which the motors and drives in this project were bought. Nowadays,

Table 4.2: Typical Inertia Ratio Limit Values from Beckhoff[80]

Application	Inertia Ratio Range
High-end Servo Drives for Maximum Accuracy	$0 < IR < 1$
Typical Servo Drives in Machining Equipment	$1 < IR < 3$
Controlling System with High Dynamics	$3 < IR < 10$
Simple applications without specific demands regarding the accuracy of positioning or dynamics	$IR > 10$

manufacturers providing servo motors with auto-tuning suggest keeping the inertia ratio under 50:1[81]. If the inertia ratio is too high, the motor cannot control the load properly which may lead to resonance and overshoot of the target parameters. If the inertia ratio is too low, it means that the motor is oversized resulting in unnecessary cost and energy consumption[79]. The inertia ratio analysis has been conducted for the crowd, hoist and swing systems and the inertia ratios are 3.0, 4.3 and 41.8, respectively. A detailed calculation of the inertia ratio for three systems is presented in Appendix G. According to the inertia ratios, motors can effectively control the dynamics of crowd and hoist systems; on the other hand, the inertia ratio of the swing system is quite large but also expected since those three systems have the motors with same specifications and the swing system requires to bear more loads (the entire upper body). Nevertheless, in this project, the accuracy of the dynamics of the swing system is not required to be high as long as the swing motion can be performed. In order to improve the inertia ratio for the swing system, the gear ratio or motor size should be increased as the dimensions of the components remain constant.

4.4.3 Validation of Shovel Model

The model was machined in the machine shop in the Department of Mechanical Engineering at University of Alberta. As for the geometric tolerances, angular dimension will deviate less than 0.5 degree and linear dimension is allowed to deviate less than 0.025 mm. The desired geometric scale was realized and physical similarity was examined by comparing desired speed and actual speed of three systems. Actual speeds were estimated using the same method as estimating the full-size shovel's speed. Take the crowd system for example, operated the crowd motor at 1528 RPM and lasted for 15 seconds, measured the crowding distance of the dipper, then the actual speed can be estimated by using the crowding distance over duration time. The same methods were applied to estimated hoist speed and swing angular speed. The comparison of desired and actual values of shovel model parameters is summarized in Table 4.3.

Table 4.3: Comparison of Desired/Actual Model Parameters

Parameter	Desired	Actual	Error
Geometry	$15:1$	$15:1$	0
Hoist Speed	$0.073m/s$	$0.07m/s$	-4.1%
Crowd Speed	$0.035m/s$	$0.034m/s$	-2.8%
Swing Speed	$2.1RPM$	$1.87RPM$	-10.9%

According to Table 4.3, it can be seen that the errors of hoist and crowd speeds are within 5%; meanwhile, the error of swing angular speed is around 10%. The error could come from the energy loss in gear transmission, servo motor drives control efficiency and human error. A slightly large error for the rotational speed could be caused by the high inertia ratio of the swing system. A high inertia ratio affects a motor's ability to achieve precise positioning and velocity. Errors of speed parameters can be decreased by applying grease to the gear train and optimizing inertia ratios. The similarity analysis and validation of the shovel model in this research is based

on the fact that the shovel model is in a good condition. Scaling of the interacting elements of the subsystem where faults are generated is not conducted. Similarity in fault modelling will provide insights into the dynamics of failure model validation which is discussed in section 6.2.1.

4.5   Control System

4.5.1   EtherCAT (Ethernet Control Automation Technology)

There are three basic motions in this shovel model: swinging, hoisting and crowding, which are actuated by three motors. There is no propel actuation. The motors are Beckhoff AX3031 with motor controllers that comply with the EtherCAT (Ethernet for Control Automation Technology) protocol. EtherCAT is a high-performance, low-cost and easy-to-use industrial Ethernet technology originally developed by Beckhoff Automation and EtherCAT protocol which is disclosed in the IEC standard IEC61158 is well suited for hard and soft real-time requirements in automation technologies, in test and measurement and many other applications[82].

Functional Principle of EtherCAT

The EtherCAT key functional principle lies in how its nodes process Ethernet frames: the EtherCAT master sends a signal (the EtherCAT equivalent of a packet) that passes through each node. Each node (EtherCAT slave device) reads the data addressed to it and writes its data back to the frame all while the frame is moving downstream[82, 83]. The EtherCAT master is the only node within a segment allowed to actively send an EtherCAT frame and all other nodes only forward the frames downstream. This principle avoids unpredictable delays and guarantees real-time capabilities[82]. The data transmission of the EtherCAT is illustrated in Figure 4.11.
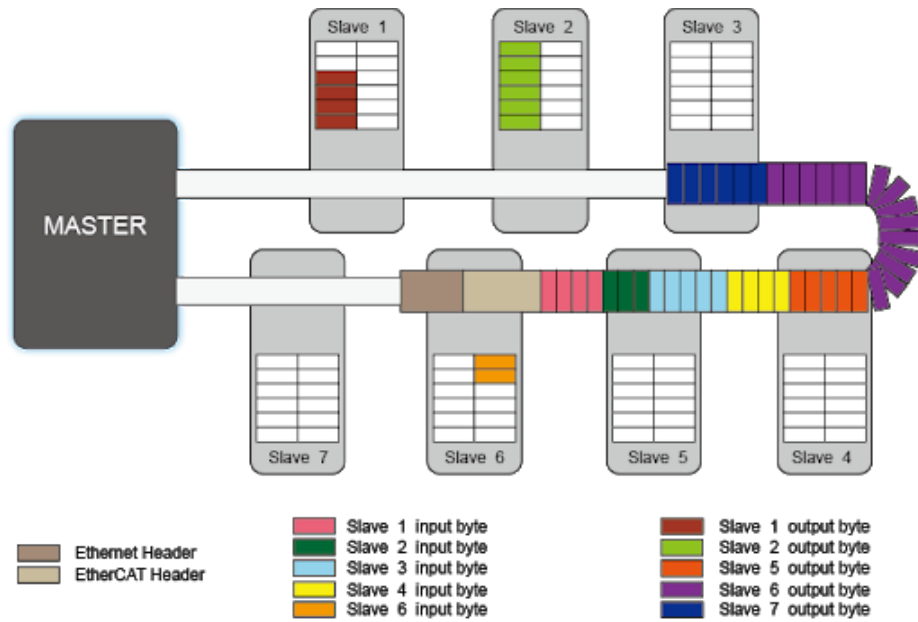
Figure 4.11: Functional Principe of EtherCAT[84]

Benefits of EtherCAT

Automation industries widely use EtherCAT technology because of various benefits which are summarized as follows[85, 86]:

- **Exceptional Performance:** EtherCAT is not only the fastest industrial Ethernet technology but it also synchronizes with nanosecond accuracy. This rapid reaction time is able to reduce the wait time during the data transmission, which can significantly improve the application efficiency;

- **Flexible Topology:** in conventional industrial Ethernet systems, there are limitations on how many switches and hubs can be cascaded, which limits the overall network topology. On the contrary, EtherCAT does not need hubs or switches, it is then virtually limitless when it comes to network topology;

- **Robustness and easy-to-use:** The network can detect potential disturbance down to the exact location, which will dramatically reduce the time needed to troubleshoot. During the startup, the network compares the planned and actual layouts to detect any discrepancies;

For those reasons, EtherCAT can be widely found in various applications such as robotics, machine tools, test benches, measurement systems, automated guided vehicles and so on[83–85].

4.5.2 EtherCAT Devices Configuration

EtherCAT technology makes the physical installation of Beckhoff devices easier. The basic CPU module (CX1020) is the core of the whole configuration, which is equipped with a 1 GHz Intel CPU and embedded Windows CE 6 operating system. A digital compact servo drive (AX5206) is connected to the CPU module with an Ethernet cable and also connected to the other servo drive through Ethernet cables. Servo drive 1 can actuate two servo motors (AM3031) which are for the crowd and hoist functions. Servo drive 2 controls the third Beckhoff servo motor that is used for the swing motion. An AC to DC power supply (TDK Lambda DDP240-24-1) can provide enough power to the system. In order to control the motion of servo motors, a PC with TwinCAT PLC software is required and connected to the CPU module with an Ethernet cable. The control signals move downstream from the EtherCAT master (PC and CPU module) to the EtherCAT slaves (servo motors) and also the master can receive the feedback from the slave's motions. The complete EtherCAT device configuration is illustrated in Figure 4.12.
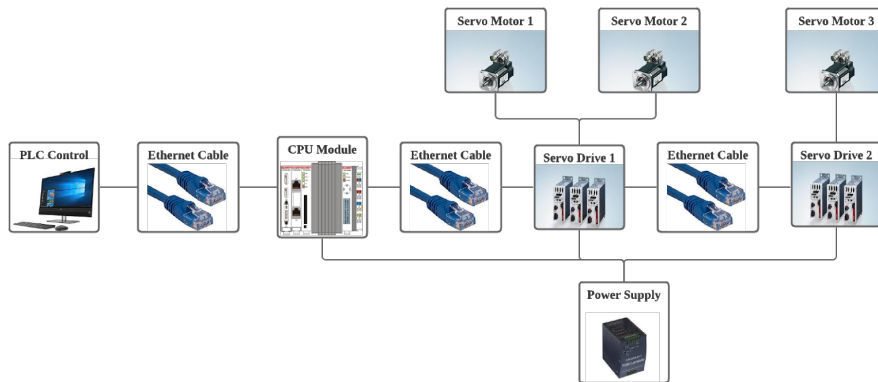
Figure 4.12: EtherCAT Device Configuration

4.5.3 Automation Control

The automation control was performed in *"TwinCAT PLC control"* software. To make the motor control procedure more user-friendly, a visualization interface was developed, which is shown in Figure 4.13. The interface consists of four categories that are motor status, manual control, iterative motion and complete work cycle motion.
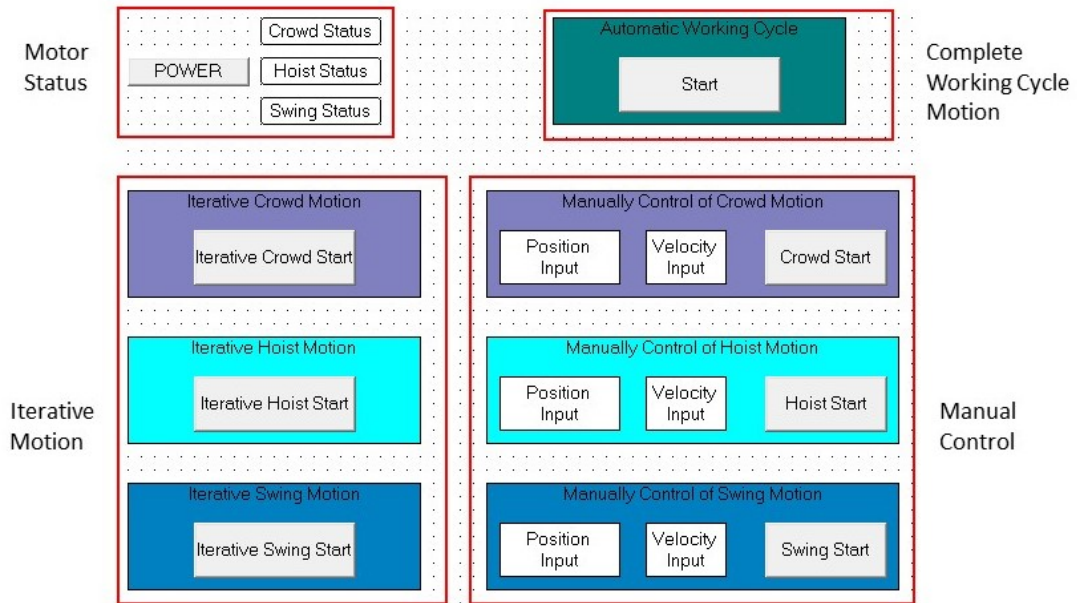
Figure 4.13: Motor Control Interface

Before controlling motors, it is important to check the conditions of motors which includes links between motors and PLC software, Etherent connection, and etc. Those can be checked automatically in the "Motor Status" category by simply clicking the POWER button. If the status for the motor turns to green, it means the motor is ready and vice versa. The POWER button can also be used for emergency situations and motor power off after the experiments.

The "Manual Control" category was created for testing of motors and model validation. Take the hoist motor for example, find the "manually control of hoist motion" square and click the "position input" and "velocity input". Then a number pad will

show up, enter the number that is of interest. Here, a positive number for the position input represents a motion that the dipper is moving up and vice versa. Velocity input is set to be a scalar variable, only magnitude of which will be considered. Once the selection of position and velocity is finished, hit the "hoist start" button. The procedure also works for the crowd and swing motions; as for the direction, a positive position input for the crowd motion is to extend the dipper and a positive position input for the swing motion is to make the shovel rotate clockwise.

The "Iterative Motion" category was developed for simulating an iterative motion for each system. As mentioned earlier, one of the primary values of physical modelling is that the elements that needed to be analyzed should only be considered. If the fault is seeded in a system, then only that system would be analyzed; in other words, the motion of that system would only be performed. The iterative mode for each system can keep the attention only on the system that is of interest and also make data analysis more efficient. The iterative mode for each system starts from the pre-digging position, which is shown in Figure E.2. As the iterative modes begin, the dipper will be hoisted up and then move down iteratively for the hoist motion, the dipper will extend and then extract iteratively for the crowd system and the shovel will rotate to the dumping point and back to the bank iteratively for the swing system. Lastly, the iterative mode of each system not only can work independently, but also work together, which is to say that, for example, the iterative mode of the crowd system can be initiated while the iterative mode of the hoist system is performing.

The last category, "automatic working cycle", can be considered as an "upgrade version" of the iteration mode. Compared to "Iterative Motion", the "automatic working cycle" collaborates three systems to perform a common working cycle of cable shovels by conducting the iterative modes in a "specified pattern". According to the similarity analysis and common work cycle of cable shovels, the "automatic working cycle" starts with the pre-digging position, the hoist motor and the crowd motor run at 465 RPM and 1528 RPM, respectively at the same time for 15 seconds

in order to finish the digging process and then the swing motors is initiated at 168 RPM for 5 seconds to reach the dumping location and then swing back to the bank with the same speed for another 5 seconds. This is the full cycle that the "automatic work cycle" simulates and the cycle will run iteratively until the POWER button is pressed.

4.6   Chapter Summary

The main motive for this chapter was to construct a lab-scale shovel model that has similar mechanical properties as real mining shovels do and also provides a platform for fault detection analysis. This chapter explains the construction of the lab-scale shovel model thoroughly with four categories: advantages of physical modelling, lab-scale model structure design, similarity analysis of the shovel model and motion control.

Creating a physical model has various advantages compared to the phenomenon which was discussed in section 4.1. First of all, constructing and testing the model is more cost-effective than using a real mining shovel. To meet the experiment requirements, the mining shovel has to pause the job to install the necessary equipment such as transducers or update software. Thus, testing real shovels directly may lead to a decreased availability which is unwanted for most companies. Second, it is more convenient to do experiments in a controlled environment. Compared to the common laboratory, the mining field environment is rough and unpredictable that could inconvenience and introduce unwanted factors into the research. Third, physical modelling is able to simplify the experiment that allows the researchers to focus on the aspects important for the analysis rather than the whole phenomenon.

Before creating a shovel model, it is essential to have knowledge about modern cable shovels' basic functions and structures. Section 4.2 used the Komatsu P&H 4100XPC cable shovel as an example to study the basic structures and mechanisms of each function that are utilized in the digging phase. With the preliminary studies

of real cable shovels, the construction of a lab-scale shovel model based on Komatsu P&H 4100XPC with a scale factor of 1:15 was explained in section 4.3. To meet the experimental requirements, three basic functions were modelled: crowd, hoist and swing. Four critical components or systems were discussed in section 4.3.1 - 4.3.4, which included gantry assembly, lower works, hoist system and crowd system assemblies.

With the completion of the shovel model construction, it is necessary to validate the model before doing any testing. Section 4.4.1 performed similitude analysis of the model regarding scale ratio, linear and rotational velocity ratios and power ratio. Besides, inertia effects discussed in section 4.4.2 have been taken into consideration. Lastly, section 4.4.3 conducted the validation process by comparing the desired and actual model parameters.

Section 4.5 gave a full description of the control system to realize the mobility of the shovel model. EtherCAT is a common and reliable automation control technology in various industries and section 4.5.1 explained the function principle and benefits of this control technology. EtherCAT devices including CPU module, servo drives and servo motors were configured to drive the hoist, crowd and swing motions, which were well discussed in section 4.5.2. Last but not least, the PLC motor control interface was explained in section 4.5.3. The visualization interface consisted of four parts: motor status, manual control, iterative motion for each system and automatic working cycle simulation.

Chapter 5

Condition Monitoring and Fault Detection

The ideal maintenance strategy is to make repair plans based on the condition of components. With the help of condition monitoring, incipient component failure can be identified before it develops into trouble that is hard to be controlled. In order to have an insight into parts condition, vibration analysis has been proved to be one of the most effective methods to detect faults in machine systems. The scope of this chapter is to detect the existence of artificial faults in the shovel model by using various digital signal processing techniques

This chapter is structured as follows. The data acquisition system is designed and tested first. After that, common failure modes and fault location are determined; meanwhile, the design and implementation of experimental trials are discussed. Using the statistical features of the waveforms, a time-domain analysis is carried out on the acceleration signal to disclose the existence of faults and the effectiveness of statistical parameters are compared. Following the time-domain analysis, frequency and time-frequency domains analyses are applied and, then the performance and limitations of the various approaches are discussed.

5.1 Data Acquisition System

Vibration analysis will be performed throughout the fault detection experiment. As mentioned in the literature review 2.3, vibration signature in the standard condition and faulty condition are different; accordingly, the vibration change in a machine can be considered as an indicator of the fault. Monitoring the vibration change provides complete observability of the system condition. The PC-based DAQ system depends on each of the following system elements: transducers and sensors, signal conditioning, DAQ hardware and computer[87]. Figure 5.1 illustrates the sensing and data acquisition elements of the system. The rest of this section will cover more details of each element in the DAQ system.
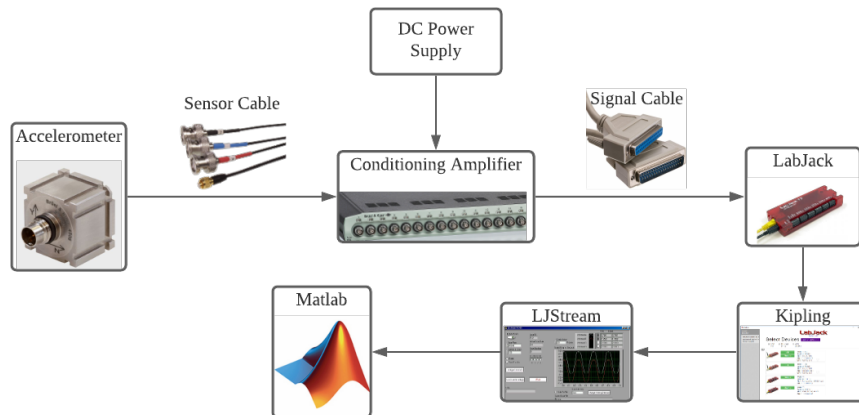
Figure 5.1: Sensing and Data Acquisition Elements

Vibration is the mechanical oscillation about the equilibrium position of a machine or components[88]. Accelerometer, velocity transducer and proximity probe (displacement measurement) are common transducers for measuring the vibration level[10, 89]. Among those common transducers, accelerometers are easy to install[89] and provide broad frequency and dynamic ranges[10]. In this experiment, Bruel & Kjaer's 4506-B triaxial accelerometer was used since its high-sensitivity and broad frequency range[90] can cover the frequencies of interest (shown in Appendix H) of the scaled shovel model. For mounting the accelerometer adhesively on the flat planes, the thin,

Poly-carbonate mounting clip (UA-1408) was used. This mounting pad, shown in Figure 5.2, can secure the cable and reduce the chance of cable-induced noise.

Figure 5.2: Thin, Poly-carbonate Mounting Clip for Accelerometer[91]

The vibration signal is then transmitted to a conditioning amplifier through the AO-0526 cable which is shown in Figure 5.3. The conditioning amplifier was used because accelerometers typically generate small voltages (micro-volts) so that the amplifier has to increase a voltage signal to a level suitable for digitization by the DAQ hardware. Typically, DAQ hardware is calibrated for input voltages in the 0 to 10V range[92]. In this experiment, Bruel & Kjaer's 16-channel Type 2694 conditioning amplifier was selected.
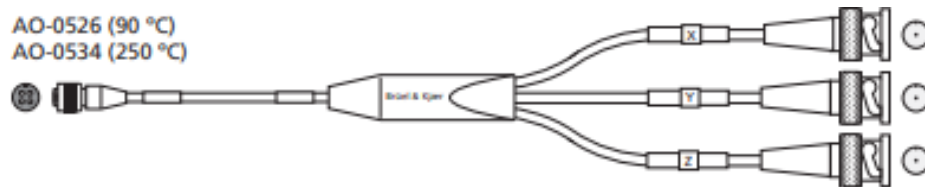
Figure 5.3: Thin, Poly-carbonate Mounting Clip for Accelerometer[91]

After the conditioning amplifier, the amplified data is then transmitted to the DAQ hardware through a D-subminiature cable. The DAQ hardware works as an interface between a computer and signals from the outside world by converting incoming analog signals to digital signals that can be readable and manipulated by computers. In this project, LabJack T7 is chosen to be the DAQ hardware. This device has a high-speed 16-bit analog to digital capability and $1\mu V$ noise-free analog input resolution.

Overall, the data acquisition system consists of transducers and sensors, signal conditioning, DAQ hardware and a computer. The model number and more information about each element are summarized in Table 5.1. Before using the DAQ system to collect vibration data of the shovel model, a waveform generator was used to validate the DAQ system. The validation of the DAQ system is included in Appendix I.

Table 5.1: A Summary of DAQ Elements

DAQ Element	Hardware Brand	Model Number	Function	Important Features
Transducer and Sensor	Bruel & Kjaer	Type 4506-B	Triaxial Accelerometer	high sensitivity and wide frequency range
Signal Conditioning	Bruel & Kjaer	Type 2694-A	Conditioning Amplifier	Multi-channel and multiplexing capability
DAQ Hardware	LabJack	T7	Analog to Digital Converter	16-bit high speed and 1μV noise-free low resolution
Computer (Software)	Kipling	3.1.17	LabJack connection and configuration	LabJack connection and configuration
	LJStream	3.1.17	Data Logging	100 ksamples/second Stream Speed
	Matlab	R2019b	Post-Processing	Signal Processing

5.2 Failure Modes of Experimental

The free motion of the shovel under the fault-free condition can be considered as a healthy state. As mentioned earlier, different failure modes can produce a distinctive vibration response. Common time behaviour characteristics can be summarized into three categories: abrupt, incipient and intermittent response, which are illustrated in Figure 5.4. Abrupt faults show step-like behaviour: a fault term changes abruptly from the normal value to a faulty value. Incipient faults show drift-like behaviour: a fault term gradually changes from the fault value to a faulty value. Last but not least, intermittent faults have a temporary effect: a faulty term changes from the normal value to the faulty value and returns to the normal value after a small amount of time[93].

To study fault detection on cable shovel models, two classes of structural artificial defects are selected: bolt looseness and shaft wear. When the shaft wear failure is introduced, gear misalignment may also be triggered, which will be explained in section 5.2.2. There are mainly two reasons behind the faults selection: first, those faults can represent common failure modes in the real cable shovels; second, these faults represent different time behaviour characteristics. To be specific, misalignment has an abrupt nature, whereas looseness shows intermittent effect. The ability to detect failures with different characteristics can prove that the designed shovel is a valid prototype for failure detection on real shovels.

5.2.1 Bolt Looseness

The first failure mode chosen for the fault detection study is bolt looseness. There are two main causes of bolt loosening: spontaneous bolt loosening and slackening. Spontaneous bolt loosening happens due to variable shock, vibration and dynamics loads; whereas slackening bolt loosening is caused by settlement, creep and relaxation[94]. Bolt looseness failure is common on mining shovels, which not only brings production
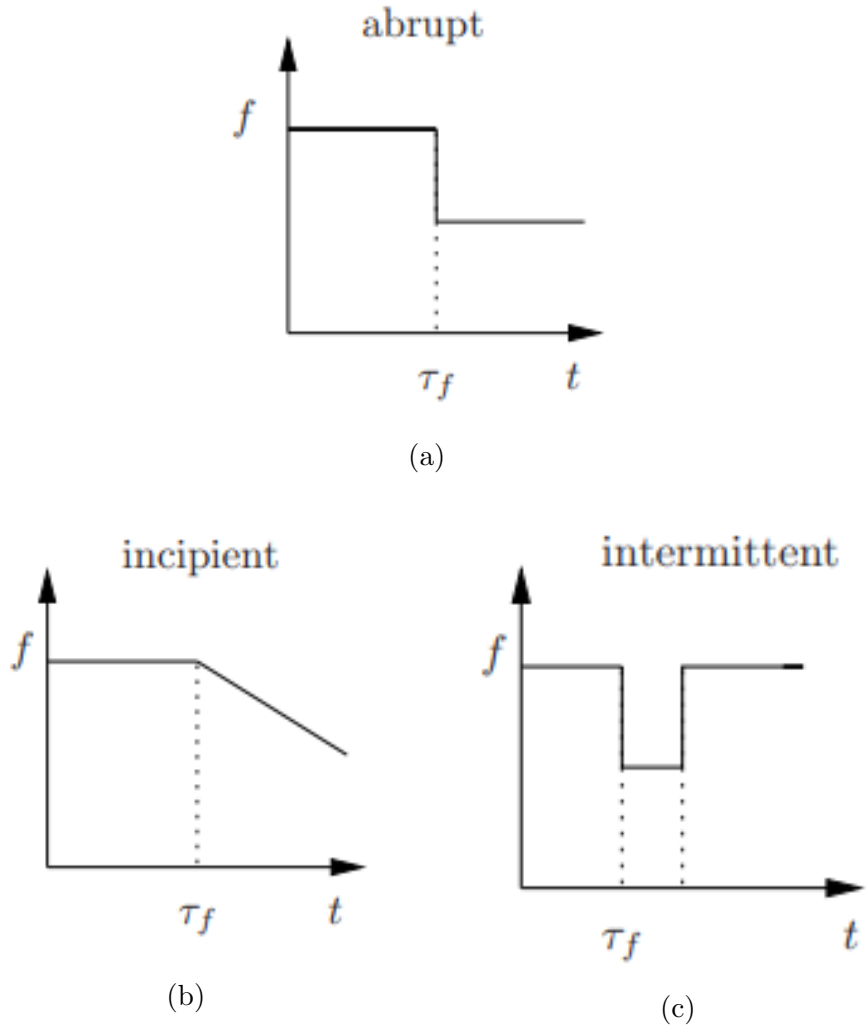
Figure 5.4: Common Time Behaviour Characteristics of Faults[93]

to a standstill and costs thousands of dollars but also could pose a significant safety hazard.

The failure of bolt looseness is seeded by changing the torque on each bolt located at the bearing block as illustrated in Figure 5.5. The bolt chosen for fastening the bearing block and bearing is M6 and A2-70. According to the fastening standard[95], the tightening torque is 8.8 Nm. In order to quantify the looseness, a torque wrench was used to alter bolt torque. Within the range of the maximum tightening torque for the selected bolt, four torques were chosen for the study: 0 Nm, 1.1 Nm, 4.5 Nm and 6.7 Nm. To study the vibration change due to bolt looseness, various
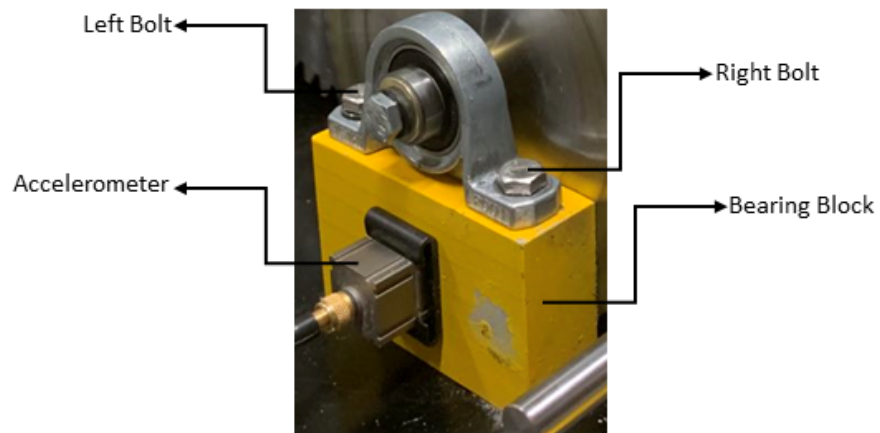
(a)
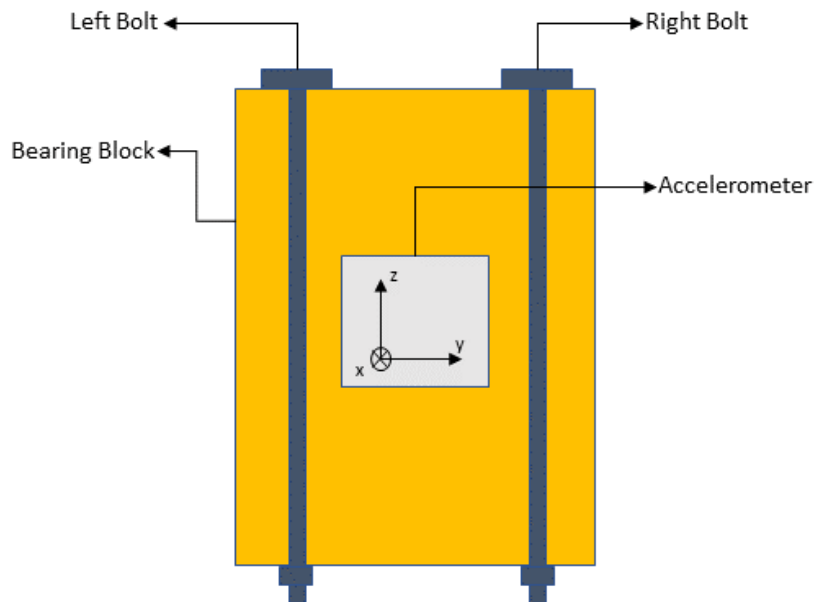
(b)

Figure 5.5: Bolt Looseness Location and Illustration

experiments have been performed. The experimental trial is summarized in Table 5.2. Experiment 1 to 3 is analyzing the vibration level of bolts with balanced torques; on the other hand, experiment 4 and 5 is to analyze the vibration level of two bolts with unbalanced torques.

Table 5.2: Experiment Trial for Bolt Looseness Fault

Experiment Order	Left Bolt Torque (Nm)	Right Bolt Torque (Nm)
1	6.7	6.7
2	4.5	4.5
3	1.1	1.1
4	6.7	0
5	1.1	0

5.2.2 Shaft Wear

The second failure mode selected for the fault detection study is shaft wear. This failure is usually caused by a poor fit between the shaft and bearing, which produces unwanted friction and heat that wear the shaft. However, in the shovel's application, shaft wear in the gearbox can trigger other problems such as gear misalignment. Because of shaft wear (shaft diameter diminishing), the shaft will then rotate at a variable angle which can cause yaw and pitch misalignment shown in Figure 2.16a and 2.16b. There are two reasons for selecting a shaft wear failure mode: first, shaft wear is one of the most common structural failures in mining equipment[34, 57, 58]; second, in the gearbox system, shaft wear often trigger other failures such as gear deterioration and bearings failure. In this research, the artificial shaft wear can lead to angular gear misalignment. As a result, the vibration level change reveals the combination effect of shaft wear and angular misalignment.

Wear is the damaging, gradual removal of material at the solid surfaces. Excessive friction can cause deformation or material removal of a component. The failure of shaft wear is seeded by changing the shaft diameter where contacts with the bearing as shown in Figure 5.6. Since wear is a fault that gradually removes the material at solid surfaces, a diameter change is able to represent the presence of wear. In addition, these diameter changes ($0.5mm$, $1mm$, and $2mm$) were chosen to mimic the gradual

74

change of the wear fault and were too small to damage other components in the system. The diameter of the healthy shaft is 12 mm and the faulty shaft diameter
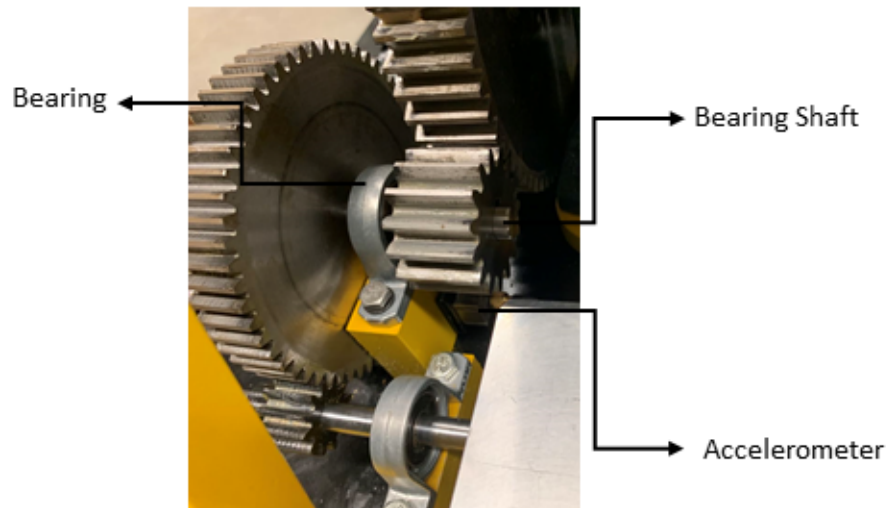
(a)
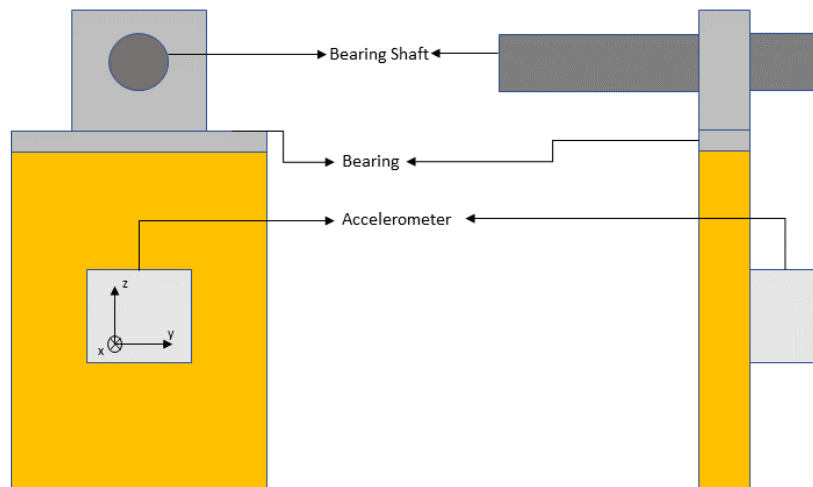
(b)

Figure 5.6: Shaft Wear Location and Illustration

is 11.5 mm, 11 mm and 10 mm, which are illustrated in Figure 5.7. To study the vibration level change due to shaft wear while other variables are kept constant (i.e., bolt tightness and shovel working process), the experiment trial for the shaft wear failure mode is summarized in Table 5.3.
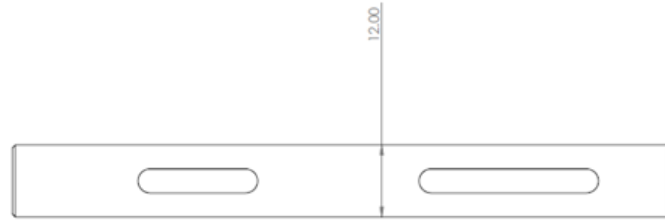
(a) Healthy Shaft
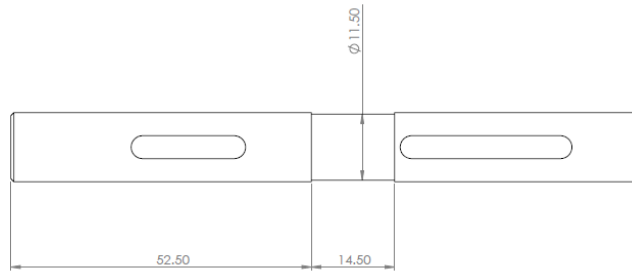
(b) Faulty Shaft with 0.5 mm Diameter Difference
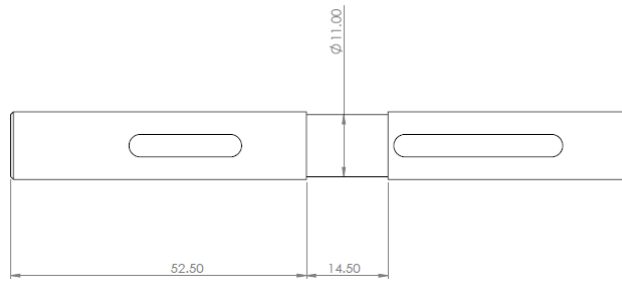
(c) Faulty Shaft with 1 mm Diameter Difference
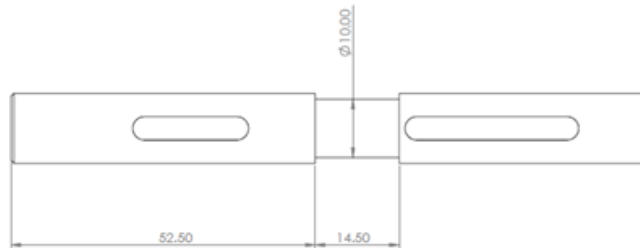
(d) Faulty Shaft with 2 mm Diameter Difference

Figure 5.7: Illustration of Good Shaft and Faulty Shafts

5.3 Fault Detection

After the baseline was established, experimental trials for bolt looseness and shaft wear were conducted and acceleration signals were collected. In this section, fault

Table 5.3: Experiment Trial for Shaft Wear Fault

Experiment Order	Shaft Diameter (mm)	Diameter Difference (mm)
1	12	0
2	11.5	0.5
3	11	1
4	10	2

detection will be explored by using common digital signal processing techniques including time-domain, frequency-domain, and time-frequency domain analyses.

5.3.1 Time-Domain Analysis

The time-domain analysis used in this section is based on statistical parameters which have been discussed in section 2.3.2 and Appendix B. Statistical parameters shown in Figure 2.17 can be used to detect faults based on the assumption that the presence of faults will change such parameters. The time-domain analysis based on the statistical parameters applied to both faults, bolt looseness and shaft wear, will be discussed more as follows.

Bolt Looseness

The statistical parameters for the fault of bolt looseness were calculated from the raw data which are the voltage output of the accelerometer whose sensitivity is 100 mV/g. Since the voltage-acceleration conversion is linear, it would be then sufficient just to analyze the voltage data directly as the trends would be the same. There are 7 statistical features being considered in the research, which include standard deviation, skewness, kurtosis, peak-to-peak, mean, RMS, and crest factor. Table 5.4 and 5.5 summarize those 7 statistical parameters regarding the three axes for balanced and unbalanced torques as well as the parameter change (in %) for faulty conditions,

which considers the healthy state (6.7 Nm - 6.7 Nm torque) as a baseline.

To study the statistical features change due to the presence of faults, mean and standard deviation provide the first insight. As shown in Table 5.4, the statistical-parameter mean is relatively stable for both balanced and unbalanced bolt looseness regardless of the acceleration orientation (x, y or z axis). For whatever the axis or bolt torque is, the changes of mean due to bolt looseness remain between 5% and 10% showing that the central tendency of probability for balanced or unbalanced torque is relatively unchanged; in other words, the average of acceleration of the subsystem with loosening bolts remains at a certain level and statistical parameter *mean* is not a good indicator to detect the fault of bolt looseness. Standard deviation is a statistical feature that measures the dispersion of a dataset relative to its mean. According to Table 5.4, the standard deviation, regardless of the acceleration orientation, is decreasing as the bolts get loose for both balanced and unbalanced torque. The standard deviation changes are within the range of 20% - 50% and 55% - 70% for the balanced and unbalanced torque, respectively. The standard deviation parameter shows a phenomenon that the tighter the bolts the more dispersive of the acceleration data, which may be due to the fact that tight bolts can give the system a better mechanical connection leading to an extensive vibration. Apart from the finding that the more loose the bolts the lower the standard deviation, the drop of the standard deviation for unbalanced bolt torques is dramatically higher (about 2×) than the balanced bolt torques(e.g., -64% for $1.1-0Nm$ vs -26% for $1.1-1.1Nm$ on the x axis). Therefore, the standard deviation is a good indicator of bolt looseness condition (the lower the standard deviation the lower the torque) and can also be used to distinguish balanced and unbalanced bolts.

Root Mean Square (RMS) and peak-to-peak value are commonly used for vibration analysis. RMS is an effective parameter for alternating voltages or currents, whose definition is also similar to standard deviation. According to Table 5.4, RMS has the same trends as the standard deviation: RMS is decreasing as the bolts get loose

Table 5.4: Statistical Parameters for Bolt Looseness (Part 1)

	Axis	Balanced Torque Nm			Unbalanced Torque Nm	
		6.7-6.7	4.5-4.5	1.1-1.1	6.7-0	1.1-0
Mean	x	0.0021 -	0.0019 -9.52%	0.0020 -4.76%	0.0020 -4.76%	0.0020 -4.76%
	y	0.0032 -	0.0034 +6.25%	0.0031 -3.13%	0.0030 -6.25%	0.0030 -6.25%
	z	0.0011 -	0.0010 -9.09%	0.0010 -9.09%	0.0010 -10.00%	0.0010 -10.00%
Standard Deviation	x	0.0200 -	0.0157 -21.50%	0.0149 -25.50%	0.0090 -55.50%	0.0072 -64.00%
	y	0.0210 -	0.0161 -23.33%	0.0133 -36.67%	0.0070 -66.67%	0.0069 -67.14%
	z	0.0190 -	0.0108 -43.16%	0.0093 -51.05%	0.0065 -65.79%	0.0059 -68.95%
RMS	x	0.0201 -	0.0158 -21.39%	0.0147 -26.87%	0.0087 -56.72%	0.0075 -62.69%
	y	0.0213 -	0.0149 -30.05%	0.0134 -37.09%	0.0076 -64.32%	0.0074 -65.26%
	z	0.0192 -	0.0108 -43.75%	0.0091 -52.60%	0.0065 -66.15%	0.0059 -69.27%
Peak to Peak	x	1.1263 -	0.7621 -32.34%	1.0319 -8.38%	0.2678 -76.22%	0.2425 -78.47%
	y	1.0123 -	0.8898 -12.10%	0.6321 -37.56%	0.1746 -82.75%	0.1355 -86.61%
	z	1.0524 -	0.6267 -40.45%	0.4574 -56.54%	0.1806 -82.84%	0.1216 -88.45%

Table 5.5: Statistical Parameters for Bolt Looseness (Part 2)

		Balanced Torque Nm			Unbalanced Torque Nm	
	Axis	6.7-6.7	4.5-4.5	1.1-1.1	6.7-0	1.1-0
Skewness	x	-2.9216	-1.3630	-1.3116	-0.0371	0.1606
	y	0.1463	0.5661	1.7318	-0.2029	-0.0495
	z	0.5905	-1.5699	0.6577	-0.0241	0.1042
Kurtosis	x	184.9570	163.1704	273.5644	10.9320	8.4045
	y	114.7603	111.2320	105.1210	9.8970	9.3624
	z	174.6859	123.4994	83.9806	9.9302	8.3433
Crest Factor	x	37.2731	32.3726	40.9706	17.0534	14.0877
		-	-13.15%	+9.92%	-54.25%	-62.20%
	y	35.3884	27.2893	23.2491	13.1311	10.4276
		-	-7.49%	-8.43%	-48.28%	-58.93%
	z	31.5719	29.7997	27.4249	12.3895	9.1477
		-	-5.61%	-13.14%	-60.76%	-71.03%

for both balanced and unbalanced torques regardless of the acceleration orientations. Besides, RMS can also be used to differentiate between balanced and unbalanced bolt torques: the change of the RMS for the unbalanced bolt torque is about 2× larger than the balanced bolt torques (e.g., -63% for $1.1 - 0Nm$ vs -27% for $1.1 - 1.1Nm$ on the x axis). As a result, RMS can be a good indicator of bolt looseness condition (the higher the RMS the tighter the bolts) and bolt torque balancing condition. The peak-to-peak value specifies the difference between positive and negative peaks. From Table 5.4, it can be seen that peak-to-peak value generally follows the rule that the tighter the bolt the higher the peak-to-peak value for balanced and unbalanced bolt torques except for x-axis (the peak-to-peak value for 1.1 Nm - 1.1 Nm is higher than the value for 4.5 Nm - 4.5 Nm). This exception could be explained by the fact

that, as shown in Figure 5.5, bolts mainly stable the bearing block on y and z axes. Peak-to-peak value not only can be used to examine the bolt looseness condition for y and z axes, but it can also easily differentiate the balanced and unbalanced bolt torques by the peak-to-peak value changes (e.g., -86% for $1.1 - 0Nm$ vs -38% for $1.1 - 1.1Nm$)

Skewness and kurtosis are the third and fourth moments of the distribution, which describes the shapes of the distribution. Skewness measures the asymmetry of the probability distribution about its mean. A perfectly symmetrical distribution will have a skewness of 0 and the more the skewness value is closer to 0 the more symmetrical the distribution is. A detailed interpretation of skewness value and its corresponding asymmetry is included in Appendix B. As seen in Table 5.5, it does not show a clear relationship between skewness and bolt torques. Although skewness is not a good indicator of bolt looseness condition it is interesting to find that the distributions of unbalanced bolt torques are all fairly symmetrical (absolute value of the skewness is less than 0.5) whereas the distribution of balanced bolt torques are skewed (absolute value of the skewness is larger than 0.5). Hence, the shape of the distribution of vibration can be used to categorize the bolt torque balancing condition: unbalanced bolt torques tend to have a moderately symmetrical distribution; on the other hand, the distributions of the balanced bolt torques are more or less skewed. Kurtosis is another common statistical parameter to interpret the shape(tail heaviness) of the distribution, more details can be found in Appendix B. As shown in Table 5.5, the kurtosis value is decreasing as the bolt torques decrease regardless of bolt balancing condition except for the x-axis, showing that as the bolts are getting loose the distribution of vibration is transforming from heavy-tailed distribution to normal distribution. It once again proves the previous hypothesis that tight bolts provide better mechanical connection leading to more vibration in the system. Moreover, the distributions of vibration for unbalanced bolts torques are much closer to the normal distribution: the average kurtosis value for balanced bolt torques is about

81

150 whereas for unbalanced bolt torques, the average kurtosis value is about 10. This 15× difference makes kurtosis a good indicator of bolt balance condition.

The crest factor is one of the most important elements in impulsive metrics which are properties related to the peaks of the signal. The crest factor, sometimes called the ratio of peak-to-average, is found by the peak value divided by the RMS. The crest factor can provide an early warning for faults when they first develop as faults often reveal themselves with changes in the peakness of the signal before they manifest in the energy represented by the signal root mean squared[96]. As seen in Table 5.5, the crest factor is decreasing as the bolt torque decreases for y and z axes regardless of the bolt torque balancing condition. In other words, due to the presence of bolt looseness, the peak of the vibration signal decreases. Accordingly, crest factor can be used as a good indicator of bolt looseness condition (the lower the crest factor the lower the torque for y and z axes); in addition, it can also categorize the bolt torque balancing conditions: for balanced bolt torques, the average crest factor is 32 whereas the average crest factor for unbalanced bolt torque is 12.5 for the configuration in this project.

Common time-domain statistical parameters including standard deviation, mean, RMS, peak-to-peak, skewness, kurtosis and crest factor have been discussed. Some can be used to determine the bolt looseness condition and some can categorize the balanced and unbalanced bolt torques. Table 5.6 summarizes the related bolt looseness issues that statistical parameters can be applied to. Later, statistical parameters will be also applied to determine the presence of shaft wear.

Shaft Wear

Similar to the time-domain analysis for the fault of bolt looseness, the same 7 statistical parameters of the vibration data (voltage output directly from the accelerometer) have been used for the fault detection purpose. Table 5.7 and Table 5.8 summarize the statistical parameters of the healthy shaft and three faulty shafts and it also

Table 5.6: Statistical Parameters Applicability to Bolt Looseness Related Issues

Statistical Parameters	Bolt Looseness Condition		Bolt Torque Balance Condition
Standard Deviation	✓	x, y and z axes	✓
Mean	×	-	×
RMS	✓	x, y and z axes	✓
Peak to Peak	✓	y and z axes	✓
Skewness	×	-	✓
Kurtosis	✓	y and z axes	✓
Crest Factor	✓	y and z axes	✓

includes the difference of the parameter (in %) between the healthy and fault shafts.

Mean and standard deviation are commonly used in vibration analysis. The mean of the vibration signal for the shaft wear is relatively stable, within the range of less than 10% variation, regardless of the shaft wear condition or the accelerometer orientation. The small fluctuation of the mean cannot reveal the presence of shaft wear; in other words, mean, the average of vibration data of the fault, is not the detector of shaft wear fault. Although the use of the mean failed to detect the fault, the dispersion of the dataset (i.e., standard deviation) could be useful for fault detection. As shown in Table 5.7, the standard deviation increases when the shaft wear gets worse no matter which axis is considered. This trend can be easily explained by the fact that the excessive clearance between the bearing and shaft allows two more degree-of-freedom added to the system[52] that leads to an increase in standard deviation. Moreover, the least standard deviation increase is as high as around 30% corresponding to the 0.5mm diameter difference shaft. Therefore, the standard deviation is a good indicator of the presence of shaft wear.

RMS, compared to mean or average, is an effective measure for alternating voltages

Table 5.7: Statistical Parameters for Shaft Wear (Part 1)

	Axis	Healthy Shaft	0.5mm Diameter Diff.	1mm Diameter Diff.	2mm Diameter Diff.
Mean	x	0.0024	0.0025	0.0025	0.0025
		-	+4.17%	+4.17%	0.00%
	y	0.0031	0.0034	0.0031	0.0034
		-	+9.68%	0.00%	+9.68%
	z	0.0010	0.0011	0.0011	0.0011
		-	+7.00%	+8.00%	+8.00%
Standard Deviation	x	0.0042	0.0061	0.0115	0.0184
		-	+45.24%	+173.81%	+338.10%
	y	0.0059	0.0075	0.0112	0.0167
		-	+27.12%	+89.83%	+183.05%
	z	0.0044	0.0059	0.0096	0.0142
		-	+34.09%	+118.18%	+222.73%
RMS	x	0.0048	0.0066	0.0118	0.0185
		-	+37.50%	+145.83%	+285.42%
	y	0.0067	0.0083	0.0116	0.0172
		-	+23.88%	+73.13%	+156.72%
	z	0.0045	0.0061	0.0097	0.0143
		-	+35.56%	+115.56%	+217.78%
Peak to Peak	x	0.0853	0.1980	0.6163	0.3738
		-	+132.12%	+622.51%	+338.22%
	y	0.0875	0.2106	0.4818	0.2949
		-	+140.69%	+450.63%	+237.03%
	z	0.0676	0.1932	0.4285	0.2292
		-	+185.8%	+533.88%	+239.05%

Table 5.8: Statistical Parameters for Shaft Wear (Part 2)

	Axis	Healthy Shaft	0.5mm Diameter Diff.	1mm Diameter Diff.	2mm Diameter Diff.
Skewness	x	-0.0022	0.2359	3.36365	0.0873
	y	-0.2724	-0.0631	0.9814	-0.1898
	z	-0.2246	0.2344	-2.1256	0.0171
Kurtosis	x	7.4010	28.5078	150.7038	11.8397
		-	+285.19%	+1936.26%	+59.97%
	y	5.9563	12.6753	79.3813	8.6686
		-	+112.80%	+1232.73%	+45.54%
	z	6.3541	40.34129	137.2526	8.42332
		-	+534.88%	+2060.06%	+52.56%
Crest Factor	x	9.5506	16.8364	27.9665	11.4777
		-	+76.29%	+192.82%	+20.18%
	y	6.8280	13.3693	24.2815	9.2004
		-	+95.80%	+255.62%	+34.75%
	z	7.6401	20.2106	24.0101	10.4032
		-	+164.53%	+214.26%	+36.17%

or currents. As shown in Table 5.7, RMS is increasing when the shaft wear condition gets worse for all three axes. The expansion of the clearance between the bearing and shaft results in the increase of the RMS and because of this, RMS is able to indicate the presence of shaft wear in the system. Peak-to-peak value is another common statistical feature for vibration analysis. It can be seen, from Table 5.7, that the peak-to-peak values of faults are considerably higher than the peak-to-peak value of the healthy shaft. Nevertheless, the relation between the peak-to-peak value and shaft wear condition seems not monotonic as RMS or standard deviation does. An indicator of fault is determined based on the difference between the healthy component

and faulty components whereas the condition of a fault is determined based on the comparison between multiple faulty components. In other words, if there is a obvious change of a statistical feature between healthy component and faulty components then it can say that the fault exists; if there is certain relationship (e.g., monotonic) between a statistical feature and faulty condition's change then the condition of the fault can be estimated. Accordingly, the peak-to-peak value can be considered as the indicator of the shaft wear but cannot be used to analyze the wear condition.

The next statistical parameters, skewness and kurtosis, are used to describe the shape of the distribution. Skewness measures the asymmetry of the probability distribution about its meanwhile kurtosis interprets the tail heaviness of the distribution. As shown in Table 5.8, the shapes of the majority of shafts (healthy shaft and faulty shafts with 0.5mm and 2mm diameter difference) for all orientations (x, y and z axes) are fairly symmetric (absolute skewness values are less than 0.5); meanwhile, the distribution shapes of the faulty shaft with 1mm diameter difference are highly skewed based on the fact that its absolute skewness values are greater than 1. Overall, there is not a significant shape difference between the good shaft and faulty shafts; in addition, skewness does not present a steady shift as the shaft wear condition gets worse. For those reasons, skewness can neither detect shaft wear fault nor be an indicator of shaft wear condition. Kurtosis, the other parameter interpreting the shape of the distribution, can be utilized to determine the presence of shaft wear. Although kurtosis does not reveal a monotonic trend when shaft wear gets worse, there is a significant change between the good shaft and faulty shafts: 310%, 1742% and 46% increase for the faulty shafts with 0.5mm, 1mm and 2mm diameter difference, respectively. Therefore, kurtosis can be used as an indicator of the presence of shaft wear but cannot determine shaft wear condition.

The crest factor, the ratio of peak-to-average, is one of the elements in impulsive metrics that are related to the peaks of the signal. According to the crest factor values shown in Table 5.8, a clear monotonic trend with respect to the shaft wear condition

is not revealed despite a prominent change between the good shaft and faulty shafts: 112%, 220%, 30% gain of the faulty shafts with 0.5mm, 1mm and 2mm diameter difference, respectively. Hence, crest factor, similar to kurtosis and peak-to-peak, can determine the presence of shaft wear but cannot estimate the shaft wear condition.

Common time-domain statistical parameters have been discussed for the failure of shaft wear and it is evident that time-domain can be used for shaft wear fault detection. Table 5.9 summarizes those statistical parameters' application in terms of shaft wear.

Table 5.9: Statistical Parameters Applicability to Shaft Wear

Statistical Parameters	Shaft Wear Fault Detection	Shaft Wear Condition Estimation	
Standard Deviation	✓	✓	The larger the standard deviation the worse the wear condition
Mean	✕	✕	-
RMS	✓	✓	The larger the RMS the worse the wear condition
Peak to Peak	✓	✕	-
Skewness	✕	✕	-
Kurtosis	✓	✕	-
Crest Factor	✓	✕	-

5.3.2 Frequency and Time-Frequency Domains

Frequency-domain analysis is another common approach used to understand a machine's condition with received signals. The frequency domain can extract information based on the frequency characteristics that may not be easily observed from the time domain. Fast Fourier Transform (FFT) is an efficient algorithm for computing the

Discrete Fourier Transform (DFT) and its inverse for stationary or nearly stationary systems, which was discussed in section 2.3.2. Since the model is not stationary in this experiment, FFT is not reliable. Power spectrum, another important signal processing technique in the frequency domain, describes the distribution of power into frequency components composing that signal. The power spectrum is generally defined as the Fourier transform of the auto-correlation function[65] and the power spectrum equation has been well discussed in section 2.3.2. Although the power spectrum, unlike the Fourier transform, does not have phase information it is well suitable to the situation where the phase is not considered useful or data containing a lot of noise (phase information is easily corrupted by noise)[65]. According to the FFT example of bolt looseness shown in Appendix J, the results of the Fourier transform are not quite meaningful and contaminated by noise. Due to the model with time-varying behaviour and high noise-to-signal ratio, power spectrum analysis is applicable to the project.

Sometimes, valuable time-series information of the spectrum components is included in the phase characteristics of the Fourier transform[97], which is hard to find in the frequency domain. Instead, the time-frequency domain can reveal time and frequency information; besides, it can also be applied to the non-stationary waveform signals. Short-time Fourier transform (STFT) is one of the most common time-frequency domain analysis techniques for condition monitoring and fault detection applications. More information about STFT including STFT equations has been summarized in section 2.3.2. Hence, frequency domain analysis (i.e., power spectrum analysis) and time-frequency domain analysis (i.e., STFT) will be applied to bolt looseness and shaft wear failures as follows.

Bolt Looseness

The power spectral analysis has been carried out for the fault of bolt looseness in Matlab by using the function *"pspectrum"*. This function performed power spectral

calculation by dividing the waveform into a number of overlapping segments and then assemble the power spectra obtained from each segment to construct the final power spectrum, and this method is called *spectral averaging*[65] and has been well discussed in section 2.3.2. Then, the function automatically converts the output to decibels using $10\log_{10}(p)$ where p is the power spectrum output[98]. The results of power spectrum analysis for bolt looseness are presented in Figure 5.8.

According to the outcome of the power spectrum analysis of bolt looseness, it can be seen that:

1. Generally speaking, the tighter the torque the larger the value of the power spectrum of the signal regardless of the balance condition of bolt torque;

2. For the unbalanced bolt torque combination (6.7-0 Nm and 1.1-0 Nm), the signal power spectrum values are moderately smaller than the power spectrum corresponding to the balanced bolt torque combination (6.7-6.7 Nm, 4.5-4.5 Nm and 1.1-1.1 Nm);

These results are expected and align with the conclusion in the time-domain analysis. A tighter bolt torque, which is to say a steady or fixed structure, leads to a better mechanical connection that in turn shows a high power in the frequency range.

The power spectrum should not be compared based on some specific frequencies since the vibration signal could be affected by other components' movement (i.e., drum rotation, dipper handle extension, etc.) or noise. Instead, the mean of the power spectrum of each bolt torque condition could better represent its power level. The average of each power spectrum of bolt looseness for three axes is shown in Figure 5.9.

From the averaged power spectrum of bolt looseness, the conclusions drawn previously are now more obvious: firstly, the tighter the torque of the bolt the higher the power level of the signal regardless of the bolt balance condition; secondly, unbalanced bolt torque severely affects the energy level of the vibration signal due to a significant
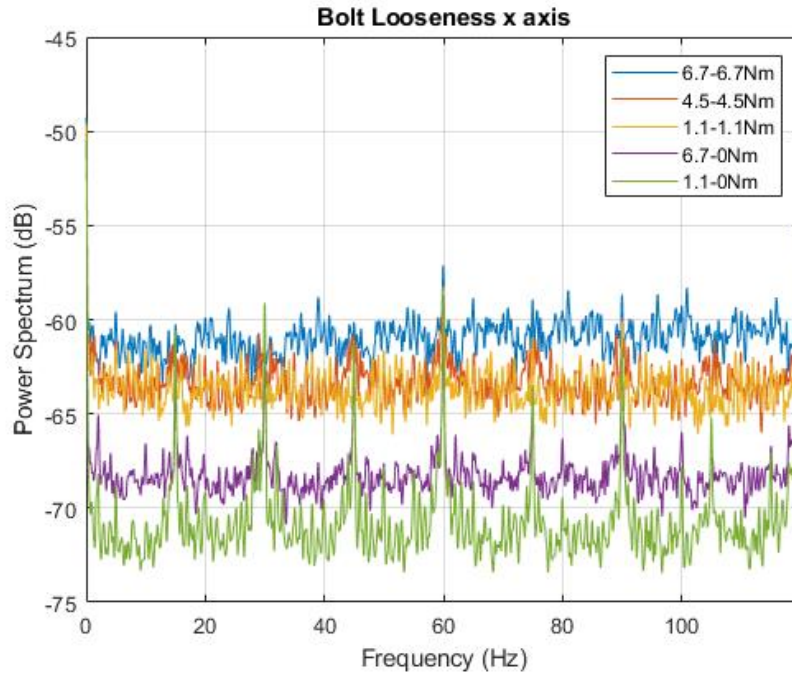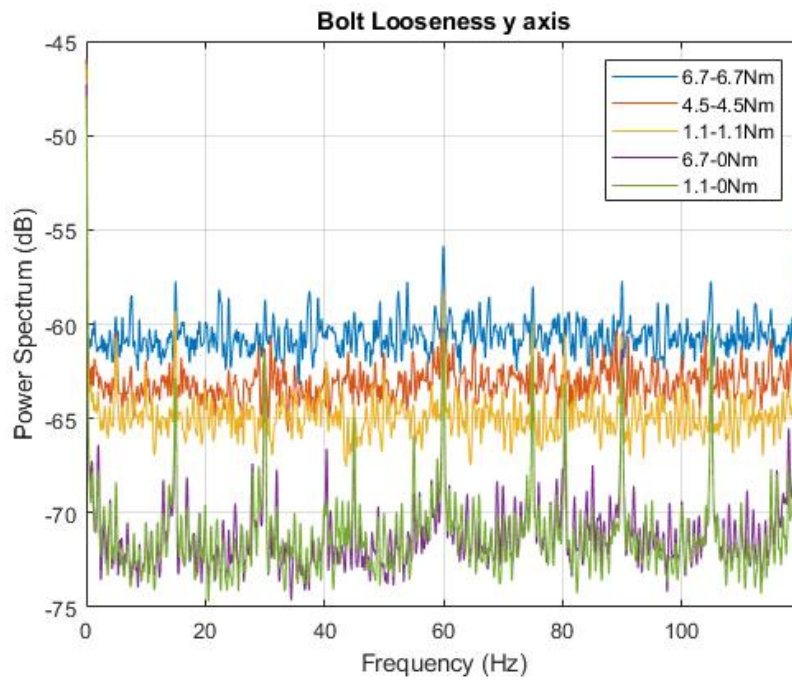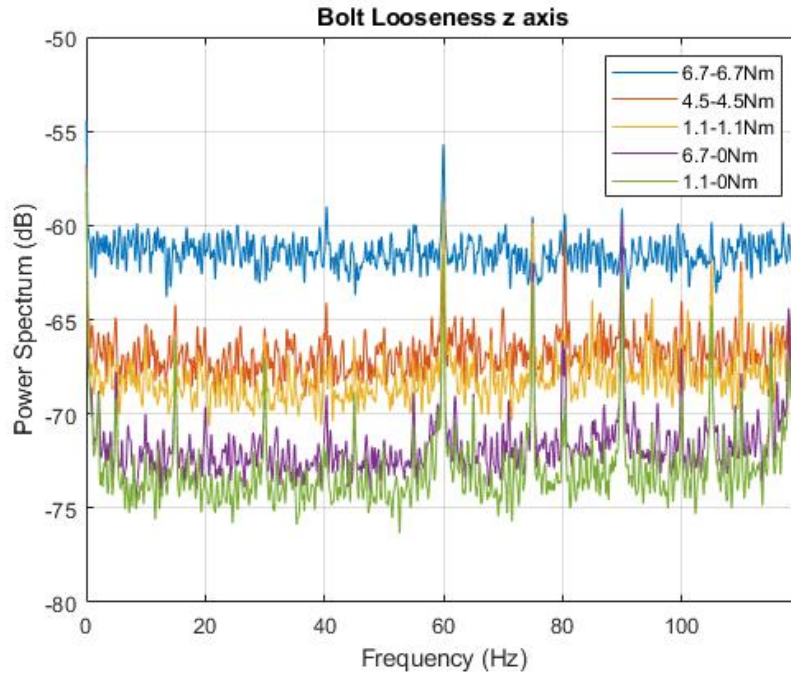
Figure 5.8: Power Spectrum Analysis for Bolt Looseness

drop of the average power for unbalanced bolt torque (6.7-0 Nm vs. 6.7-6.7 Nm and 1.1-0 Nm vs. 1.1-1.1 Nm).

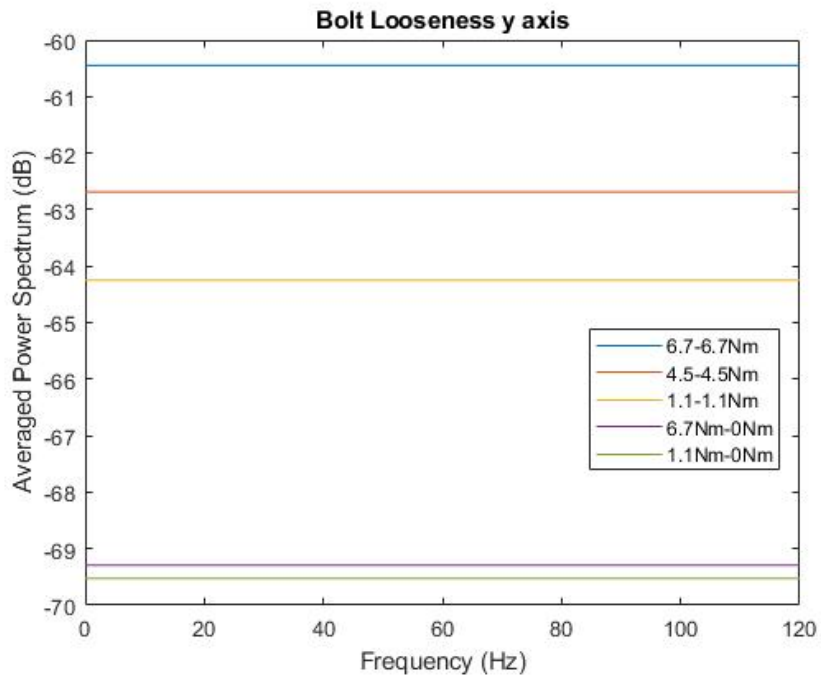Figure 5.8: Power Spectrum Analysis for Bolt Looseness (cont.)

Overall, from the power spectrum analysis and the mean of each power spectrum for bolt looseness discussed above, it can prove that the power spectrum analysis in the frequency domain is one of the most effective methods to determine the presence of bolt looseness. In addition, the time-frequency approach has also been applied to fault detection, which will be discussed next.

The short-time Fourier transform (STFT), analyzing how the frequency content of nonstationary signal changes over time, has been performed for the fault of bolt looseness in Matlab by using the *"stft"* function. This function calculates the STFT of the vibration signal by using a sliding analysis window over the signal and calculating the discrete Fourier transform of the windowed data[99]. A theory background of the STFT calculation has been covered in section 2.3.2. The results of the STFT analysis for bolt looseness are presented in Figure 5.10; since the phenomenon of x, y and z axes are quite similar, the results for y-axis will only be discussed here and results for the other two axes will be included in Appendix K.

Figure 5.10a, 5.10b and 5.10c represent the STFT for balanced bolt torque while
Figure 5.10d and 5.10e represent the STFT for unbalanced bolt torque. Here, the
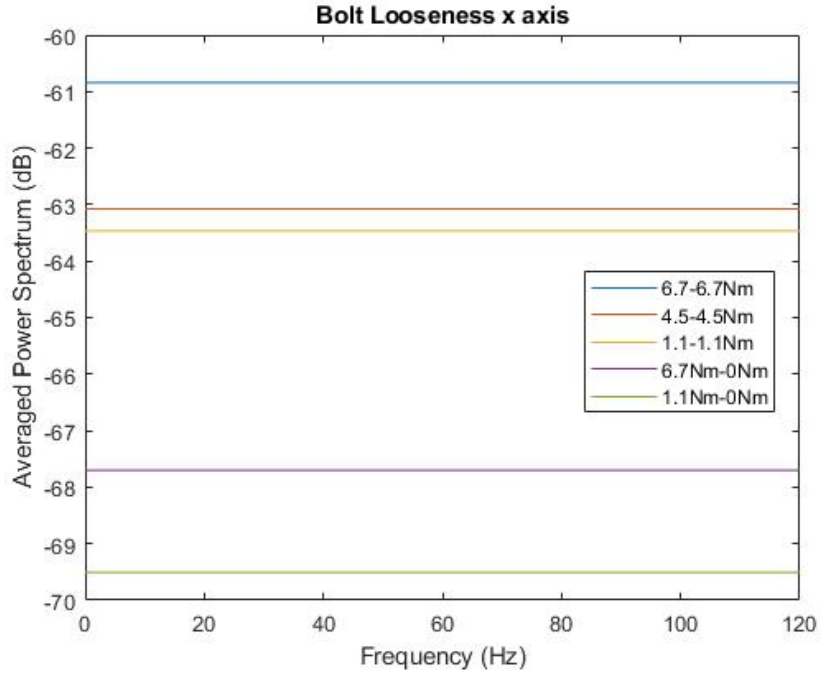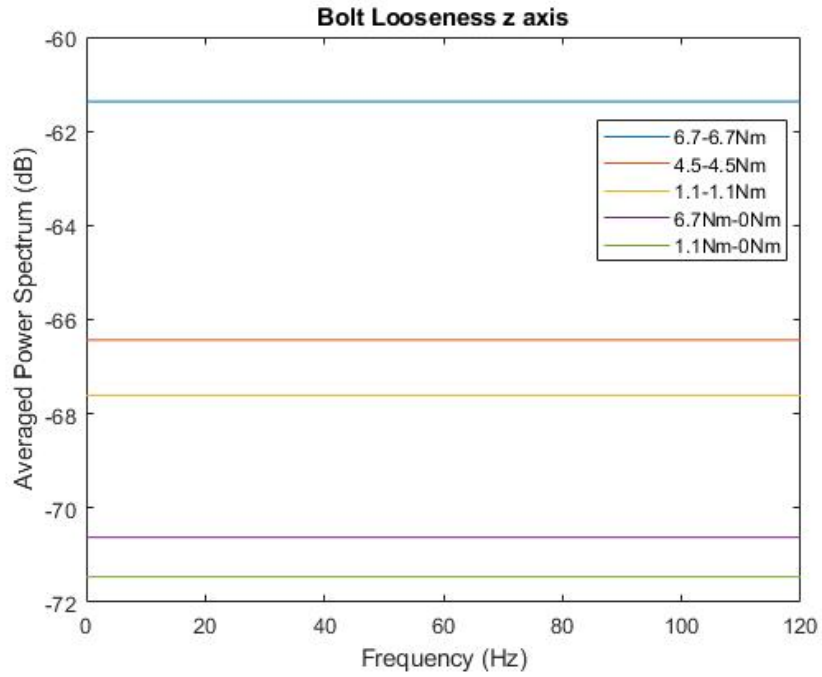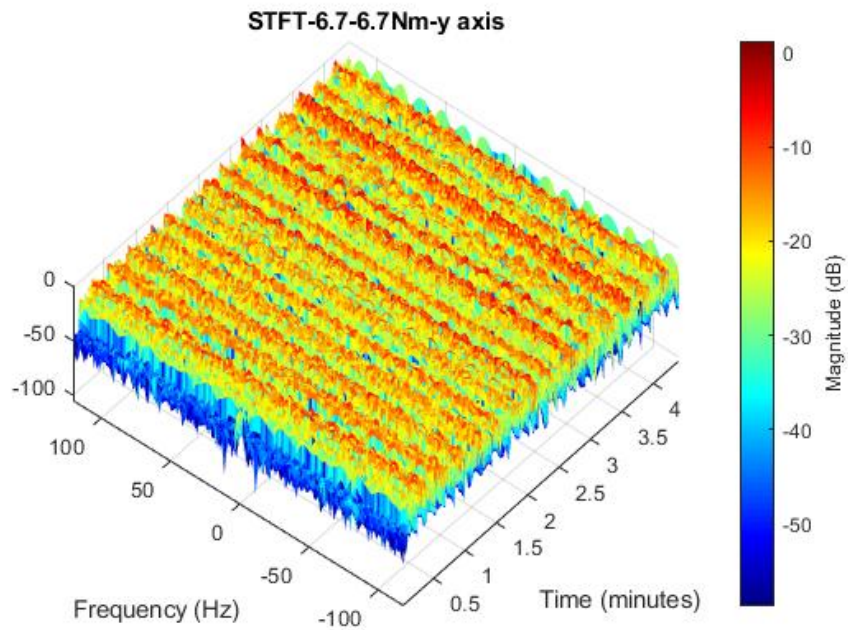

(a)

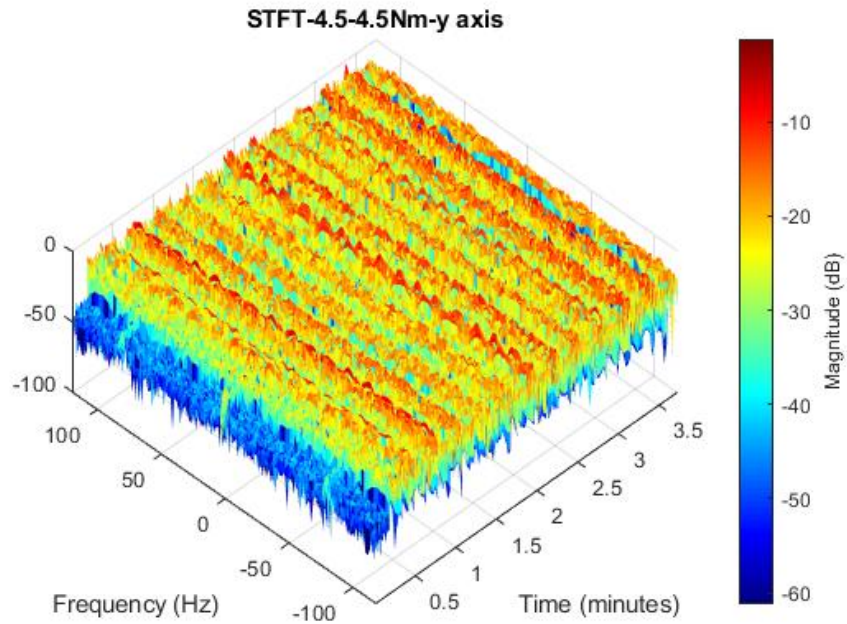(b)

Figure 5.9: Average Power Spectrum for Bolt Looseness

(c)

Figure 5.9: Average Power Spectrum for Bolt Looseness (cont.)

(a)

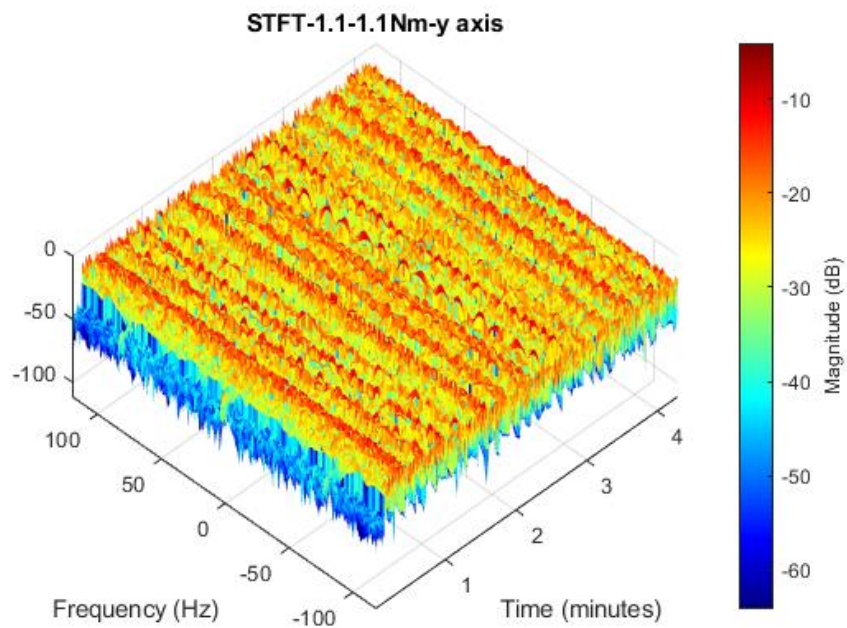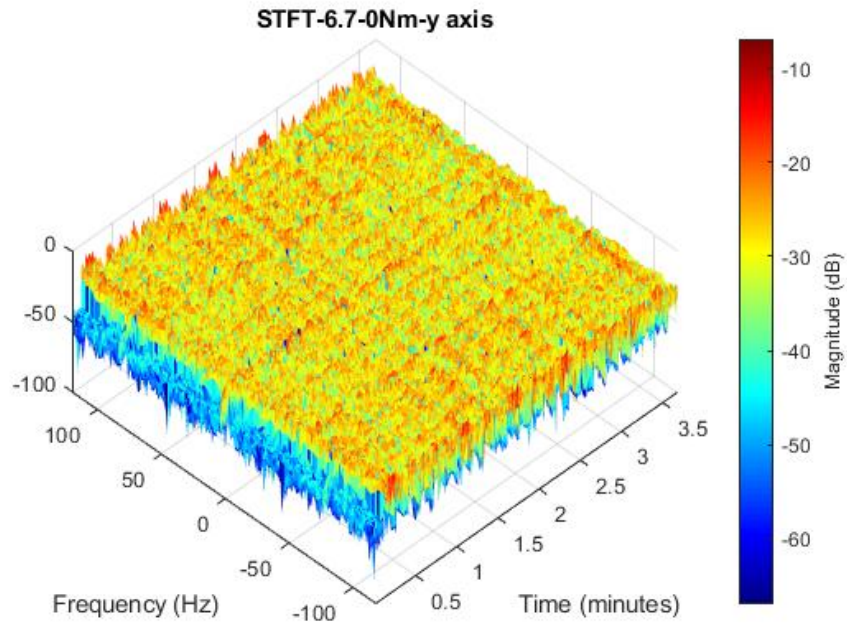Figure 5.10: Short-Time Fourier Transform of Bolt Looseness on y-axis
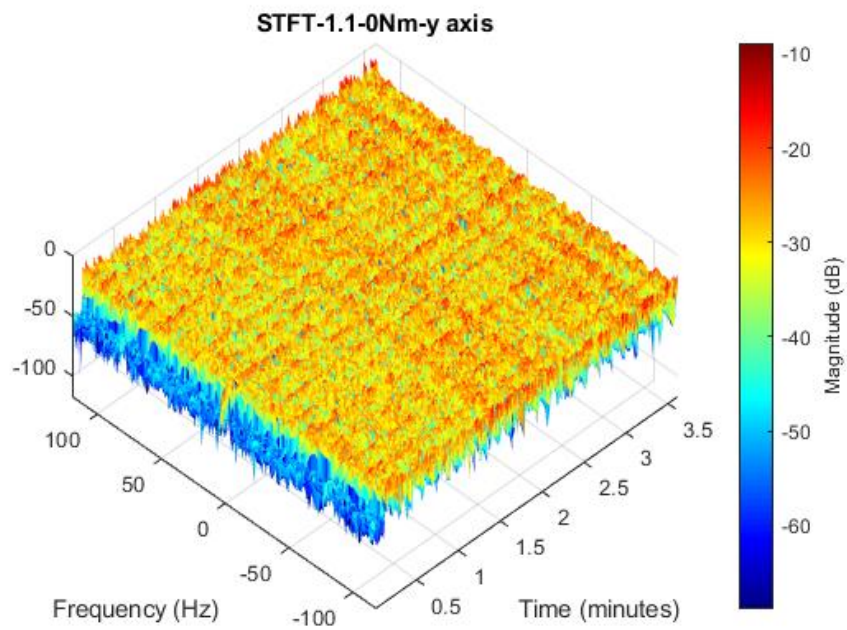
STFT-4.5-4.5Nm-y axis

(b)

STFT-1.1-1.1Nm-y axis

(c)

Figure 5.10: Short-Time Fourier Transform of Bolt Looseness on y-axis (cont.)

magnitude of the power of the frequency is illustrated using a color bar: red represents a high power, green represents medium power and blue represents low power. From

STFT-6.7-0Nm-y axis

(d)

STFT-1.1-0Nm-y axis

(e)

Figure 5.10: Short-Time Fourier Transform of Bolt Looseness on y-axis (cont.)

Figure 5.10a, 5.10b and 5.10c, it is apparent that the power of frequency is not evenly distributed along the timeline but with a periodic pattern: it is red then turns to

green (or yellow) and turns to red again. This periodic pattern of the frequency power matches the pattern of the shovel model's operating conditions that the dipper moves up and down regularly. Accordingly, in the situation where the bolt torques are balanced, the power of frequency content of the signal is higher when the dipper is moving up and vice versa. As for unbalanced bolt torques, as shown in Figure 5.10d and 5.10e, it can be seen that there is not a clear pattern of the power of frequency over time. In other words, the power of the frequency content of the vibration signal does not get affected due to the model's operation. Although STFT cannot determine the bolt looseness condition, it is a good indicator to distinguish balanced and unbalanced bolts.

Frequency domain and time-frequency domain analyses have been applied to detect the presence of bolt looseness in this section. In the frequency domain, power spectrum analysis was performed to determine the bolt looseness condition and bolts balance issues; meanwhile, in the time-frequency domain, short-time Fourier transform was used to detect the bolts balance configuration. According to their performance, it is recommended that use the STFT first to determine the bolts torque balance configuration and then use power spectrum analysis to determine the bolt looseness condition, the higher the power spectrum values the tighter the bolts. Later, power spectrum analysis and STFT will also be performed to detect shaft wear conditions.
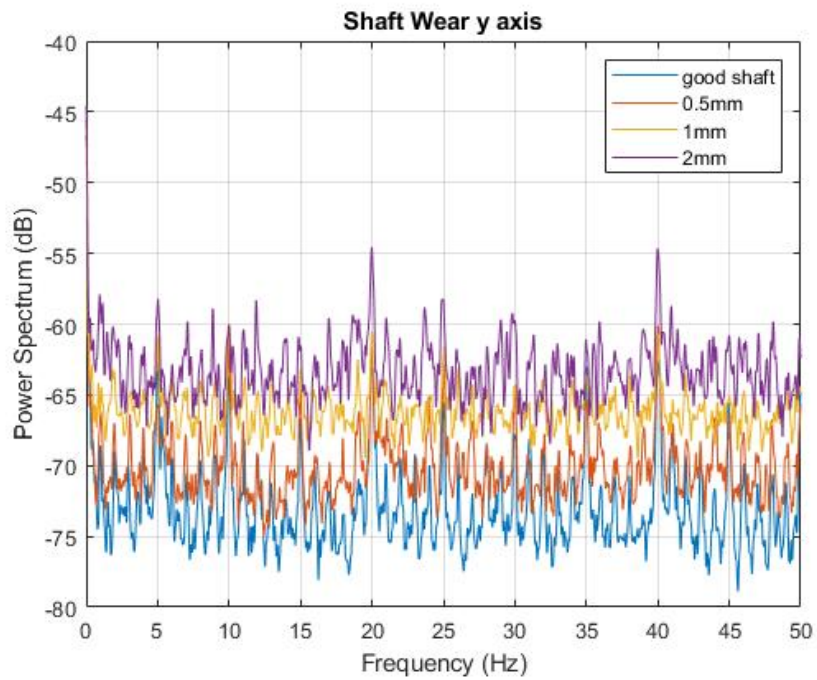
Shaft Wear

In order to determine the presence of shaft wear, power spectrum analysis and short-time Fourier transform will also be applied. Similar to the detection of bolt looseness, power spectral analysis has been conducted in Matlab by using the function *"pspec-trum"*. The results of power spectral analysis for shaft wear are presented in Figure 5.11, where "good shaft", "0.5mm", "1mm" and "2mm" represents healthy shaft and faulty shafts with diameter difference of 0.5mm, 1mm and 2mm, respectively.

Based on the outcomes of power spectral analysis of shaft wear, it can be seen that
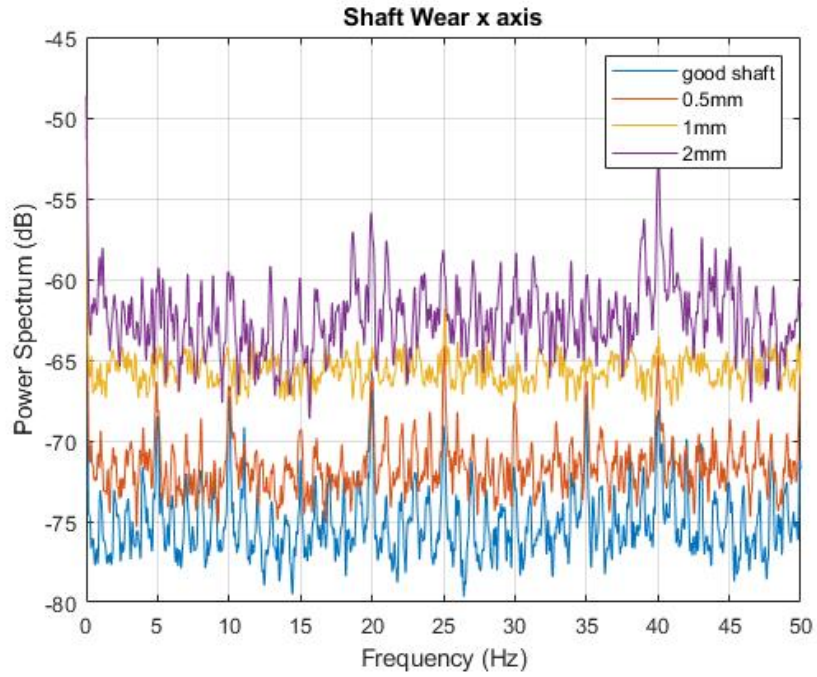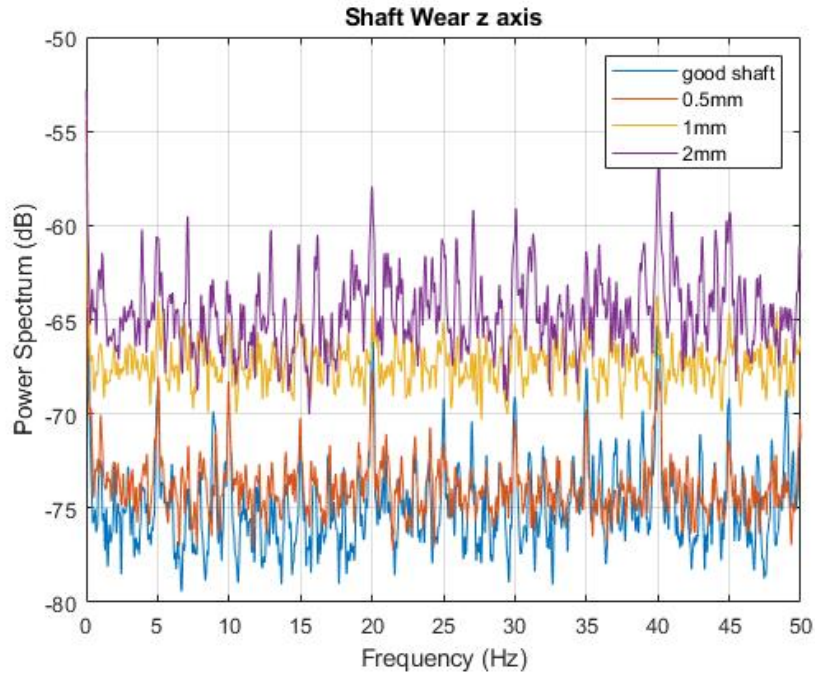
Figure 5.11: Power Spectrum Analysis for Shaft Wear

the worse the shaft wear condition the higher the value of the power spectrum of the

signal no matter which axis is considered. This phenomenon is expected and aligned

(c)

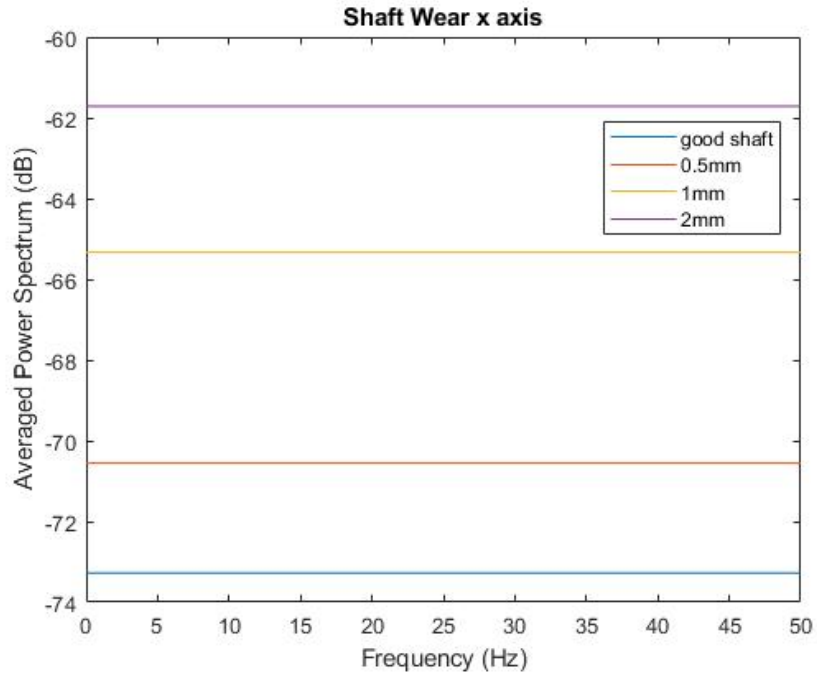Figure 5.11: Power Spectrum Analysis for Shaft Wear (cont.)

with the standard deviation or RMS in the time-domain analysis. As shaft wear gets worse, unwanted mechanical interaction will occur such as gear misalignment that could increase the energy in the frequency range.

For similar reasons, the vibration signal could be influenced by other components' movements and analyzing the power spectrum based on some specified frequencies is not reasonable. In order to visualize the power level, the mean of the power spectrum of each shaft (one healthy shaft and three faulty shafts) were calculated and is shown in Figure 5.12. From the averaged power spectrum of shaft wear, it is easy to conclude that a worse shaft wear condition can increase the energy level of the frequency content of the vibration signal.

Therefore, according to the power spectrum analysis and the mean power spectrum for shaft wear discussed above, the power spectrum analysis in the frequency domain can effectively determine the shaft wear condition. Besides, the time-frequency approach has also been applied to detect the shaft wear fault, which will be discussed

next.

To analyze how the frequency content of nonstationary signals changes over time,

(a)
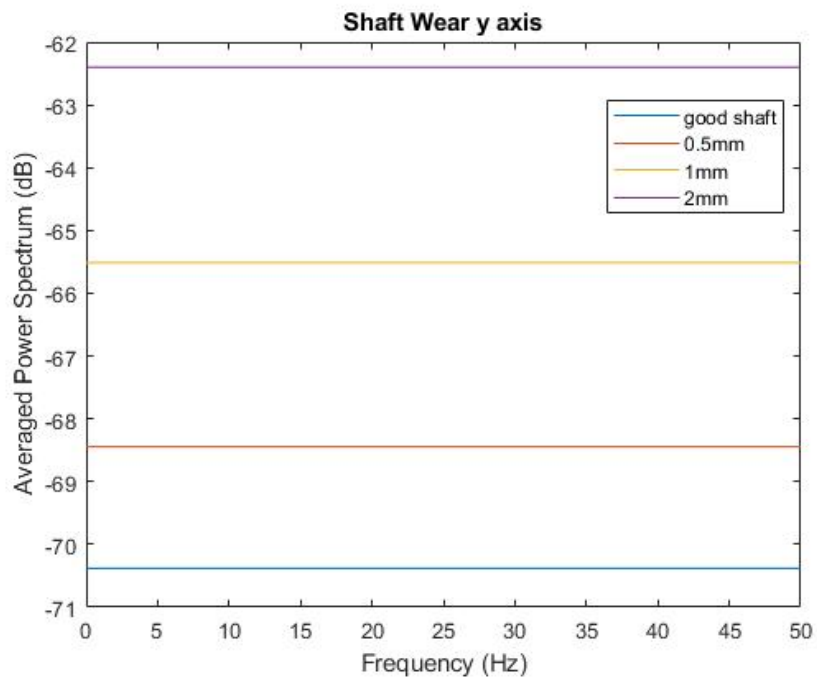
(b)

Figure 5.12: Average Power Spectrum for Shaft Wear

Figure 5.12: Average Power Spectrum for Shaft Wear (cont.)

the short-time Fourier transform has been conducted for the failure of shaft wear in Matlab by using the *"stft"* function. The results of the STFT analysis for shaft wear are illustrated in Figure K.3; s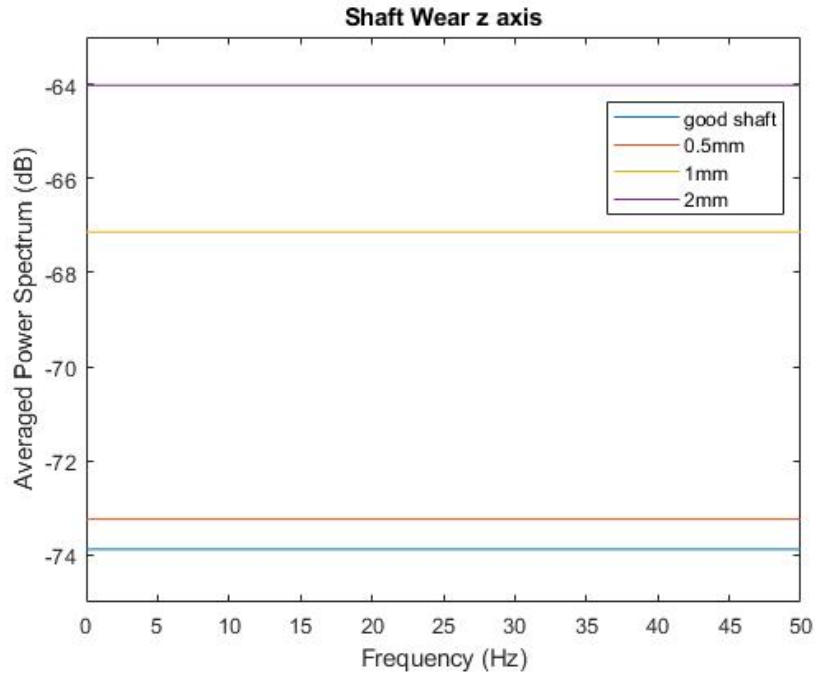ince the phenomenon of x, y and z axes are quite similar, only results for the y axis will be discussed here and results for the other two axes will be included in Appendix K.

From Figure 5.13a to 5.13d, the shaft wear condition is getting worse and at the same time, a pattern is gradually formed: when the shaft wear condition is okay (i.e., Figure 5.13a and 5.13b) the energy levels of the frequency are low and more importantly, it does not show a relationship between power level and time; in other words, before the shaft wear condition gets worse, the power of the vibration signal is not affected by the shovel model's operation mode. As the shaft wear condition is getting worse (i.e., Figure 5.13c and 5.13d), an apparent periodic pattern is gradually developed. This periodic pattern (it shows red first then turns to green or yellow and then turns to red again) matches the shovel model's operation setting (the dipper is

set to move up and then move down), which means that as the shaft wear is getting worse the power level of the vibration signal is affected by the model's operation
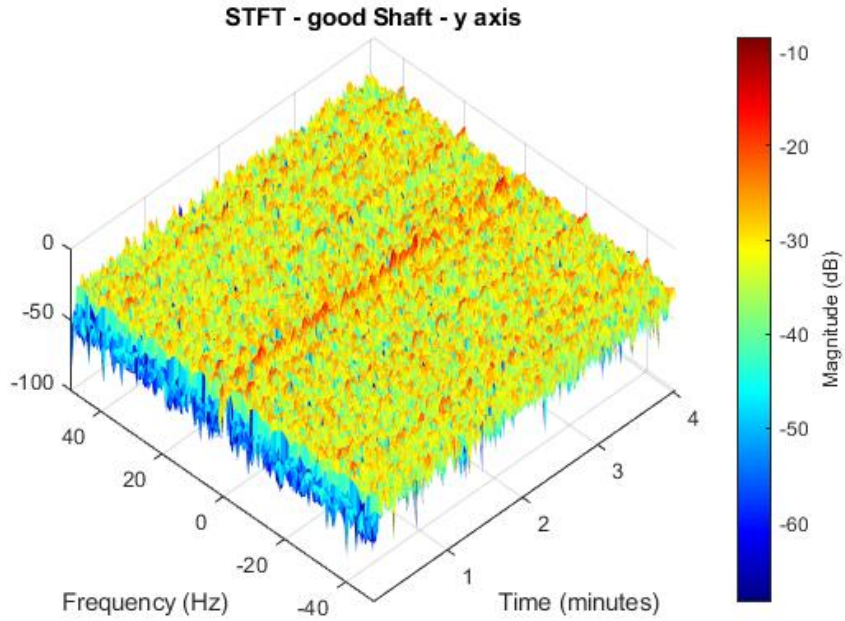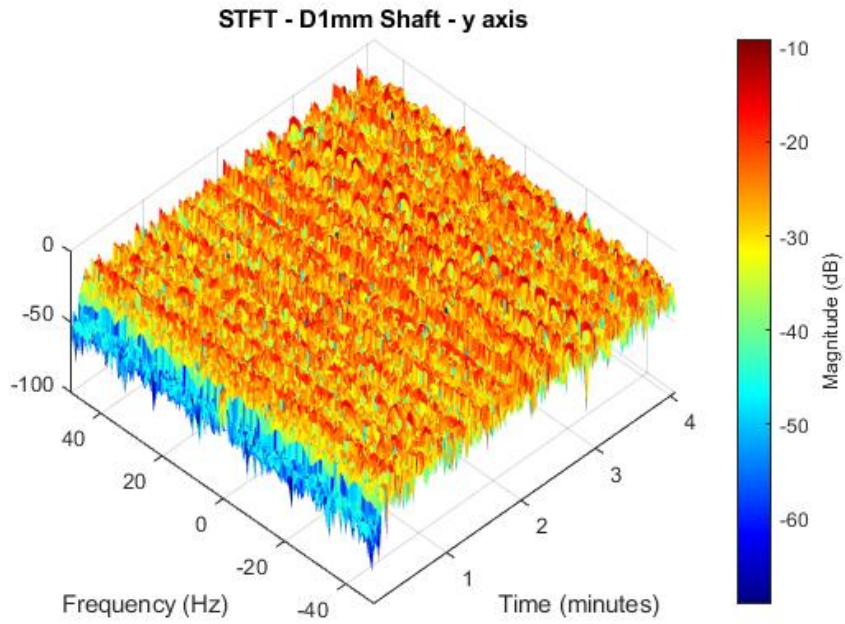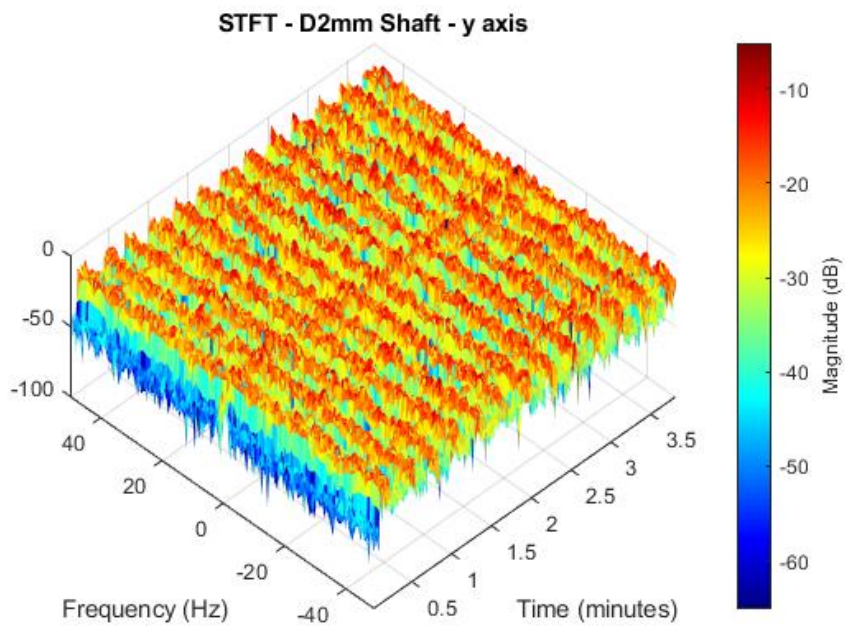

(a)
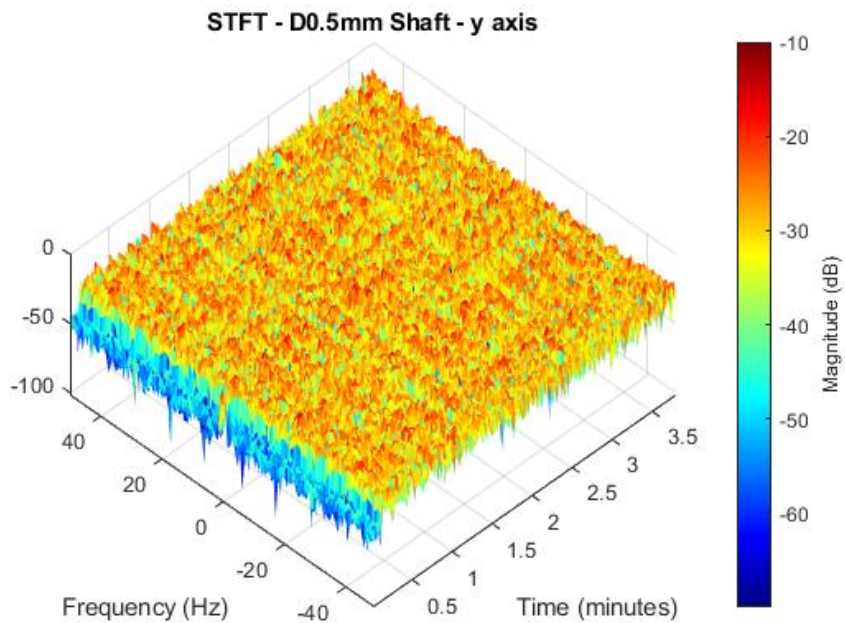
(b)

Figure 5.13: Short-Time Fourier Transform of Shaft Wear on y-axis

(c)

(d)

Figure 5.13: Short-Time Fourier Transform of Shaft Wear on y-axis (cont.)

mode. Therefore, based on the characteristics of the relationship between shaft wear condition and model's operation configuration, STFT can be used as the fault indi-

cator: the shaft wear should be checked as the energy of the frequency content of the vibration signal follows the model's operating configuration pattern.

In this section, frequency domain and time-frequency domain approaches have been performed to determine the presence of shaft wear. Based on the discussion above, power spectral analysis and short-time Fourier transform are both effective methods to detect the wear condition of shafts but STFT is a visualization tool whereas power spectral analysis makes it more quantitative. Having considered their performance and limitations, it is recommended to use STFT first to "visualize" the shaft wear condition and then power spectral analysis can be performed to confirm the presence of the fault.

5.4   Chapter Summary

The main motive of this chapter is to perform condition monitoring and fault detection on the developed shovel model. Fault detection analysis provides an insight into the machine's condition which helps the implementation of the predictive maintenance scheme.

Vibration analysis is one of the most effective methods using condition-monitoring strategies to detect faults in machine systems. The principle of the vibration analysis is based on the fact that vibration levels in healthy and faulty conditions are different. Due to its effectiveness, vibration analysis was leveraged to detect two common failure modes seeded in the shovel model.

To collect vibration data of the shovel model, section 5.1 provided an overview of the data acquisition system. Section 5.2 introduced two failure modes selected in this research: bolt looseness and shaft wear. The reasons for choosing those faults are because they are common failure modes in the real cable shovel models and have different behavioural characteristics in mechanical systems. The implementation and experiment trials of bolt looseness and shaft wear were discussed in sections 5.2.1 and 5.2.2, respectively.

Time domain, frequency domain and time-frequency domain analyses have been applied to detect the seeded faults in section 5.3. Statistical features of vibration signal in the time domain for bolt looseness and shaft wear were extracted and analyzed in section 5.3.1. Most of those can successfully separate components with faulty conditions from normal. The effectiveness of the statistical parameters for fault detection has also been summarized for both failure modes. In section 5.3.2, frequency domain and time-frequency domain analyses were performed. Power spectrum analysis was utilized instead of the classic Fast Fourier Transform because FFT is not good at dealing with non-stationary data and noise. For a system with time-varying behavior, the time-frequency domain analysis would make more sense. Short-time Fourier transform (STFT) was conducted for both failure modes and it provided an effective visualization aid to differentiate faulty components from normal ones.

The findings of this chapter are summarized as follows:

- From vibration analysis, it can be seen that the characteristics of the function of tight bolts and normal shaft are different: fastened bolts provide a good mechanical connection that leads to an increased vibration level whereas a shaft with the good condition will rotate steadily that will not increase the vibration level;

- In the time-domain analysis, statistical parameters not only successfully detect the presence of faults but also offer insights into fault conditions (e.g., balanced or unbalanced bolt torque, how bad the wear is, and etc.)

- Power spectrum analysis and STFT have shown their performance and limits in fault detection. STFT can easily disclose the existence of faults with its graphic ability and power spectrum analysis can quantitatively determine the presences of faults and fault condition.

Chapter 6

Conclusion and Future Work

Cable shovels are playing an essential role in overburden removal and ore material collection in large-scale surface mining operations and the availability of shovels is critical to their production. As mentioned earlier, predictive maintenance-the most effective maintenance strategy or certain types of shovel failure modes-allows repair plans to be made based on the expected condition of components. It can not only push the usage limit but also avoid unexpected shutdowns due to breakdowns (and possible consequential damage). The adoption of condition monitoring and fault detection is needed to aid the implementation of predictive maintenance.

Vibration analysis is one of the most effective methods used by condition-monitoring strategies to identify incipient component failures. The exploration of the fault detection techniques on full-size cable shovels is not feasible as the initial approach would require several shutdowns and cannot be studied in a controlled space. Therefore, a lab-scale cable shovel with a potential for fault detection analysis has been well studied in this research.

6.1 Conclusions

The lab-scale cable shovel research consists of two major objectives: first, design, development and fabrication of a shovel model with an inherent time-varying behaviour; second, access the observability of the presence of faults through vibration analysis

during the operation mode.

A lab-scale cable shovel has been developed to simulate the fundamental operation processes of full-size mining shovels. In order to reach the goal of this study, the model was designed with four distinct characteristics: firstly, the model is able to realize three imperative functions during the operation process which are hoist, crowd and swing; secondly, to replicate the real cable shovel as well as possible, the main systems were built with identical or similar working mechanisms as the industrial shovels; thirdly, a robust control system using industrial programmable language was developed to simulate primary shovel operational motions; lastly, the shovel model provided a platform for fault seeding and implementation of transducers and sensors. Vibration data were collected under normal and faulty conditions, time and frequency domain analyses were performed for fault detection.

Time-domain analysis based on the statistical features of the vibration signals has been performed to disclose the existence of artificial failures. The effectiveness and limitations of statistical parameters have been compared. As for bolt looseness fault, it was found that standard deviation, RMS, peak-to-peak, kurtosis and crest factor could be used to determine the bolt looseness condition; meanwhile, the standard deviation, RMS, peak-to-peak, skewness, kurtosis and crest factor has shown their performance to distinguish balanced and unbalanced bolt torques. As for shaft wear, the standard deviation, RMS, peak-to-peak, kurtosis and crest factor were proved as good indicators of detecting the existence of shaft wear failure.

Frequency and time-frequency domain analyses were used to extract vibration signatures of the system under normal and faulty conditions. Power spectral analysis and short-time Fourier transform (STFT) were adopted to quantitatively and visually differentiate the faulty components from normal ones. It was shown that power spectrum analysis can be used to detect the bolt looseness condition and also differentiate the balanced bolts from unbalanced ones based on the fact that balanced tighten bolts tend to have higher energy of vibration signal. With the help of STFT,

the balance condition of bolts can be easily determined since the energy of vibration signal of balanced bolts tends to be influenced by the shovel's working process. Speaking of the shaft wear failure, power spectrum analysis has proved its performance of detecting the presence of shaft wear according to the finding that energy of signal increases as the shaft wear condition gets worse; meanwhile, STFT was also shown as a good indicator of detecting the shaft wear from the finding that as the shaft wear condition gets worse, the energy of vibration signal tends to gets influenced by the shovel's working process.

The conclusions of this research are summarized as followings:

- A lab-scale cable shovel model has been designed and fabricated which has fundamental functions to simulate the operation mode and provide a platform for various studies (e.g., fault detection);

- Time-domain analysis based on the statistical parameters of the vibration signal can be used to extract vibration signatures of mechanical systems;

- Power spectral analysis along with STFT is an effective approach to monitor the condition of the non-stationary systems with structural defects.

6.2 Future Work

This research has the potential for further exploration which roughly can be categorized into two aspects: physical modelling and fault detection and diagnosis which will be discussed in the following remaining sections.

6.2.1 Physical Modelling

Improvements regarding the physical modelling can be categorized into four aspects: structure modification, similitude in fault modelling, ground-tool interaction and remote control. First, for structure modification, some basic functions of cable shovels

are not included in this lab-scale shovel model. At the moment, the propel function is not considered which is replaced by aluminum extrusion. Also, for the bucket assembly, it is recommended to install bucket teeth and design an automatic dipper door to simulate soil-tool interaction and dumping mode. Besides, the design of power transmission needs to be changed: replace gears using set screws with gears and keys. Second, for similitude in fault modelling, as well as scaling the dimensions of the laboratory scale system, scaling of the interacting elements of the subsystem where faults are being generated should be done. This will be useful for producing fault features that are more representative of those expected in a full-scale machine and will provide insights into the physics of failure model validation for digital twin development. Third, the fault detection analysis is conducted under the free movement of the shovel model. However, some faults may reveal themselves during the digging process. It is highly recommended to include soil-tool interaction in further research; last but not least, the current shovel model is controlled using EtherCAT technology requiring communication from a local computer through Ethernet cables. For those researchers interested in this shovel model but do not have access to the lab (geographic limitation or safety control), a remote control would be an asset to this project. Publishing mechanical design and control scheme can help other researchers make and use their own systems.

6.2.2 Fault Detection and Diagnosis

The research can not only be improved in the area of physical modelling, it can also get better in fault detection and diagnosis. First, the proposed vibration analysis can detect anomalies but it cannot diagnose faults. Although knowing the area or system where the fault happens it still takes maintenance specialists an amount of time to filter the fault; therefore, the finding of faults can be more efficient if the fault diagnosis is developed. Second, vibration analysis showed an effective approach to condition monitoring for the shovel model. The next step would be to test it on the full-size

cable shovels. There are various factors that a shovel at a mine would be exposed to which include: operator influence, weather, ore material, maintenance personnel, etc. Third, although statistical parameters, power spectrum analysis and STFT showed good performance for fault detection, some other DSP techniques can be tried as well: principal component analysis (PCA) for dimension reduction and classification, Hilbert-Huang Transform (HHT) for instantaneous frequency extraction, statistical features in the frequency domain, etc.

Cable shovels are playing a critical role in large-scale surface mining operations. Keeping machines in a good condition can prevent unnecessary shutdowns, high maintenance costs and lost production. Vibration analysis is one of the most effective methods used in condition-monitoring to detect faults in machine systems. However, conducting vibration analysis directly on actual mining machines is not practical; on the contrary, a lab-scale shovel model is easier and cost-efficient to be manipulated. This research developed and fabricated a lab-scale shovel model with inherent time-varying behaviours. The shovel model was designed with similarity analysis and has been conducted a validation process before experiments. Statistical parameters, power spectrum analysis and Short-Time Fourier transform have been applied to detect bolt looseness and shaft wear in the system and their effectiveness and limitation have also been discussed. This research provided a lab-scale shovel with a potential for fault detection and it can also be improved in the aspects of physical modelling and fault diagnosis.

Bibliography

[1]   M. A. Raza and S. Frimpong, "Mechanics of electric rope shovel performance and reliability in formation excavation," *Lagrangian mechanics*, pp. 107–133, 2017.

[2]   N. Yousefi, "System level monitoring for time-varying conditions with application to ground engaging equipment," 2015.

[3]   J. Rodríguez, L. Morán, J. Pontt, J. Espinoza, R. Díaz, and E. Silva, "Operating experience of shovel drives for mining applications," *IEEE Transactions on Industry Applications*, vol. 40, no. 2, pp. 664–671, 2004.

[4]   W. E. Allen and J. N. Sundermeyer, "A structural health monitoring system for earthmoving machines," in *2005 IEEE International Conference on Electro Information Technology*, IEEE, 2005, 5–pp.

[5]   Y Yin, G. Grondin, K. Obaia, and A. Elwi, "Fatigue life prediction of heavy mining equipment. part 1: Fatigue load assessment and crack growth rate tests," *Journal of Constructional Steel Research*, vol. 63, no. 11, pp. 1494–1505, 2007.

[6]   B. S. Dhillon, *Mining equipment reliability*. Springer, 2008.

[7]   R. A. Hall and L. K. Daneshmend, "Reliability modelling of surface mining equipment: Data gathering and analysis methodologies," *International journal of surface mining, reclamation and environment*, vol. 17, no. 3, pp. 139–155, 2003.

[8]   D. J. Edwards, G. D. Holt, and F. C. Harris, "Predicting downtime costs of tracked hydraulic excavators operating in the uk opencast mining industry," *Construction Management & Economics*, vol. 20, no. 7, pp. 581–591, 2002.

[9]   J. Trout, *Vibration analysis explained*, https://www.reliableplant.com/vibration-analysis-31569, 2020.

[10] R. B. Randall, *Vibration-based condition monitoring: industrial, aerospace and automotive applications*. John Wiley & Sons, 2011.

[11] M. Lipsett and R. Y. Moghaddam, "Modeling excavator-soil interaction," in *Bifurcations, Instabilities and Degradations in Geomaterials*, Springer, 2011, pp. 347–366.

[12] S. Blouin, A. Hemami, and M. Lipsett, "Review of resistive force models for earthmoving processes," *Journal of Aerospace Engineering*, vol. 14, no. 3, pp. 102–111, 2001.

[13] A Hemami, S Goulet, and M Aubertin, "Resistance of particulate media to excavation: Application to bucket loading," *International Journal of Surface Mining and Reclamation*, vol. 8, no. 3, pp. 125–129, 1994.

[14] A. N. Zelenin, V. I. Balovnev, I. P. Kerov, *et al.*, "Machines for moving the earth.," *Machines for moving the earth.*, 1986.

[15] L Daneshmend, C Hendricks, S Wu, and M Scoble, "Design of a mining shovel simulator," *Innovative mine design for the 21st century*, pp. 551–561, 1993.

[16] C Hendricks, L Daneshmend, S Wu, and M Scoble, "Design of a simulator for productivity analysis of electric mining shovels," in *Proc., 2nd Int. Symp. on Mine Mechanization and Automation*, 1993, pp. 329–336.

[17] P. Vähä and M. Skibniewski, "Dynamic model of excavator," *Journal of aerospace engineering*, vol. 6, no. 2, pp. 148–158, 1993.

[18] S. Frimpong and Y. Hu, "Intelligent cable shovel excavation modeling and simulation," *International Journal of Geomechanics*, vol. 8, no. 1, pp. 2–10, 2008.

[19] S. Frimpong, Y. Hu, and K. Awuah-Offei, "Mechanics of cable shovel-formation interactions in surface mining excavations," *Journal of terramechanics*, vol. 42, no. 1, pp. 15–33, 2005.

[20] A. Koivo, M Thoma, E Kocaoglan, and J Andrade-Cetto, "Modeling and control of excavator dynamics during digging operation," *Journal of aerospace engineering*, vol. 9, no. 1, pp. 10–18, 1996.

[21] A. Koivo, "Kinematics of excavators (backhoes) for transferring surface material," *Journal of Aerospace Engineering*, vol. 7, no. 1, pp. 17–32, 1994.

[22] H Araya, M Kakuzen, N Kimura, and N Hayashi, "Automatic control system for hydraulic shovels," in *Proc., USA-Japan Symp. on Flexible Automation—Crossing Bridges: Advances in Flexible Automation and Robotics*, 1988.

[23] N. Shi, *A new approach to improving cable shovel dipper design for cutting soft rock and soils*. ProQuest, 2008.

[24] R. Rasimarzabadi, "Granular material flow into cable shovel dippers," 2016.

[25] J. Hadjigeorgiou, "Studies of machine-ground interaction in surface mines," PhD thesis, McGill University Libraries, 1993.

[26] N. Goodman, *Ways of worldmaking*. Hackett Publishing, 1978, vol. 51.

[27] S. J. Kline, *Similitude and approximation theory*. Springer Science & Business Media, 2012.

[28] H. L. Langhaar, *Dimensional analysis and theory of models*, BOOK. Robert E. Krieger publishing company, 1980.

[29] C. P. Coutinho, A. J. Baptista, and J. D. Rodrigues, "Reduced scale models based on similitude theory: A review up to 2015," *Engineering Structures*, vol. 119, pp. 81–94, 2016.

[30] E. Szücs, *Similitude and modelling*. Elsevier, 2012.

[31] G. J. Simitses and J. Rezaeepazhand, "Structural similitude and scaling laws for laminated beam-plates," 1992.

[32] P. D. Tomlingson, *Equipment management: Key to equipment reliability and productivity in mining*. SME, 2009.

[33] R. Kothamasu, S. H. Huang, and W. H. VerDuin, "System health monitoring and prognostics—a review of current paradigms and practices," *The International Journal of Advanced Manufacturing Technology*, vol. 28, no. 9-10, pp. 1012–1024, 2006.

[34] C. Scheffer and P. Girdhar, *Practical machinery vibration analysis and predictive maintenance*. Elsevier, 2004.

[35] *Introduction to predictive maintenance with matlab*, https://de.mathworks.com/content/dam/mathworks/ebook/predictive-maintenance-ebook-part1.pdf, 2019.

[36] U. Kumar and S. Granholm, "Reliability centred maintenance: A tool for higher profitability," *Maintenance*, vol. 5, no. 3, pp. 23–26, 1990.

[37] H. Sandtorv and M. Rausand, "Rcm-closing the loop between design and operation reliability," in *Reliability Data Collection and Analysis*, Springer, 1992, pp. 265–281.

[38] A. K. Jardine, D. Lin, and D. Banjevic, "A review on machinery diagnostics and prognostics implementing condition-based maintenance," *Mechanical systems and signal processing*, vol. 20, no. 7, pp. 1483–1510, 2006.

[39] Y. Zhao, F. Xiao, J. Wen, Y. Lu, and S. Wang, "A robust pattern recognition-based fault detection and diagnosis (fdd) method for chillers," *HVAC&R Research*, vol. 20, no. 7, pp. 798–809, 2014.

[40] *Damage monitor*, http://www.cadetech.cl/en/productos/damage-monitor/index.html, 2012.

[41] *Siamflex-ms*, http://www.cadetech.cl/en/productos/siamflex/index.html, 2012.

[42] D. Nower, *Online vibration monitoring on electric mining shovels*, 2015.

[43] *Prevail remote health monitoring highlights*, https://mining.komatsu/technology/mining-intelligence/prevail-remote-health-monitoring-system, 2019.

[44] M. Timusk, M. Lipsett, and C. K. Mechefske, "Fault detection using transient machine signals," *Mechanical Systems and Signal Processing*, vol. 22, no. 7, pp. 1724–1749, 2008.

[45] M. A. Timusk, M. G. Lipsett, J. McBain, and C. K. Mechefske, "Automated operating mode classification for online monitoring systems," *Journal of vibration and acoustics*, vol. 131, no. 4, 2009.

[46] J. McBain and M. Timusk, "Fault detection in variable speed machinery: Statistical parameterization," *Journal of Sound and Vibration*, vol. 327, no. 3-5, pp. 623–646, 2009.

[47] W Bartelmus and R Zimroz, "A new feature for monitoring the condition of gearboxes in non-stationary operating conditions," *Mechanical Systems and Signal Processing*, vol. 23, no. 5, pp. 1528–1534, 2009.

[48] A. Wyłomańska, J. Obuchowski, R. Zimroz, and H. Hurd, "Periodic autoregressive modeling of vibration time series from planetary gearbox used in bucket wheel excavator," in *Cyclostationarity: Theory and Methods*, Springer, 2014, pp. 171–186.

[49] C. M. Vicuňa, "Effects of operating conditions on the acoustic emissions (ae) from planetary gearboxes," *Applied Acoustics*, vol. 77, pp. 150–158, 2014.

[50] S. K. Sar and R. Kumar, "Techniques of vibration signature analysis," *International Journal of Advanced Research in Computer and Communication Engineering*, vol. 4, no. 3, pp. 240–243, 2015.

[51] B. Peterson, "General introduction to vibration," in *Handbook of noise and vibration control*, John Wiley and Sons, New Jersey, 2007, pp. 171–179.

[52] P. Flores, C. Koshy, H. M. Lankarani, J. Ambrósio, and J. C. P. Claro, "Numerical and experimental investigation on multibody systems with revolute clearance joints," *Nonlinear Dynamics*, vol. 65, no. 4, pp. 383–398, 2011.

[53] R. Haines, "An experimental investigation into the dynamic behaviour of revolute joints with varying degrees of clearance," *Mechanism and Machine Theory*, vol. 20, no. 3, pp. 221–231, 1985.

[54] S Dubowsky, M Norris, E Aloni, and A Tamir, "An analytical and experimental study of the prediction of impacts in planar mechanical systems with clearances," 1984.

[55] P. Flores, J. Ambrósio, J. P. Claro, and H. Lankarani, "Influence of the contact—impact force model on the dynamic response of multi-body systems," *Proceedings of the Institution of Mechanical Engineers, Part K: Journal of Multi-body Dynamics*, vol. 220, no. 1, pp. 21–34, 2006.

[56] P. Flores, "A parametric study on the dynamic response of planar multibody systems with multiple clearance joints," *Nonlinear dynamics*, vol. 61, no. 4, pp. 633–653, 2010.

[57] M. A. Khan, M. A. Shahid, S. A. Ahmed, S. Z. Khan, K. A. Khan, S. A. Ali, and M. Tariq, "Gear misalignment diagnosis using statistical features of vibration and airborne sound spectrums," *Measurement*, vol. 145, pp. 419–435, 2019.

[58] R. G. Jones, "The mathematical modelling of gearbox vibration under applied lateral misalignment," PhD thesis, University of Warwick, 2012.

[59] H. Yang, J. Mathew, and L. Ma, "Vibration feature extraction techniques for fault diagnosis of rotating machinery: A literature survey," 2003.

[60] M. Lebold, K. McClintic, R. Campbell, C. Byington, and K. Maynard, "Review of vibration analysis methods for gearbox diagnostics and prognostics," in *Proceedings of the 54th meeting of the society for machinery failure prevention technology*, vol. 634, 2000, p. 16.

[61] A. K. Nandi and H. Ahmed, *Condition Monitoring with Vibration Signals: Compressive Sampling and Learning Algorithms for Rotating Machines*. John Wiley & Sons, 2020.

[62] S. Singh and D. M. Vishwakarma, "A review of vibration analysis techniques for rotating machines," *International Journal of Engineering Research & Technology*, vol. 4, no. 03, pp. 2278–0181, 2015.

[63] G. Gelle, M. Colas, and C. Servière, "Blind source separation: A new preprocessing tool for rotating machines monitoring?" *IEEE Transactions on Instrumentation and Measurement*, vol. 52, no. 3, pp. 790–795, 2003.

[64] A. Brandt, *Noise and vibration analysis: signal analysis and experimental procedures*. John Wiley & Sons, 2011.

[65] J. Semmlow, *Circuits, signals and systems for bioengineers: A MATLAB-based introduction*. Academic Press, 2017.

[66] A. K. Nandi, C. Liu, and M. D. Wong, "Intelligent vibration signal processing for condition monitoring," in *Proceedings of the International Conference Surveillance*, vol. 7, 2013, pp. 1–15.

[67] E. G. Strangas, S. Aviyente, and S. S. H. Zaidi, "Time–frequency analysis for efficient fault diagnosis and failure prognosis for interior permanent-magnet ac motors," *IEEE Transactions on Industrial Electronics*, vol. 55, no. 12, pp. 4191–4199, 2008.

[68] A. Belšak and J. Prezelj, "Analysis of vibrations and noise to determine the condition of gear units," *Advances in Vibration Analysis Research*, p. 315, 2011.

[69] H.-C. Lin, Y.-C. Ye, B.-J. Huang, and J.-L. Su, "Bearing vibration detection and analysis using enhanced fast fourier transform algorithm," *Advances in Mechanical Engineering*, vol. 8, no. 10, p. 1 687 814 016 675 080, 2016.

[70] A Primer, C. S. Burrus, and R. A. Gopinath, *Introduction to wavelets and wavelet transforms*, 1998.

[71] N. E. Huang, "Introduction to hilbert-huang transform and some recent developments," in *The Hilbert-Huang Transform in Engineering*, CRC Press, 2005, pp. 10–32.

[72] R. Isermann, *Fault-diagnosis applications: model-based condition monitoring: actuators, drives, machinery, plants, sensors, and fault-tolerant systems.* Springer Science & Business Media, 2011.

[73] G Meltzer and Y. Y. Ivanov, "Fault detection in gear drives with non-stationary rotational speed-part i: The time-frequency approach," *Mechanical Systems and Signal Processing*, vol. 17, no. 5, pp. 1033–1047, 2003.

[74] D. Zhen, J. Guo, Y. Xu, H. Zhang, and F. Gu, "A novel fault detection method for rolling bearings based on non-stationary vibration signature analysis," *Sensors*, vol. 19, no. 18, p. 3994, 2019.

[75] P. MinePro, *Peak performance practices: Excavator selection*, 2003.

[76] *P&h 4100xpc product overview*, https://mining.komatsu/docs/default-source/product-documents/surface/electric-rope-shovels/4100xpc-dc-brochure.pdf?sfvrsn=5e470a6b_48, 2018.

[77] *4100xpc electric mining shovel digital ac drive control*, http://cdn.thomasnet.com/ccp/00989656/119254.pdf, 2011.

[78] *Make the most of servo motor efficiency*, https://www.designworldonline.com/make-the-most-of-servo-motor-efficiency/, 2007.

[79] *Faq: How do i calculate the inertia of a servo-driven system?* https://www.motioncontroltips.com/faq-how-do-i-calculate-the-inertia-of-a-servo-driven-system/#:~:text=While%20it%20seems%20logical%20that,successfully%20at%20much%20higher%20ratios, 2016.

[80] *Tc3 motion designer*, https://download.beckhoff.com/download/document/motion/tcmotiondesigner_ba_en.pdf, 2017.

[81] *Motor sizing basics part 2: Load inertia*, https://blog.orientalmotor.com/motor-sizing-basics-part-2-load-inertia, 2020.

[82] *Ethercat - the ethernet fieldbus*, https://www.ethercat.org/en/technology.html, 2020.

[83] *Ethercat - the ethernet fieldbus brochure*, https://www.ethercat.org/download/documents/ETG_Brochure_EN.pdf, 2020.

[84] *Ethercat data transmission*, http://www.tpm-pac.com/EtherCAT, 2020.

[85] *Why use ethercat*, https://www.ethercat.org/en/why_use_ethercat.htm, 2020.

[86] *Ethercat: What are the user benefits*, http://www.ethercat.org/2011/us/seminar_download/files/ethercat_us_2011_04_userbenefits.pdf, 2011.

[87] *Introduction to data acquisition and signal conditioning*, https://www.industrial-electronics.com/DAQ/signal-conditioning.html, 2020.

[88] *Measuring vibration with accelerometers*, https://www.ni.com/en-ca/innovations/white-papers/06/measuring-vibration-with-accelerometers.html, 2020.

[89]   *Applications of vibration transducers*, https://rotorlab.tamu.edu/me617/Vibration%20Sensors%202012.pdf, 2012.

[90]   *High-sensitivity triaxial ccld accelerometer type 4506-b-003*, https://www.bksv.com/media/doc/Bp1838.pdf, 2020.

[91]   *Miniature triaxial piezoelectric ccld accelerometer, teds, 500mv/g, excl. cable.* https://www.bksv.com/en/products/transducers/vibration/accelerometers/4506-B-003, 2020.

[92]   *Understanding signal conditioning*, https://www.windmill.co.uk/signal-conditioning.html, 2016.

[93]   S. Donders, V. Verdult, and M. Verhaegen, "Fault detection and identification for wind turbine systems: A closed-loop analysis," *Master's thesis, University of Twente*, 2002.

[94]   *Why do bolts loosen?* https://www.nord-lock.com/insights/, 2020.

[95]   *Stainless steel fasteners - pre-load and tightening torques*, https://www.trfastenings.com/products/knowledgebase/stainless-steel-fasteners/pre-load-and-tightening-torques-coarse-metric-threads, 2020.

[96]   *Signal features*, https://www.mathworks.com/help/predmaint/ug/signal-features.html, 2020.

[97]   H. Ahmed and A. K. Nandi, *Condition Monitoring with Vibration Signals*. Wiley Online Library, 2019.

[98]   *Pspectrum*, https://www.mathworks.com/help/signal/ref/pspectrum.html#d122e124210, 2020.

[99]   *Stft*, https://www.mathworks.com/help/signal/ref/stft.html#mw_18811b9a-fc97-4bce-a361-4f7e71b414c2, 2020.

[100] B. Nayana and P Geethanjali, "Analysis of statistical time-domain features effectiveness in identification of bearing faults from vibration signal," *IEEE Sensors Journal*, vol. 17, no. 17, pp. 5618–5625, 2017.

[101] C. Altın and O. Er, "Comparison of different time and frequency domain feature extraction methods on elbow gesture's emg," *European journal of interdisciplinary studies*, vol. 2, no. 3, pp. 35–44, 2016.

[102] *Kurtosis*, https://corporatefinanceinstitute.com/resources/knowledge/other/kurtosis/, 2020.

[103] V. Venkatasubramanian, R. Rengaswamy, S. N. Kavuri, and K. Yin, "A review of process fault detection and diagnosis: Part iii: Process history based methods," *Computers & chemical engineering*, vol. 27, no. 3, pp. 327–346, 2003.

[104] S Patnayak and D. Tannant, "Performance monitoring of electric cable shovels," *International Journal of Surface Mining, Reclamation and Environment*, vol. 19, no. 4, pp. 276–294, 2005.

[105] *How to specify: Servo systems*, https://tigerquest.com/how%20to%20specify/ Servo%20Systems.php, 2021.

[106] *Moment of inertia j calculation formula*, https://www.mikipulley.co.jp/EN/ Services/Tech_data/tech24.html, 2021.

[107] *Rolling element bearing components and failing frequencies*, https://power-mi.com/content/rolling-element-bearing-components-and-failing-frequencies, 2021.

[108] C. B. Chapman and M. Pinfold, "Design engineering—a need to rethink the solution using knowledge based engineering," *Knowledge-based systems*, vol. 12, no. 5-6, pp. 257–267, 1999.

Appendix A: Dynamic Modelling of Cable Shovel

Dynamic modelling is an important aspect indicating the work mechanism and performance of cable shovels. S. Frimpong developed a fully comprehensive dynamic modelling of the earth moving machine[19] and the dynamic equation is shown below,

$$D(\boldsymbol{\Theta})\ddot{\boldsymbol{\Theta}} + C(\boldsymbol{\Theta}, \dot{\boldsymbol{\Theta}})\dot{\boldsymbol{\Theta}} + G(\boldsymbol{\Theta}) = F - F_{\text{load}}\left(F_{\text{t}}, F_{\text{n}}\right) \tag{A.1}$$

where $D(\boldsymbol{\Theta})$,$C(\boldsymbol{\Theta}, \dot{\boldsymbol{\Theta}})$ and $G(\boldsymbol{\Theta})$ represents the generalized inertia matrix, Coriolisand centripetal torque, and gravity torque respectively. $\boldsymbol{\Theta}$ is the vector of generalized variables. F is the cable shovel's breakout force and $F_{\text{load}}\left(F_{\text{t}}, F_{\text{n}}\right)$ represents the resistive force during the dipper-soil digging process. For a cable shovel, the variables in the dynamic equation are summarized from Equation A.2 to Equation A.5.

$$D(\Theta) = \begin{bmatrix} m_1 + m_2 & -m_2 d_2 s_{2c_2} \\ -m_2 d_2 s_{2c_2} & I_{zz1} + I_{zz2} + m_1 d_1^2 + m_2 \left(l_1^2 + 2l_1 d_1 c_{2c_2} + d_1^2\right) \end{bmatrix} \tag{A.2}$$

$$C(\boldsymbol{\Theta}, \dot{\boldsymbol{\Theta}}) = \begin{bmatrix} 0 & -\left(m_1 d_1 + m_2 \left(l_1 + d_2 c_{2c_2}\right)\right)\dot{\theta}_1 \\ 2\left(m_1 d_1 + m_2 \left(l_1 + d_2 c_{2c_2}\right)\right)\dot{\theta}_1 & 0 \end{bmatrix} \tag{A.3}$$

$$G(\boldsymbol{\Theta}) = \begin{bmatrix} \left(m_1 + m_2\right) g s_1 \\ \left(m_1 d_1 c_1 + m_2 \left(l_1 c_1 + d_2 c_{12c_2}\right)\right) g \end{bmatrix} \tag{A.4}$$

$$F_{\text{load}}\left(F_{\text{t}}, F_{\text{n}}\right) = \begin{bmatrix} F_{\text{t}} c_{2\theta_{\text{b}}} - F_{\text{n}} s_{2\theta_{\text{b}}} \\ F_{\text{t}}\left(l_1 + l_2\right) s_{2\theta_{\text{b}}} + F_{\text{n}}\left(l_1 + l_2\right) c_{2\theta_{\text{b}}} \end{bmatrix} \tag{A.5}$$

The nomenclature for the variables in the dynamic modelling equation is summarized in Table A.1.

Table A.1: List of Symbol for Variables in Dynamic Modelling Equation

Symbol	Description
m_1	mass of crowd arm
m_2	mass of dipper
c_i, s_i	$cos(\theta_i)$ and $sin(\theta_i)$, respectively
c_{ij}, s_{ij}	$cos(\theta_i + \theta_j)$ and $sin(\theta_i + \theta_j)$, respectively
I_{zz1}	moment of inertia of crowd arm about centroidal axis parallel to z_1-axis
I_{zz2}	moment of inertia of dipper about centroidal axis parallel to z_2-axis
l_1	length of of crowd arm from pivotal point to connection point between arm and dipper in Figure 2.2
l_2	length between dipper tip and connect point of arm and dipper in Figure 2.2
d_1	displacement between O_1 and C_1 in Figure 2.2
d_2	displacement between O_2 and C_2 in Figure 2.2
F_t	tangential reaction force
F_n	normal reaction force

Appendix B: Statistical Parameters in Time Domain

The statistical features that can be applied in the time-domain are summarized as follows[2, 100, 101],

1. ***Mean Absolute Value (MAV)***: the absolute average of data for a segment of length L.

$$\text{MAV} = \frac{1}{L} \sum_{i=1}^{L} |y_i| \tag{B.1}$$

2. ***Root Mean Square (RMS)***: RMS measures the power content in the vibration signature. RMS is a basic approach to measuring defects in the time domain but is not sensitive enough for incipient fault detection.

$$\text{RMS} = \sqrt{\frac{1}{N} \sum_{i=1}^{L} |y_i|^2} \tag{B.2}$$

3. ***Mean***: it finds the mean of the amplitude values over a sample length of the signal, it is also the first moment of the probability distribution function (pdf).

$$\text{M} = \frac{1}{L} \sum_{i=1}^{L} y_i \tag{B.3}$$

4. ***Variance (VAR)***: VAR indirectly measures the data distribution from the mean of the segment, and it is also the second central moment of a distribution.

$$VAR = \frac{1}{L} \sum_{i=1}^{L} |y_i - \mu|^2 \tag{B.4}$$

where

$$\mu = \frac{1}{L} \sum_{i=1}^{L} y_i \tag{B.5}$$

5. **Standard Deviation (STD)**: STD is the positive square root of the VAR to measure the variation of the data segment.

$$STD = \sqrt{\frac{1}{L}\sum_{i=1}^{L}|y_i - \mu|^2} \qquad (B.6)$$

6. **Skewness (SKW)**: SKW is the third moment of the distribution, to measure the asymmetry of the probability distribution about its mean.

$$\text{SKW} = \frac{\frac{1}{L}\sum_{i=1}^{L}|y_i - \mu|^3}{(\sqrt{\frac{1}{L}\sum_{i=1}^{L}|y_i - \mu|^2})^3} \qquad (B.7)$$

The relationship between the skewness value and asymmetry of the distribution is summarized as follows:

(a) if the absolute value of skewness is between 0 and 0.5, the data are fairly symmetrical;

(b) if the absolute value of skewness is between 0.5 and 1, the data are moderately skewed;

(c) if the absolute value of skewness is greater than 1, the data are highly skewed.

7. **Kurtosis (KURT)**: KURT is defined as the fourth moment of the pdf and measures the relative peakedness or flatness of distribution as compared to a normal distribution. KURT can also provide a measure of the size of the tails of the distribution.

$$\text{KURT} = \frac{\frac{1}{L}\sum_{i=1}^{L}|y_i - \mu|^4}{\left(\frac{1}{L}\sum_{i=1}^{L}|y_i - \mu|^2\right)^2} \qquad (B.8)$$

If the kurtosis value is zero or close to zero, it follows a mesokurtic distribution; if a positive excess kurtosis is obtained, it follows a leptokutic distribution; if a negative excess kurtosis is obtained, then it follows a platykurtic distribution, which are shown in Figure B.1.

When the number of features is large, multivariate statistical techniques can be utilized to compress data and reduce the dimensionality so that essential information

121
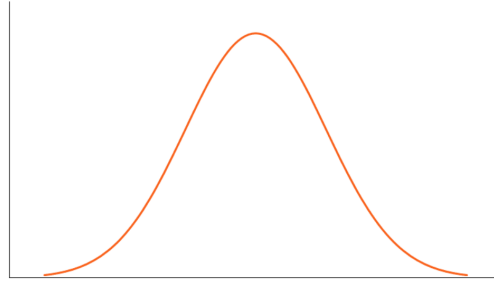
(a) Mesokurtic
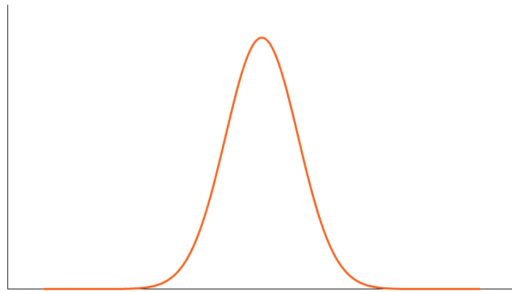
(b) Leptokurtic
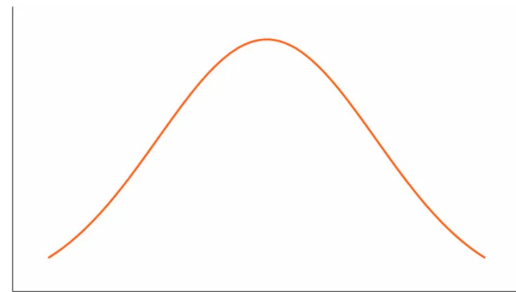
(c) Platykurtic

Figure B.1: Shapes of Distribution for Various Kurtosis [102]

is retained while background noise is eliminated. The main function of multivariate statistical techniques is to transform a number of related process variables into a smaller set of uncorrelated variables. Principal Component Analysis (PCA) is an important method in multivariate statistical techniques, it can locate factors with a lower dimension than the original data set which can fully describe the major trends in the original one[103].

Appendix C: Frequency Spectrum Statistical Features

Frequency domain features allow investigating the failure modes for mining equipment. Frequency spectrum statistical features allow a quick overview of a machine's condition without specific diagnostic capacity[66]. The common frequency spectrum statistical techniques, listed in Table C.1, are summarized by Nandi et.al.[61] and described in detail below,

Table C.1: Common Frequency Spectrum Statistical Feature

Frequency Spectrum Statistical Features	Formula
Arithmetic Mean	$\hat{x}(w) = 20 \log \left\{ \frac{\frac{1}{N} \sum_N A_n}{10^{-5}} \right\}$
Geometric Mean	$\hat{x}_{geo}(w) = \left\{ \sum_N 20 \log \left(\frac{\frac{A_n}{\sqrt{2}}}{10^{-5}} \right) \right\}$
Matched Filter RMS	$M_{frms} = 10 \log \left\{ \frac{1}{N} \sum_N \left(\frac{A_i}{A_n^{ref}} \right) \right\}$
The RMS of Spectral Difference	$R_d = \sqrt{\left\{ \frac{1}{N} \sum_N \left(P_n - P_n^{ref} \right)^2 \right\}}$
The Sum of Squares Spectral Difference	$S_d = \frac{1}{N} \sum_N \sqrt{\left(P_n + P_n^{ref} \right) * \left| P_n - P_n^{ref} \right|}$

1. **_Arithmetic Mean_**: the arithmetic mean of a frequency spectrum can be defined as,

$$\widehat{x}(w) = 20 \log \left\{ \frac{\frac{1}{N} \sum_N A_n}{10^{-5}} \right\} \tag{C.1}$$

where $\widehat{x}(w)$ represents the arithmetic mean in dBm, A_n denotes the amplitude of the nth component in a total of N components.his feature can provide the average amplitude value within the frequency range.

2. **Geometric Mean**: The geometric mean is an alternative representation of the arithmetic mean, which can be expressed below,

$$\widehat{x}_{geo}(w) = \left\{ \sum_N 20 \log \left(\frac{\frac{A_n}{\sqrt{2}}}{10^{-5}} \right) \right\} \tag{C.2}$$

3. **Matched Filter RMS**: The matched filter root mean square (RMS) requires a reference spectrum. The matched filter RMS gives the RMS amplitude of the frequency components with reference to the reference spectrum and is expressed using the following equation,

$$M_{frms} = 10 \log \left\{ \frac{1}{N} \sum_N \left(\frac{A_i}{A_n^{ref}} \right) \right\} \tag{C.3}$$

here A_n^{ref} denotes the nth component of the reference spectrum.

4. **The RMS of Spectral Difference**: The RMS of the spectrum can be computed using the following equation,

$$R_d = \sqrt{\left\{ \frac{1}{N} \sum_N \left(P_n - P_n^{ref} \right)^2 \right\}} \tag{C.4}$$

where P_n and P_n^{ref} represent the amplitude (in dB) of the incident and reference spectra respectively.

5. **The Sum of Squares of Spectral Difference**: The sum of squares of spectral difference provides greater weight to high-amplitude components and can be expressed as follows,

$$S_d = \frac{1}{N} \sum_N \sqrt{\left(P_n + P_n^{ref} \right) * \left| P_n - P_n^{ref} \right|} \tag{C.5}$$

Appendix D: Finite Element Analysis of the Shaft Looseness Fault

A finite element analysis has been conducted to investigate the impact of the shaft looseness fault for preliminary study. Solidworks simulation tool was used to simulate the fault's effect. Before setting up the simulation, the model needs to be simplified: important features will stay but unrelated parts will be left out. The simplified model is shown in Figure D.1. Prior to the simulation, assumptions and constraints were
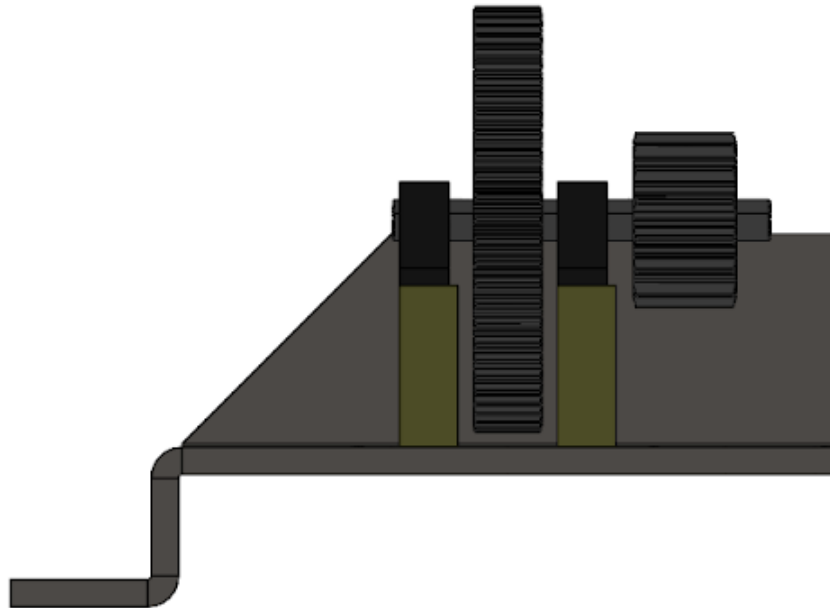
Figure D.1: Simplified Model for Shaft Looseness Simulation

made, which can be categorized into four areas including fixture, external loads, parts constraints and mesh and are shown in Table D.1

Table D.1: Assumptions and Constraints for the Shaft Looseness Simulation

Category	Assumptions and Constraints
Fixture	Bearing Support for Bearing; Fixed Geometry for Bearing Blocks
External Loads	Centrifugal Speed 1.25 rad/s for Shaft
Parts Constraints	Plate for Mounting Marked as Rigid
Mesh	Middle

The shaft looseness fault has been well discussed in section 5.2.2. Here the good shaft and faulty shafts for the FEM simulation are illustrated in Figure D.2. The comparison of stress analysis, displacement and strain simulations for the good shaft and faulty shafts are shown in Figure D.3, D.4 and D.5 respectively. From displacement analysis, it appears that the faulty shaft will not cause the system to vibrate drastically. It acts normally but the fault starts to grow which is a good scenario for the fault detection. According to the Figure D.3 and D.5, faulty shaft will cause more stress and strain around the bearing corners and bearing blocks. Among the FEM analysis, it would be a good idea to install the accelerometer on the bearing block where the vibration change can tell the severity of shaft wear condition.

(a)

(b)
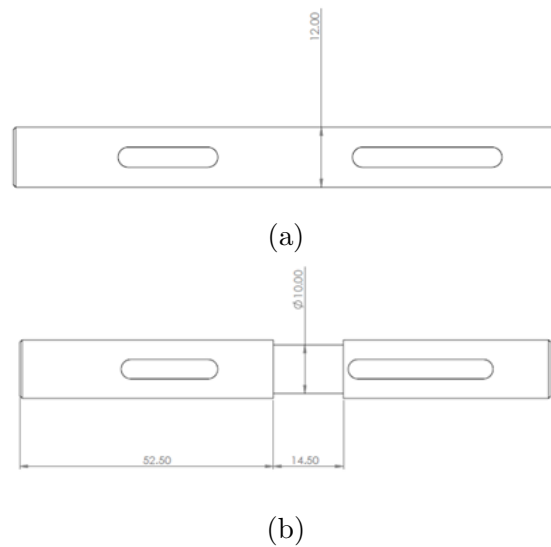
Figure D.2: Good Shaft and Faulty Used in the FEM Simulation
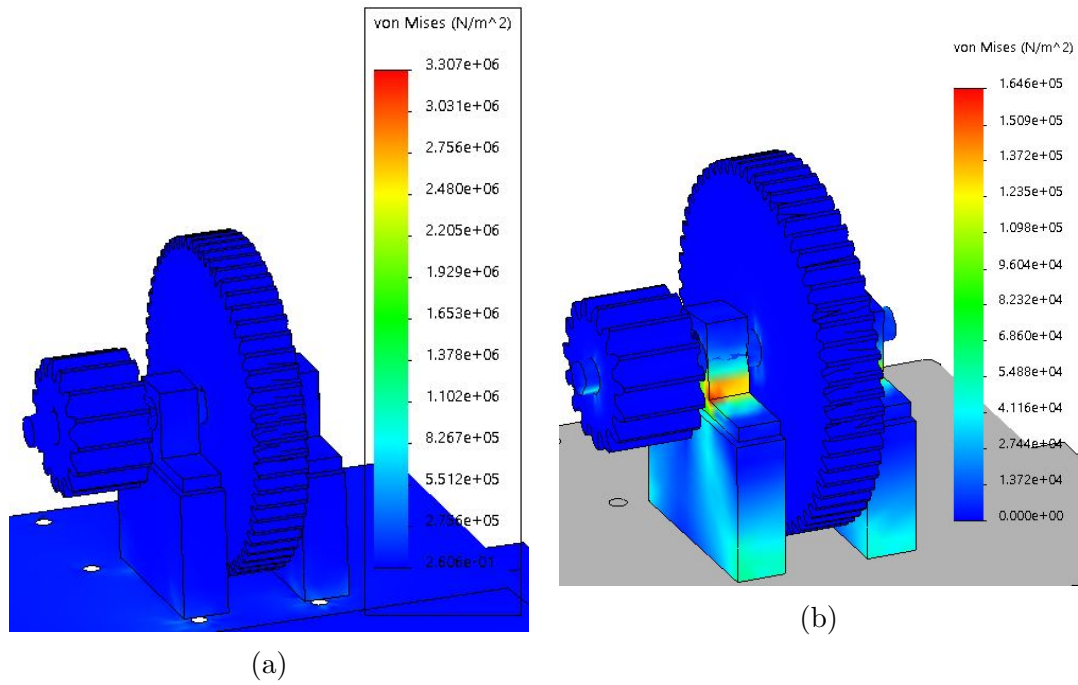
Figure D.3: Stress Analysis for Good Shaft and Faulty Shaft
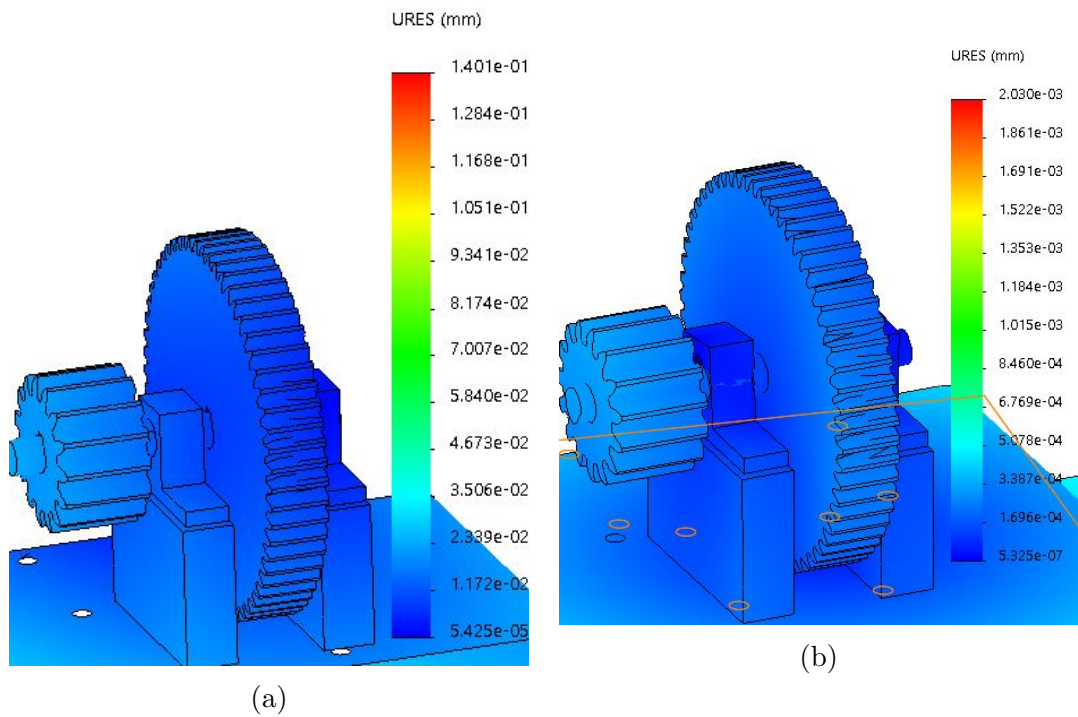
Figure D.4: Displacement Analysis for Good Shaft and Faulty Shaft

127
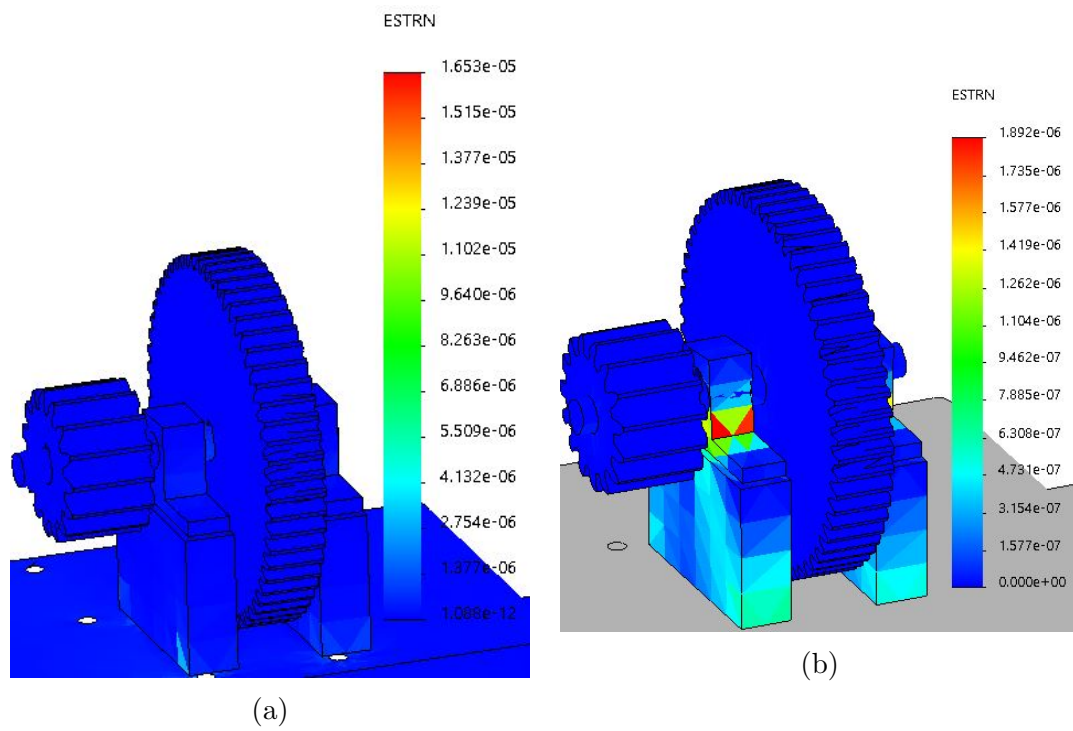
Figure D.5: Strain Analysis for Good Shaft and Faulty Shaft

Appendix E: Full-Size Shovel Linear Velocity Estimation

Even though the physical size of the shovel model is scaled down, the motion characteristics should also be scaled down properly based on the similitude and dimensional analysis. However, important factors of cable shovels such as velocities are classified information; as a result, the velocity information needs to be calculated from two aspects of collected data: moving distance and process time. P&H 4100 XPC cable shovel's component moving distance can be estimated from its brochure provided by the manufacturer, which is shown in Figure E.1.
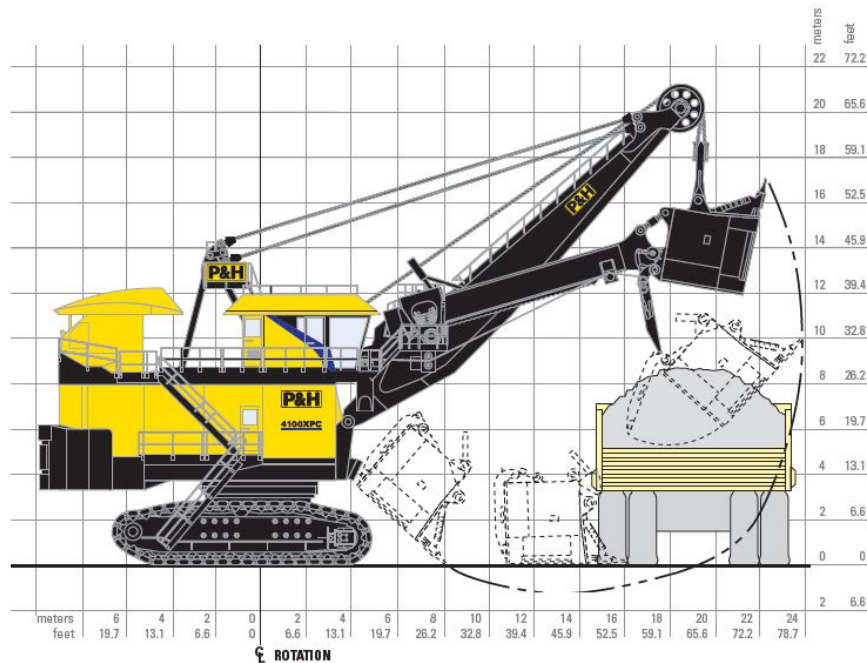
Figure E.1: P&H 4100 XPC General Specifications[76]

S. Pantnayak and D. Tannant have done magnificent research on activities recog-

nition of mining shovels, especially the model used in this experiment, P&H 4100 series[104]. Various shovel activities include digging, hoisting, swinging, dumping, waiting, etc, which are illustrated in Figure E.2.
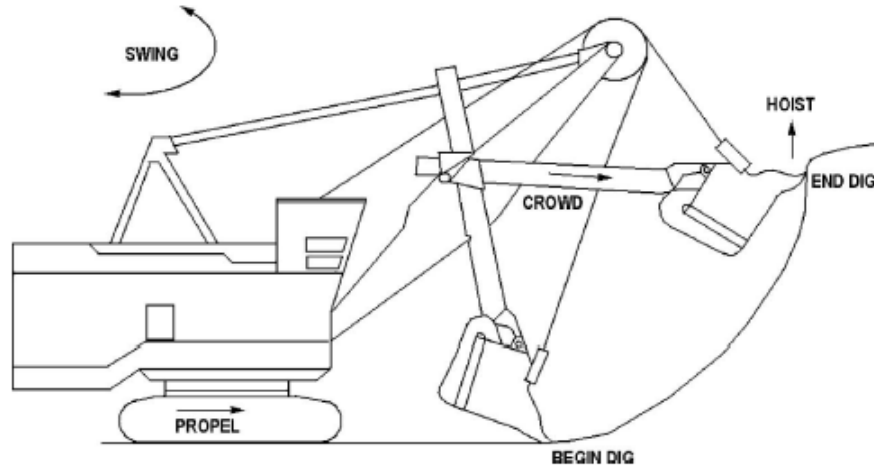
Figure E.2: Common Shovel Activities[104]

The most critical motions involving in common shovel activities are hoisting, crowding and swinging which are actuated by three AC electric motors. Moreover, the speed of the motor is proportional to the voltage and the torque is proportional to the current. In order to have a better understanding of the motions, voltage and current conditions of AC motors can be good indicators for critical parts' moving logic in the duty cycle, which then will be considered as a reference for the automated control algorithm for the model in this experiment.

S. Pantnayak and D. Tannant have collected voltage and current for hoist, crowd and swing armatures for eight different P&H 4100 shovels covering six months, and those data are illustrated in Figure E.3 to E.5. Positive and negative voltages indicate the direction of motor rotation. For the hoist motor, a positive voltage means the dipper is moving upward and a negative voltage means the dipper is moving downward. For the crowd motor, a positive voltage represents the extension of the crowd arm and a negative voltage implies the retraction of the crowd arm. As for the swing motor, the sign of the voltage depends on the position of the truck with respect to the shovel. The change of current flow can alter the speed of the motors: a reversed current flow can cancel out the motor movement usually referred to as plugging[104].
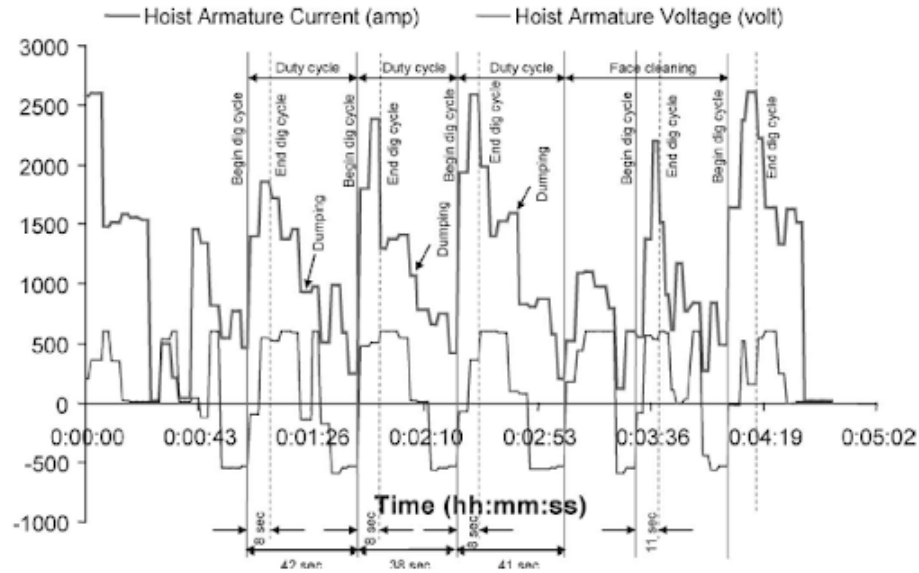
Figure E.3: Hoist Motor Response During Shovel Duty Cycle[104]
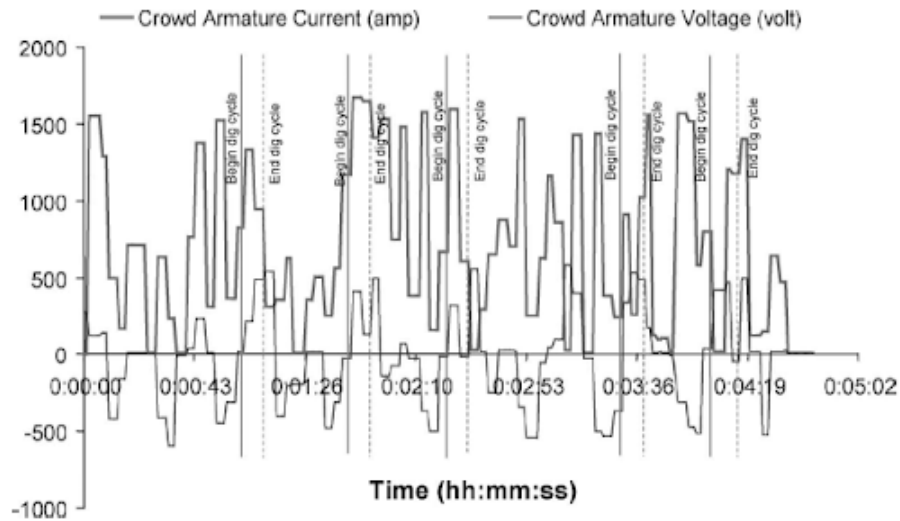
Figure E.4: Crowd Motor Response During Shovel Duty Cycle[104]

According to data recording in Figure E.3 to E.5, the dig cycle time could vary between 6 to 25 seconds. There are various factors affecting the dig cycle time including geological parameters, operator's practice, tooth design, digging trajectory, machine condition, etc. In this experiment, it is reasonable to assume that the dig cycle time is 15 seconds. In an ideal shovel duty cycle, the sequence of activities

131
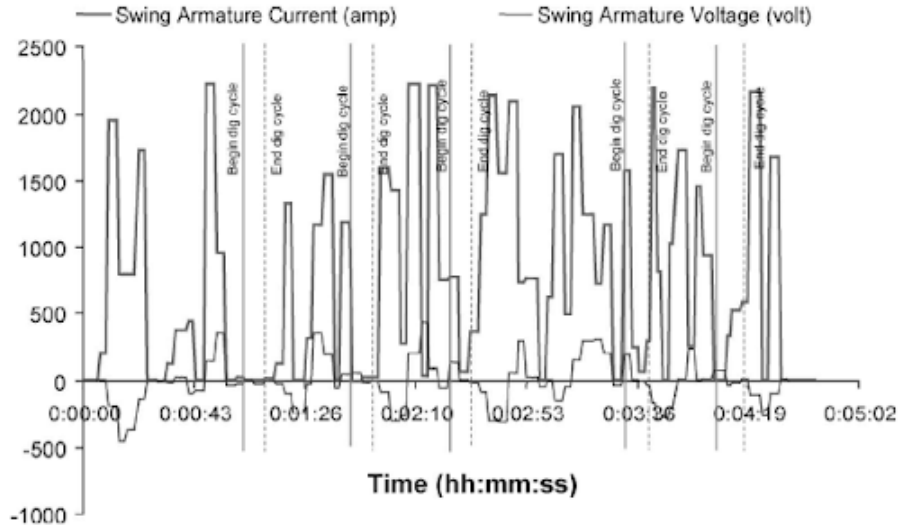
Figure E.5: Swing Motor Response During Shovel Duty Cycle[104]

includes digging, hoisting, swinging the dipper towards the truck, dumping, swinging back to the surface[104]. Despite the fact that there are some extra activities in the real shovel duty cycle such as face cleaning, material loosening, etc, this experiment will assume the duty cycle is ideal. It can also be observed that shovel duty cycle time is around 40 seconds that includes 15 seconds of dig cycle time, 5 seconds of dumping (assumed) and total swinging time. Therefore, the time of swinging towards the truck or swinging back to the face can be assumed to be 10 seconds.

From Figure E.1, it can roughly tell that during the digging process, the dipper is hoisted about 16 m and the crowding distance can be estimated as the dipper handle length which is about 8 m. During the dumping process, it is assumed that the cable shovel has to rotate 90 degrees to reach the dumping location. Therefore, based on the distance travelled by the dipper, the shovel's rotation angle and the working process (time) discussed previously, the velocity of the hoist, crowd and swing systems are summarized in Table E.1.

Table E.1: Summary of Velocity Estimation for P&H 4100 XPC

System	Velocity
Hoist	$1.067m/s$
Crowd	$0.53m/s$
Swing	1.5 RPM

Appendix F: Motor Speed Calculation

In order to satisfy the velocity requirements for the shovel model, the model motors need to be operated at 465 RPM, 1528 RPM and 168 RPM for hoist, crowd and swing systems, respectively. Motor speed calculation along with rotation radius for full-size shovel (R_p) and shovel model (R_m) are discussed as follows.

F.1   Hoist System

Drum Radius:

$$R_D = 0.03 \, \text{m}$$

Hoist Linear Velocity:

$$v_H = 0.073 \, \text{m/s}$$

Angular Velocity of Drum:

$$\omega_D = \frac{v_H}{R_D} = 23.237 \, \text{rpm}$$

Gear Ratio in Hoist System:

$$GR_H = 20$$

Hoist Motor Speed:

$$\omega_H = \omega_D \cdot GR_H = 464.732 \, \text{rpm}$$

F.2   Crowd System

Pinion Radius:

$$R_c = 14 \, \text{mm}$$

Crowd Linear Velocity:

$$v_c = 0.035 \text{ m/s}$$

Angular Velocity of Pinion:

$$\omega_c = \frac{v_c}{R_c} = 23.873 \text{ rpm}$$

Gear Ratio in crowd system:

$$GR_c = 64$$

Crowd Motor Speed:

$$\omega_C = \omega_c \cdot GR_c = 1528 \text{ rpm}$$

F.3   Swing System

Swing Angular Velocity of the Full-Size Machine:

$$\omega_D = 1.5 \text{ rpm}$$

Swing Radius of Full-Size Machine:

$$R_p = 2 \text{ m}$$

Swing Radius of Shovel Model:

$$R_m = 0.095 \text{ m}$$

Swing Angular Velocity of Shovel Model:

$$\omega_m = \frac{\omega_p}{15 \cdot \frac{R_m}{R_p}} = 2.105 \text{ rpm}$$

Gear Ratio in Swing System:

$$GR_s = 80$$

Swing Motor Speed:

$$\omega_s = \omega_m \cdot GR_s = 168.42 \text{ rpm}$$

Appendix G: Inertia Ratio Calculation

Motors are commonly used in common mechanical systems to achieve precise positioning, velocities and torques. To evaluate the motor's ability to effectively control the load, the ratio of the load inertia to the motor inertia plays an important role. The inertia ratio analysis has been conducted for the crowd, hoist and swing systems and the inertia ratios are 3.0, 4.3 and 41.8, respectively. Detailed calculations for three system are presented as follows.

G.1 Inertia Ratio Calculation for Crowd System

G.1.1 Assumption

The crowd system can be simplified into a rack-pinion linear power transmission as shown in Figure G.1.
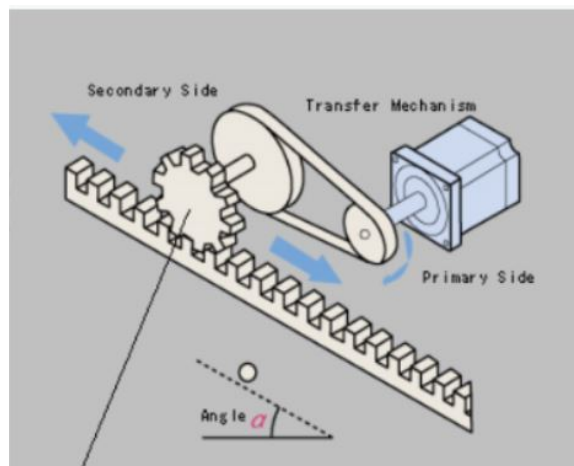
Figure G.1: Rack-Pinion Linear Power Transmission Model[105]

G.1.2 Knowns

Mass of Rack:

$$m = 15 \, \text{kg}$$

Pinion Diameter:

$$D = 28 \, \text{mm}$$

Pinion Mass:

$$m_p = 0.12 \, \text{kg}$$

Transfer Mechanism:

Primary Side Diameter:

$$D_{g1} = 22 \, \text{mm}$$

Secondary Side Diameter:

$$D_{g2} = 49 \, \text{mm}$$

Primary Side Mass:

$$m_{g1} = 1.64 \, \text{kg}$$

Secondary Side Mass:

$$m_{g2} = 4.62 \, \text{kg}$$

Gear Ratio:

$$GR = 64$$

Inertia of Motor:

$$J_M = 0.33 \ \text{kg} \cdot \text{cm}^2$$

G.1.3 Calculations

Pinion Load Inertia:

$$J_p = \frac{1}{8} \cdot m_p \cdot D^2 = \left(1.176 \cdot 10^{-5}\right) \, \text{kg} \cdot \text{m}^2$$

Load Inertia of Rack:

$$J_r = \frac{1}{4} \cdot m \cdot D^2 = 0.002 \, \text{kg} \cdot \text{m}^2$$

Moment of Inertia of the Transfer Mechanism:

$$J_g = \frac{1}{8} \cdot m_{g1} \cdot D_{g1}{}^2 + \frac{1}{8} \cdot m_{g2} \cdot \frac{D_{g2}{}^2}{GR^2} = \left(9.956 \cdot 10^{-5}\right) \, \text{kg} \cdot \text{m}^2$$

Total Load Inertia:

$$J_L = \frac{J_p + J_r}{GR^2} + J_g = \left(1.001 \cdot 10^{-4}\right) \text{ kg} \cdot \text{m}^2$$

Inertia Ratio:

$$IR = \frac{J_L}{J_M} = 3.034$$

G.2 Inertia Ratio Calculation for Hoist System

G.2.1 Assumption

The hoist system can be simplified into 1 gear set model as shown in Figure G.2
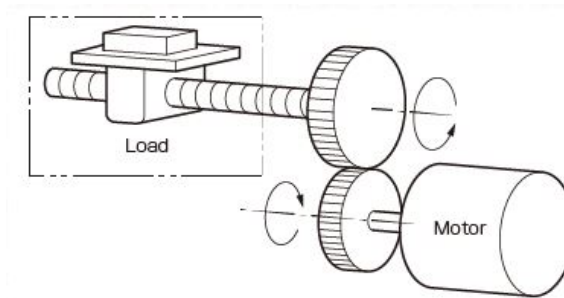
Figure G.2: 1 Gear Set Power Transmission Model[106]

G.2.2 Knowns

Drum Mass:

$$M_d = 5 \text{ kg}$$

Drum Diameter:

$$D_d = 60 \text{ mm}$$

Gear Ratio:

$$GR = 20$$

Inertia of Motor:

$$J_M = 0.33 \text{ kg} \cdot \text{cm}^2$$

Gear Box:

Mass of Pinion:

$$M_p = 1.13 \text{ kg}$$

Mass of Gear:

$$M_g = 6.4 \, \text{kg}$$

Diameter of Pinion:

$$D_p = 30 \, \text{mm}$$

Diameter of Gear:

$$D_g = 70 \, \text{mm}$$

G.2.3 Calculations

Load Inertia of Drum:

$$J_D = \frac{1}{8} \cdot M_d \cdot D_d{}^2 = 0.002 \, \text{kg} \cdot \text{m}^2$$

Inertia of Gearbox:

$$J_G = \frac{1}{8} \cdot M_p \cdot D_p{}^2 + \frac{1}{8} \cdot M_g \cdot \frac{D_g{}^2}{GR^2} = \left(1.369 \cdot 10^{-4}\right) \, \text{kg} \cdot \text{m}^2$$

Total Load of Inertia:

$$J_L = \frac{J_D}{GR^2} + J_G = \left(1.426 \cdot 10^{-4}\right) \, \text{kg} \cdot \text{m}^2$$

Inertia Ratio:

$$IR = \frac{J_L}{J_M} = 4.32$$

G.3 Inertia Ratio Calculation for Swing System

G.3.1 Assumptions

The swing system is simplified into the 1 gear set model as shown in Figure G.2. The upper body can simplified into three main components: crowd system, hoist system and top plate. For the simplicity, those components are treated as solid cylinder which is shown in Figure G.3.
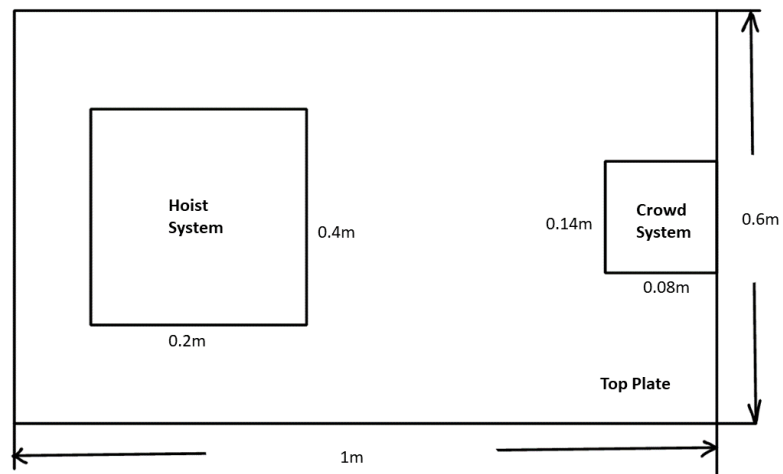
(a)
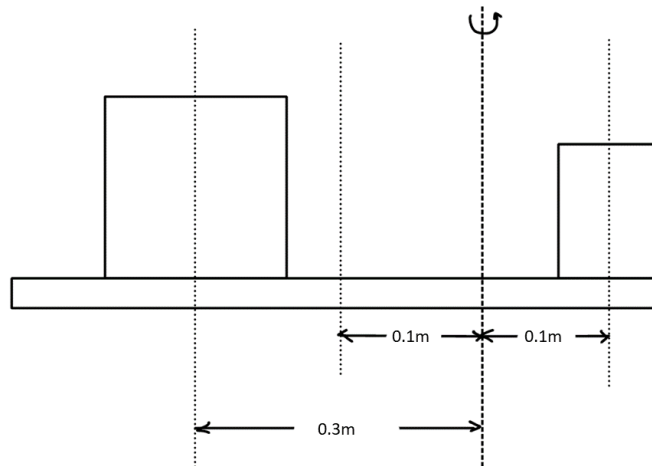
(b)

Figure G.3: Dimensions for Main Components for Inertia of the Swing System

G.3.2 Knowns

Crowd System

Crowd System Mass:

$$m_c = 22 \, \text{kg}$$

Crowd System Dimension:

$$A_c = 0.08 \, \text{m}, \qquad B_c = 0.14 \, \text{m}$$

Distance Between the Crowd System to the Rotational Axis:

$$d_c = 0.1 \text{ m}$$

Hoist System

Hoist System Mass:

$$m_h = 28 \text{ kg}$$

Hoist System Dimension:

$$A_h = 0.2 \text{ m}, \qquad B_h = 0.4 \text{ m}$$

Distance Between the Hoist System to the Rotational Axis:

$$d_h = 0.3 \text{ m}$$

Top Plate

Top Plate Mass:

$$m_p = 45 \text{ kg}$$

Top Plate Dimension:

$$A_p = 1 \text{ m}, \qquad B_p = 0.6 \text{ m}$$

Distance Between the Top Plate to the Rotational Axis:

$$d_p = 0.1 \text{ m}$$

Gear Box

Mass of Pinion:

$$m_{g1} = 0.1 \text{ kg}$$

Mass of Gear:

$$m_{g2} = 1.5 \text{ kg}$$

Diameter of Pinion:

$$D_{g1} = 15 \text{ mm}$$

Diameter of Gear:

$$D_{g2} = 90 \text{ mm}$$

Gear Ratio:

$$GR = 80$$

Inertia of Motor:

$$J_M = 0.33 \ \text{kg} \cdot \text{cm}^2$$

G.3.3   Calculations

Inertia of External Load from the Hoist System:

$$J_h = \frac{1}{12} \cdot m_h \cdot \left(A_h{}^2 + B_h{}^2\right) + m_h \cdot d_h{}^2 = 2.987 \ \text{kg} \cdot \text{m}^2$$

Inertia of External Load from the Crowd System:

$$J_c = \frac{1}{12} \cdot m_c \cdot \left(A_c{}^2 + B_c{}^2\right) + m_c \cdot d_c{}^2 = 0.268 \ \text{kg} \cdot \text{m}^2$$

Inertia of External Load from the Top Plate:

$$J_p = \frac{1}{12} \cdot m_p \cdot \left(A_p{}^2 + B_p{}^2\right) + m_p \cdot d_p{}^2 = 5.55 \ \text{kg} \cdot \text{m}^2$$

Total Inertia of External Load:

$$J_E = J_h + J_c + J_p = 8.804 \ \text{kg} \cdot \text{m}^2$$

Inertia of Gear Box:

$$J_G = \frac{1}{8} \cdot m_{g1} \cdot D_{g1}{}^2 + \frac{1}{8} \cdot m_{g2} \cdot \frac{D_{g2}{}^2}{GR^2} = \left(3.05 \cdot 10^{-6}\right) \ \text{kg} \cdot \text{m}^2$$

Inertia of Load:

$$J_L = \frac{J_E}{GR^2} + J_G = 0.001 \ \text{kg} \cdot \text{m}^2$$

Inertia Ratio:

$$IR = \frac{J_L}{J_M} = 41.78$$

Appendix H: Frequency of Interest in Hoist System

In order to select a proper accelerometer, frequencies of components in the system play an important role. Failure modes have been discussed in Chapter 5.2.1 and 5.2.2 and decided to be seeded in the hoist system. The frequencies of components in the hoist system mainly focus on the gearbox and bearing which are shown in Figure H.1 and H.2.
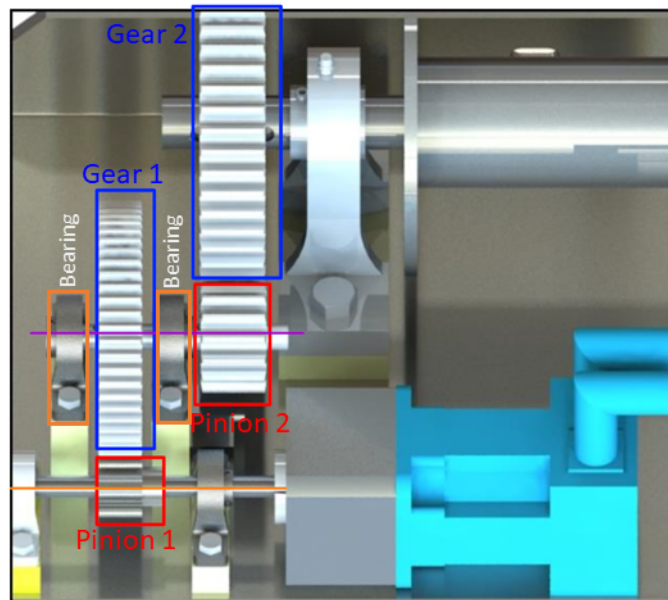
Figure H.1: Gear Train in the Hoist System

H.1   Knowns

Pinion 1 and Gear 1:
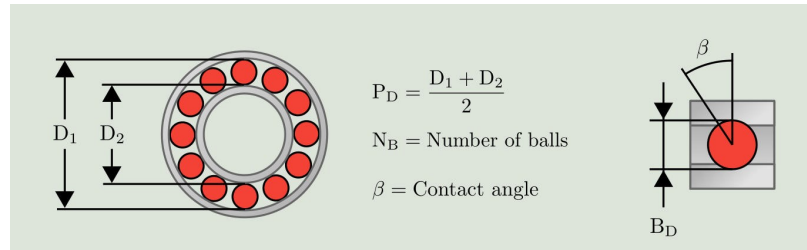
Figure H.2: Nomenclature for Bearing[107]

Number of Tooth for Pinion 1:

$$N_{p1} = 12$$

Number of Tooth for Gear 1:

$$N_{g1} = 60$$

Pinion 1 Shaft Frequency:

$$f_{p1} = 7.75 \text{ Hz}$$

Pinion 2 and Gear 2:

Number of Tooth for Pinion 2:

$$N_{p2} = 15$$

Number of Tooth for Gear 2:

$$N_{g2} = 60$$

Bearing:

Outer Diameter:

$$D_1 = 25.26 \text{ mm}$$

Inner Diameter:

$$D_2 = 20.5 \text{ mm}$$

Ball Diameter:

$$B_D = 4.76 \text{ mm}$$

Number of Balls:

$$N_B = 8$$

Contact Angle:

$$\beta = 0$$

H.2 Calculations

Pinion 1 and Gear 1:

Gear 1 Shaft Frequency:

$$f_{g1} = f_{p1} \cdot \frac{N_{p1}}{N_{g1}} = 1.55 \text{ Hz}$$

Gear Mesh Frequency:

$$f_{mesh1} = f_{p1} \cdot N_{p1} = 93 \text{ Hz}$$

Pinion 2 and Gear 2:

Pinion 2 Shaft Frequency:

$$f_{p2} = f_{g1} = 1.55 \text{ Hz}$$

Gear 2 Shaft Frequency:

$$f_{g2} = f_{p2} \cdot \frac{N_{p2}}{N_{g2}} = 0.388 \text{ Hz}$$

Gear Mesh Frequency:

$$f_{mesh2} = f_{p2} \cdot N_{p2} = 23.25 \text{ Hz}$$

Bearing:

Pitch Diameter:
$$P_D = \frac{D_1 + D_2}{2} = 0.023 \text{ m}$$

Ball Pass Frequency Outer:
$$\text{BPFO} = f_{p2} \cdot \frac{N_B}{2} \cdot \left(1 - \frac{B_D}{P_D} \cdot \cos(\beta)\right) = 4.91 \text{ Hz}$$

Ball Pass Frequency Inner:
$$\text{BPFI} = f_{p2} \cdot \frac{N_B}{2} \cdot \left(1 + \frac{B_D}{P_D} \cdot \cos(\beta)\right) = 7.49 \text{ Hz}$$

Ball Spin Frequency:
$$\text{BSF} = f_{p2} \cdot \frac{P_D}{B_D} \cdot \left(1 - \left(\frac{B_D}{P_D} \cdot \cos(\beta)\right)^2\right) = 7.128 \text{ Hz}$$

Fundamental Train Frequency:
$$\text{FTF} = f_{p2} \cdot \frac{1}{2} \cdot \left(1 - \frac{B_D}{P_D} \cdot \cos(\beta)\right) = 0.614 \text{ Hz}$$

Appendix I: Data Acquisition System Validation

The PC-based DAQ system consists of transducers and sensors, signal conditioning, DAQ hardware and a computer. The DAQ system is specifically designed for the fault detection experiment using vibration sensors. The specifications and features of each element in the DAQ system are mentioned in section 5.1. Before collecting any vibration data, the DAQ system is required to validate the setting of each element. Accordingly, the data and conclusion would be more convincing.

In order to validate the designed DAQ system, a waveform generator was used instead of the accelerometer since it can send out a sine wave signal with known features (frequency and amplitude). If Matlab can give a sine wave matching the one from the waveform generator then the DAQ system's settings are ready for the later experiment. Figure I.1 illustrates the rationale of the validation of the DAQ system.
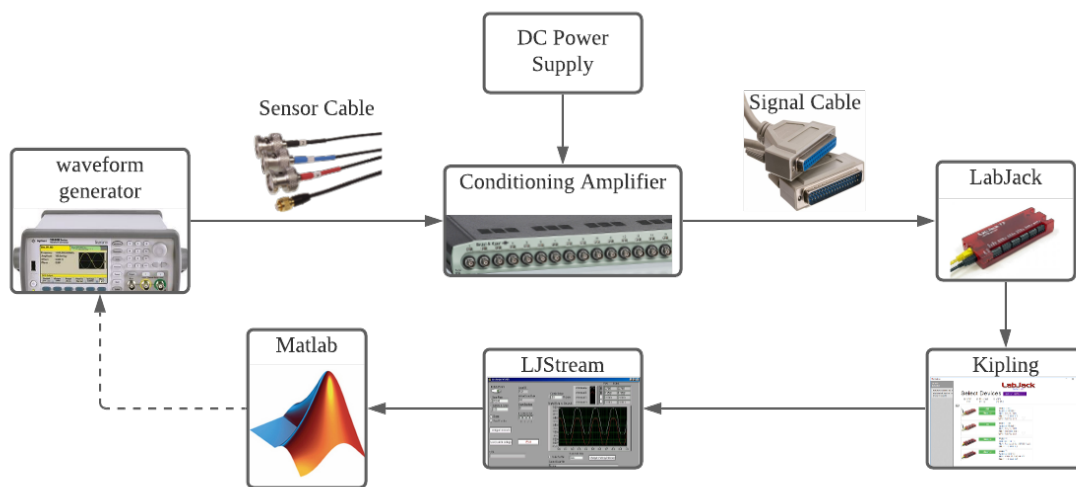
Figure I.1: The Rationale of the Validation of DAQ system

There are two sine waves generated by the waveform generator for the validation of the DAQ system. The sine what characteristics are summarized in Table I.1. The time series and frequency response for each sine wave is shown in Figures I.2 and I.3. It is clear from the time series that the waves generated are sine waves; in addition, from its frequency response, the important features such as amplitude and frequency are extracted accurately. Hence, the information from Matlab matches the waves created from the generator. As a result, the designed DAQ system is validated.

Table I.1: Important Features of Sine Waves

Sine Wave	Frequency (Hz)	Amplitude (V)	Sampling Rate (Hz)
I	25	8	125
II	4	6	50

(a)   (b)
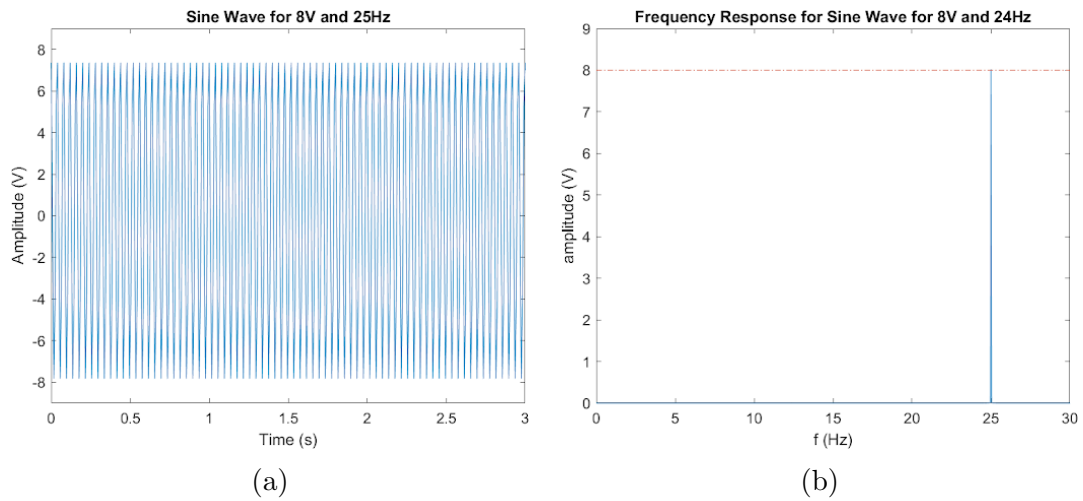
Figure I.2: 8V and 25Hz Sine Wave Sampled at 125Hz

(a)   (b)
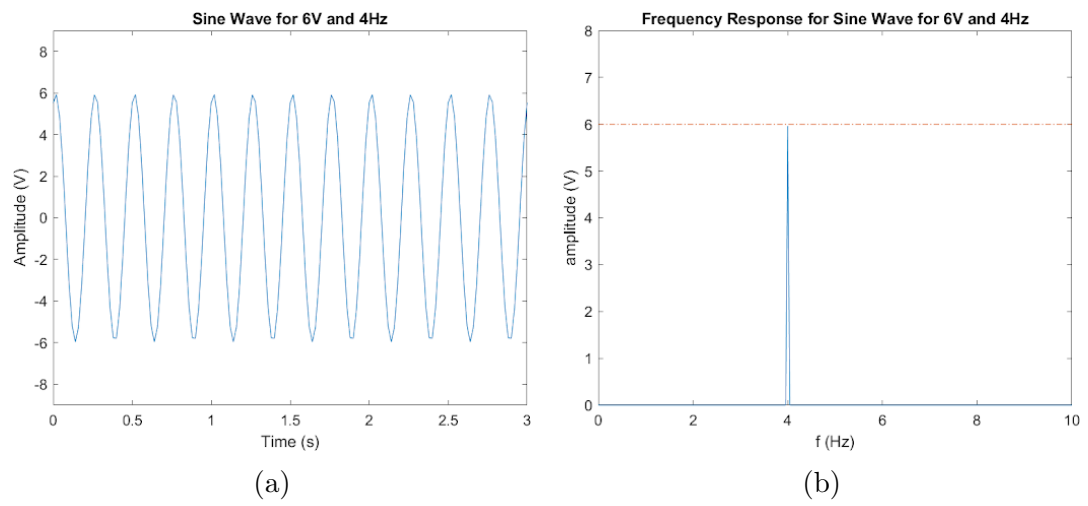
Figure I.3: 6V and 4Hz Sine Wave Sampled at 50Hz

Appendix J: Inapplicability of Fast Fourier Transform

Fast Fourier Transform (FFT) is an efficient algorithm for computing the Discrete Fourier Transform (DFT) and its inverse for stationary or nearly stationary systems. However, for the current project, the shovel model is in operation mode and movement is fast enough that it cannot be treated as stationary. An example of the FFT result for 6.7-6.7 Nm on the y-axis is shown in Figure J.1. From the FFT example, it can be seen that the signal is contaminated by noise and the expected frequencies are not clear. Therefore, FFT is not an effective method to detect the presence of a fault in our application.
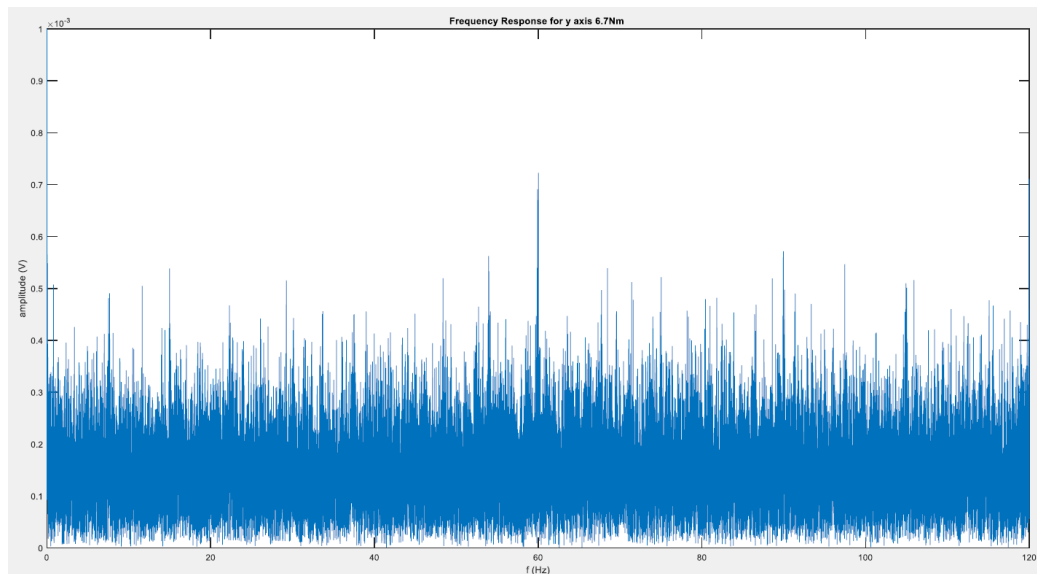
Plate J.1: Example of FFT of 6.7-6.7 Nm on the y-axis

Appendix K: Short Time Fourier Transform Results

The short-time Fourier transform (STFT) analyzes how the frequency content of nonstationary signal changes over time. It has been performed for the fault of bolt looseness and shaft wear in Matlab by using the "stft" function. The STFT results for the y-axis have been presented for both failure modes. In this Appendix, the STFT results on the x and z axes will be illustrated.

K.1   STFT Results for Bolt Looseness
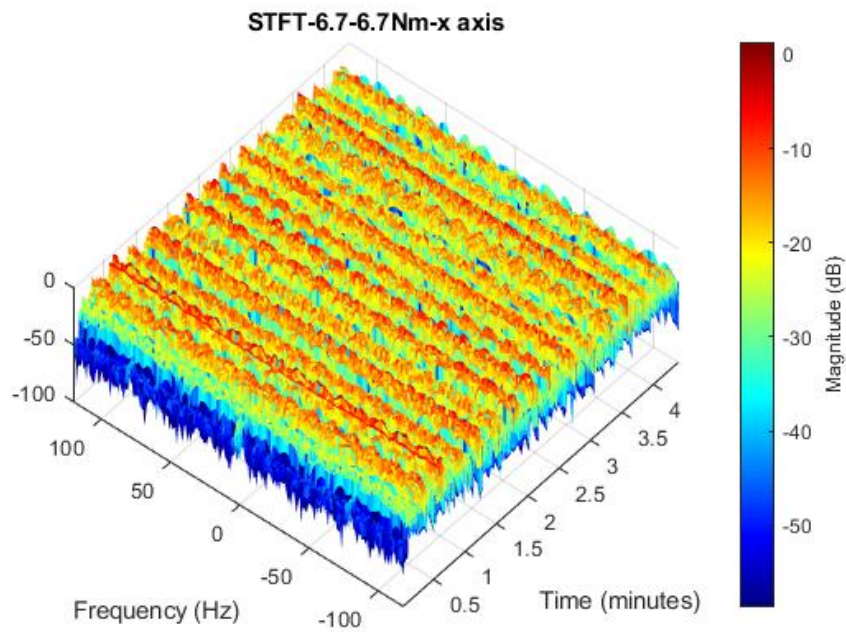
(a)

Figure K.1: Short-Time Fourier Transform of Bolt Looseness on the x-axis
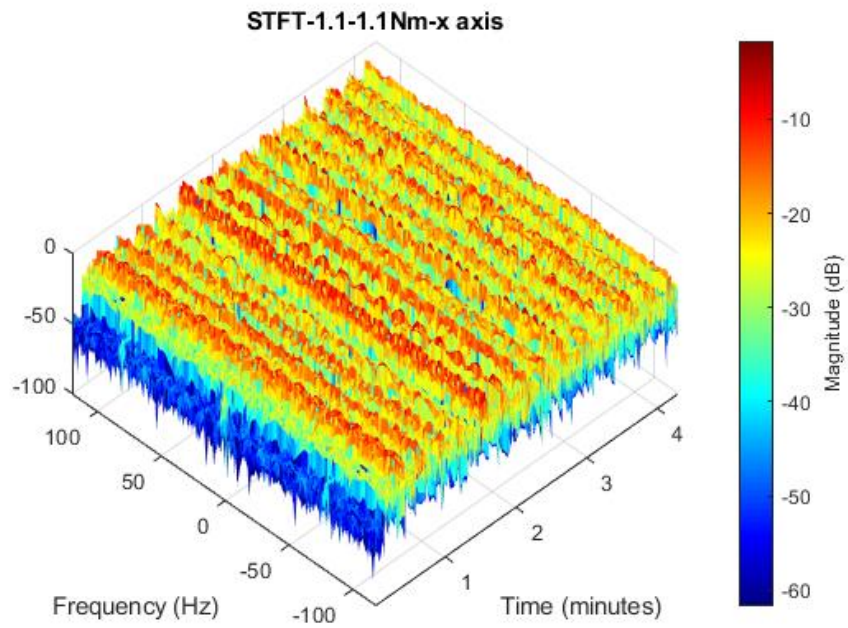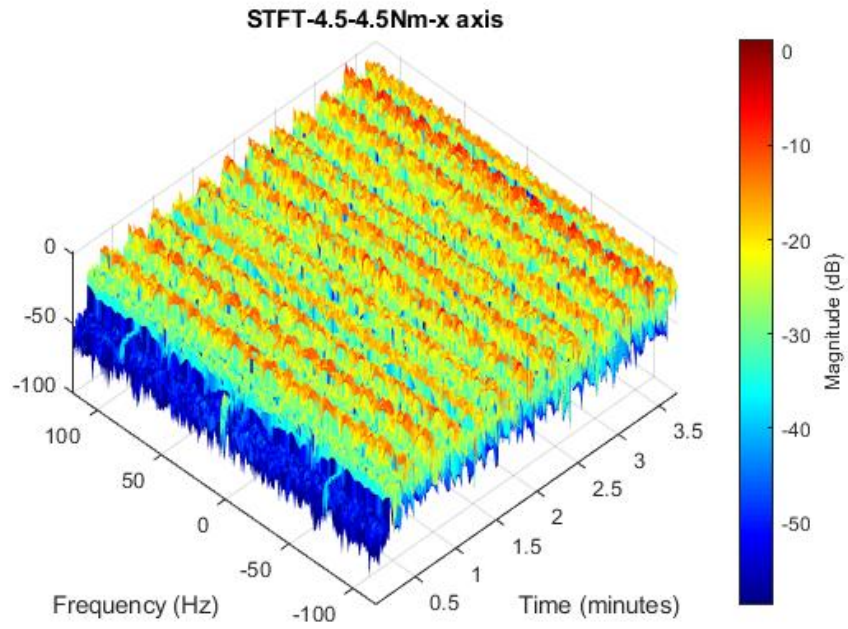
STFT-4.5-4.5Nm-x axis

(b)

STFT-1.1-1.1Nm-x axis

(c)

Figure K.1: Short-Time Fourier Transform of Bolt Looseness on the x-axis (cont.)

STFT-6.7-0Nm-x axis

(d)

STFT-1.1-0Nm-x axis

(e)

Figure K.1: Short-Time Fourier Transform of Bolt Looseness on the x-axis (cont.)

STFT-6.7-6.7Nm-z axis

(a)

Figure K.2: Short-Time Fourier Transform of Bolt Looseness on the z-axis

153

(b)

(c)

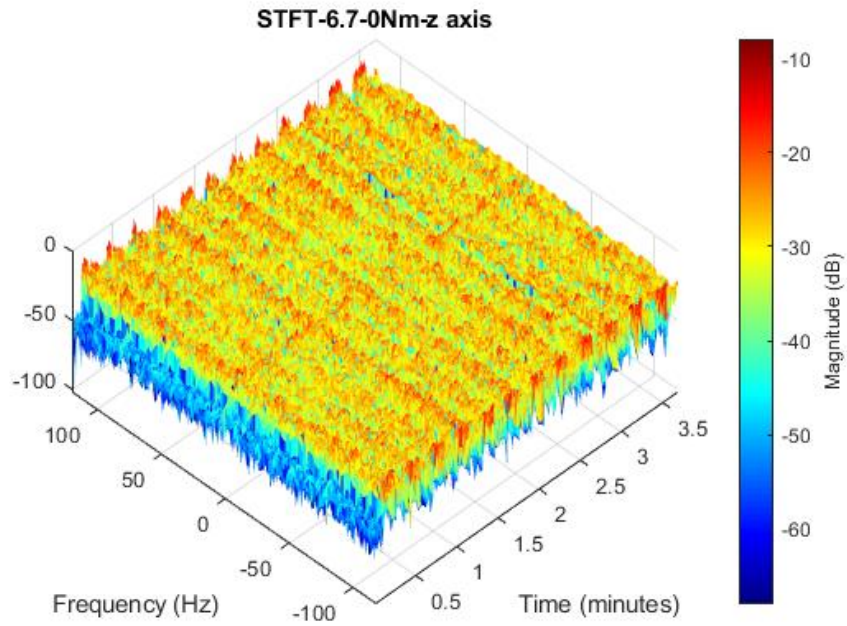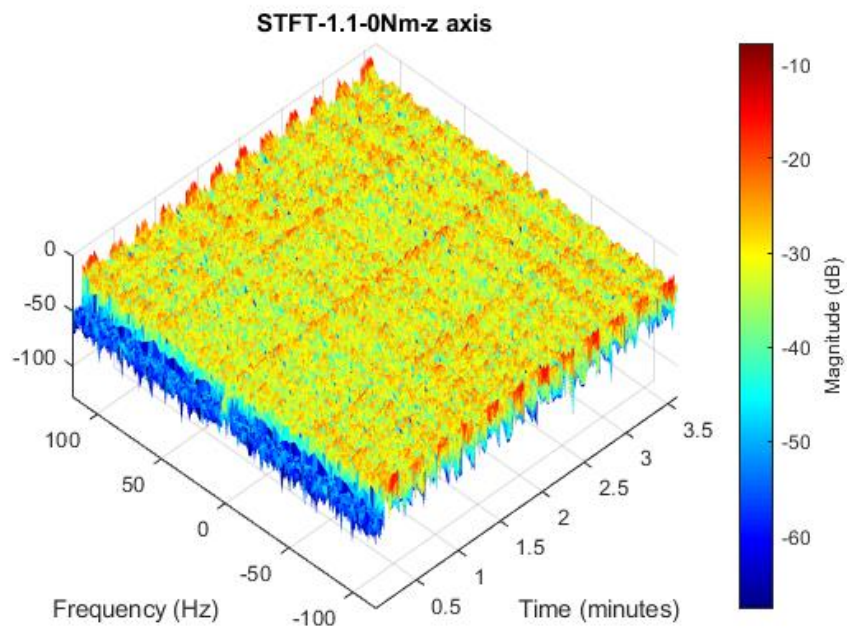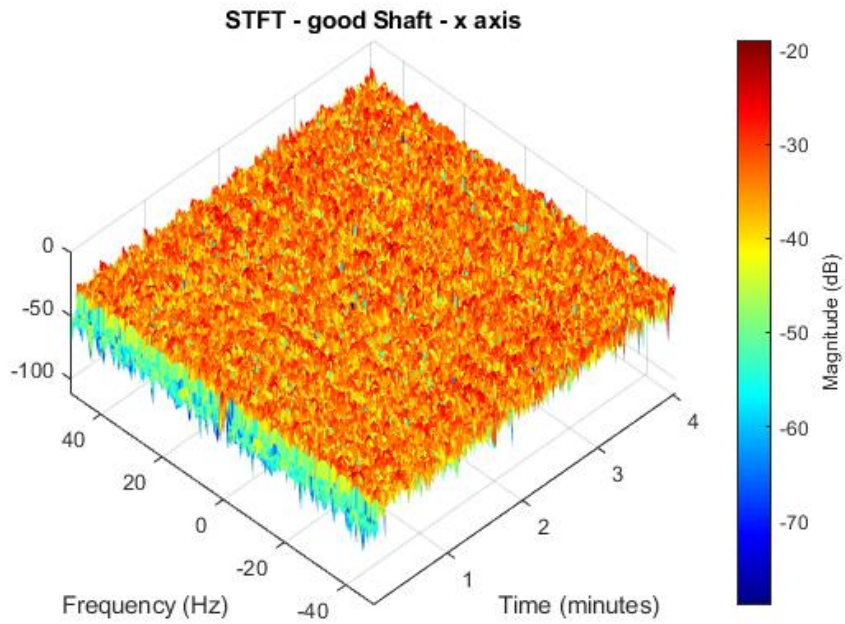Figure K.2: Short-Time Fourier Transform of Bolt Looseness on the z-axis (cont.)

STFT-6.7-0Nm-z axis

(d)

STFT-1.1-0Nm-z axis
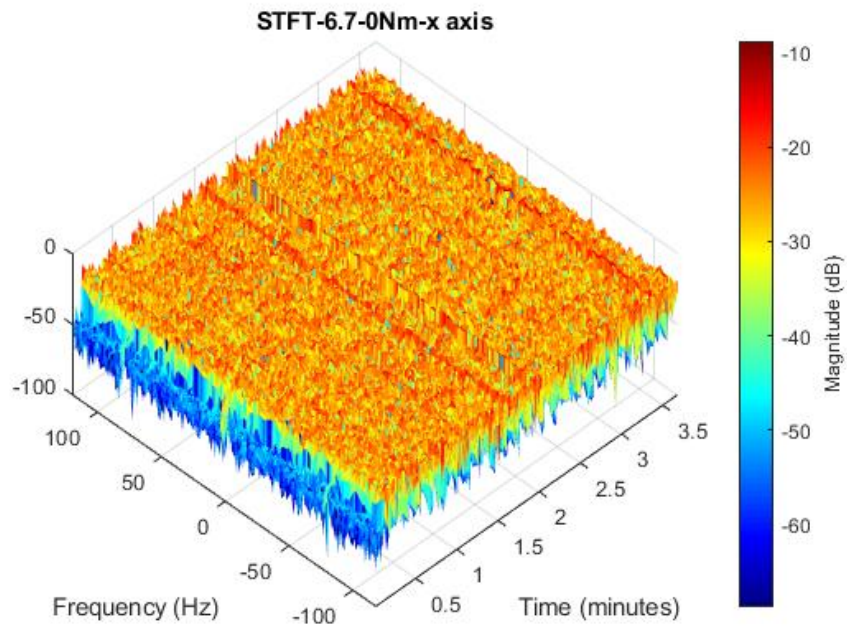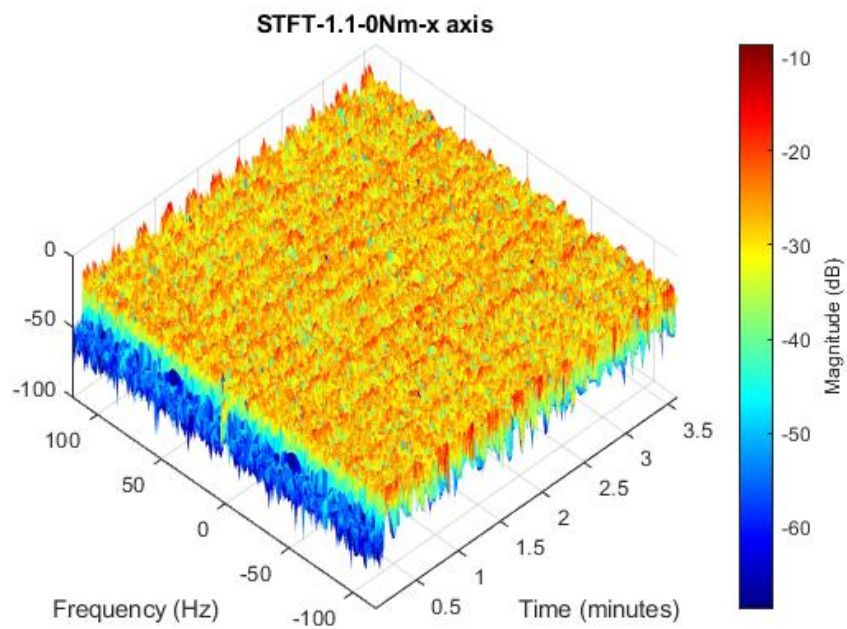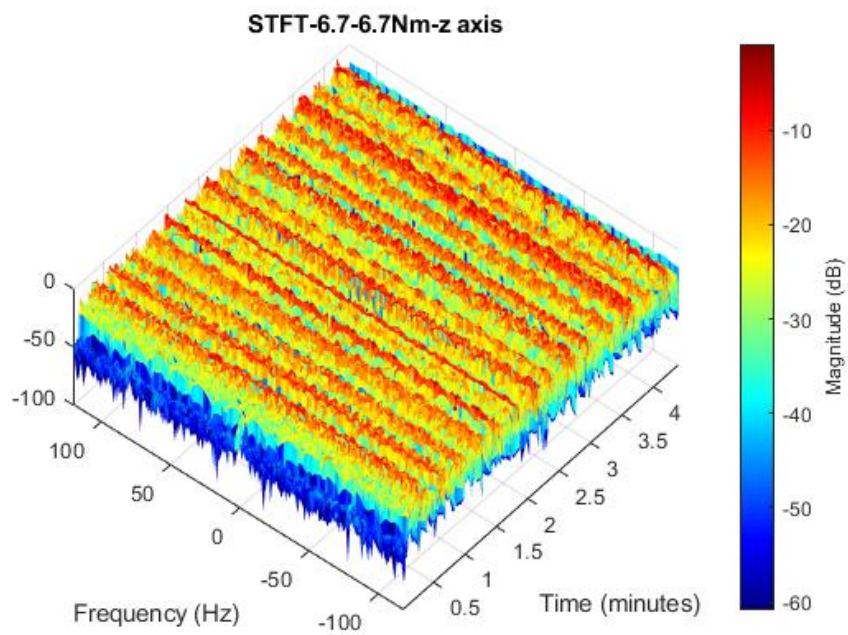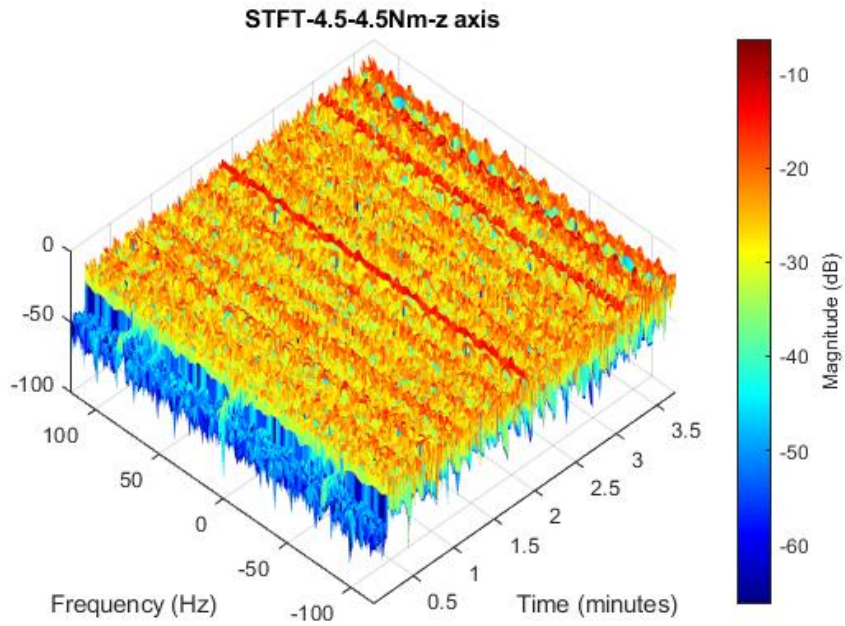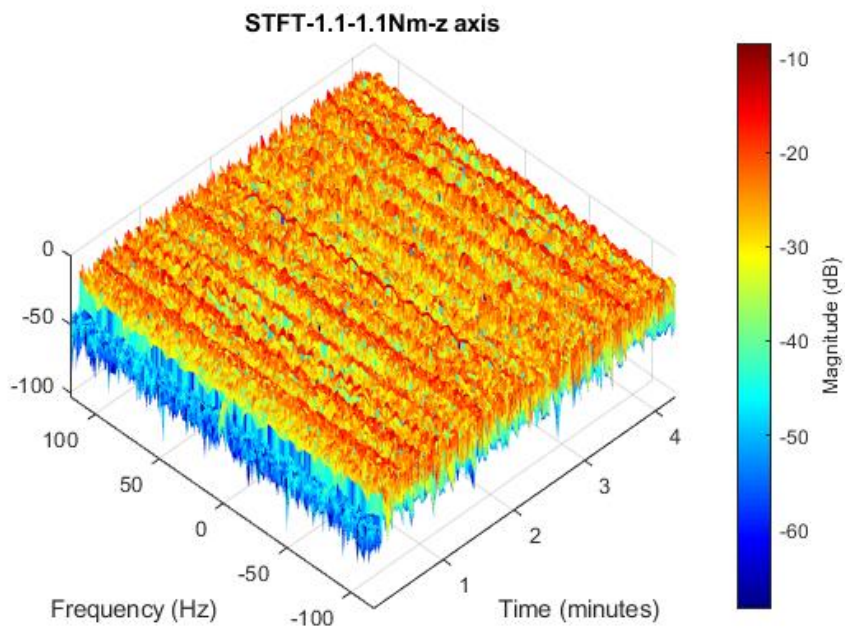
(e)

Figure K.2: Short-Time Fourier Transform of Bolt Looseness on the z-axis (cont.)

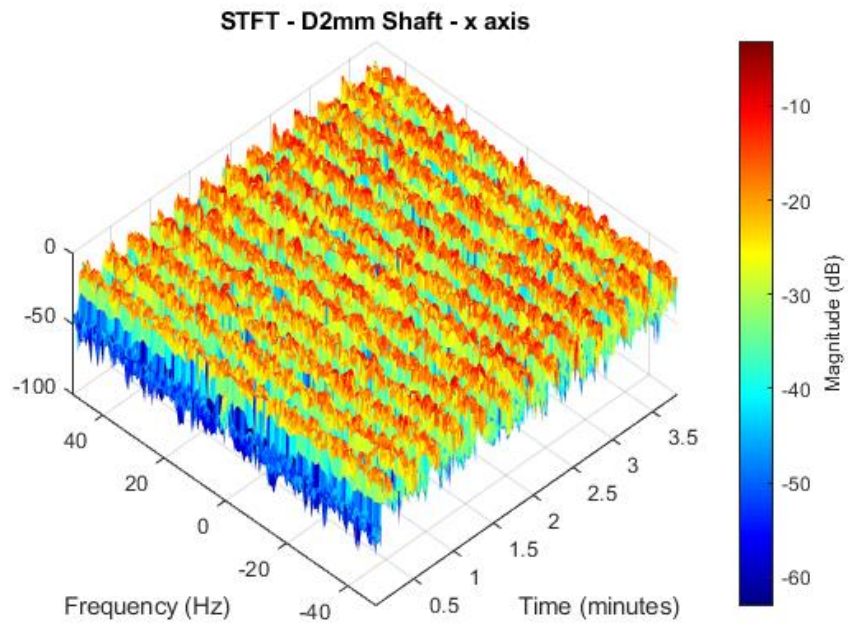## K.2   STFT Results for Shaft Wear

(a)
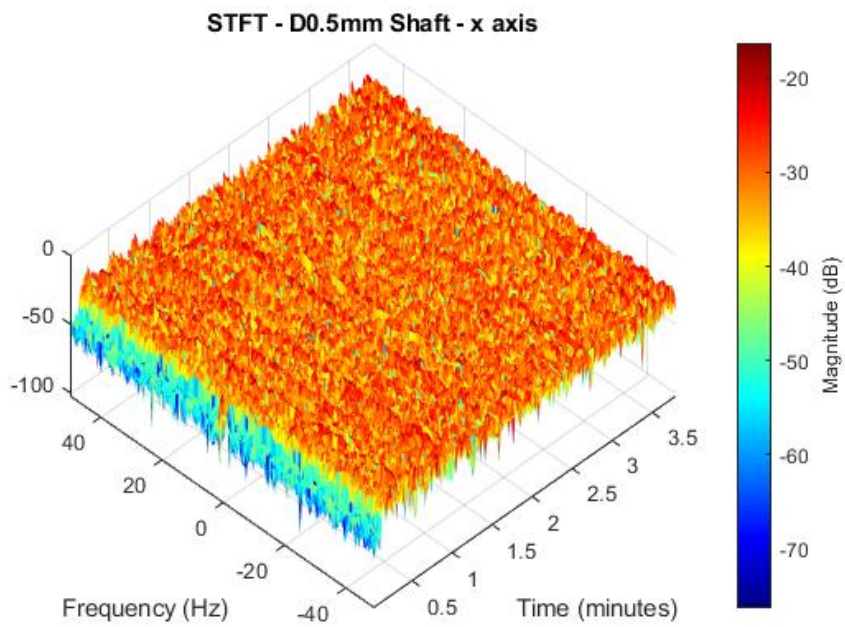
(b)

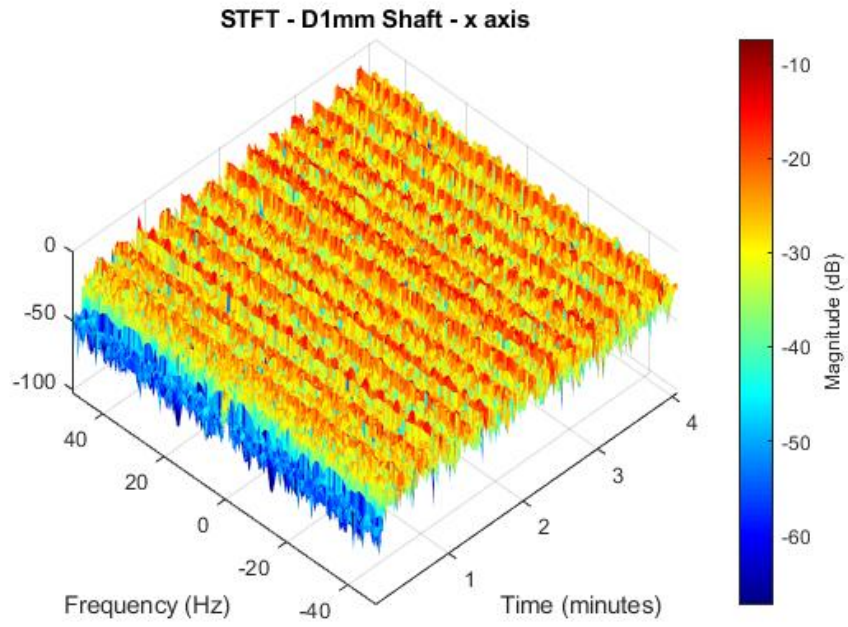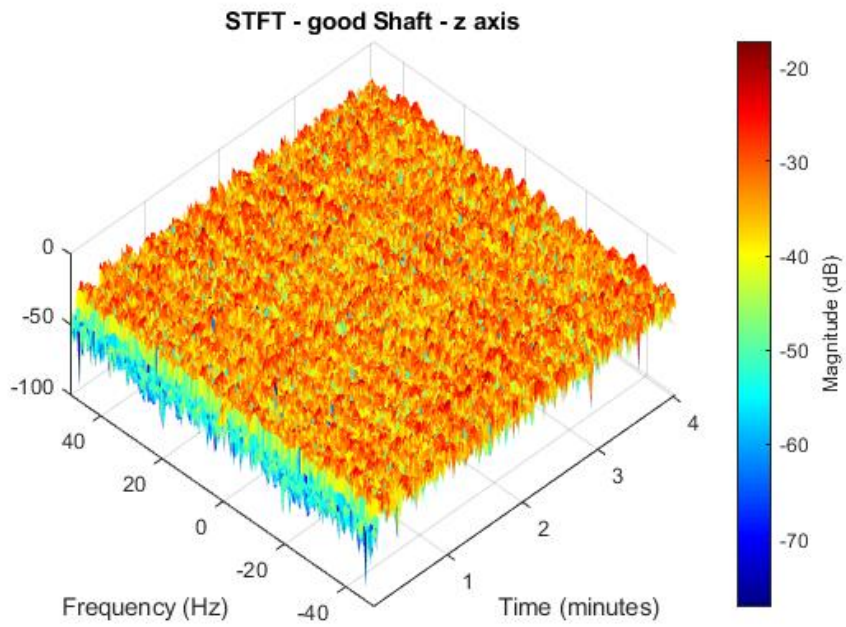Figure K.3: Short-Time Fourier Transform of Shaft Wear on the x-axis
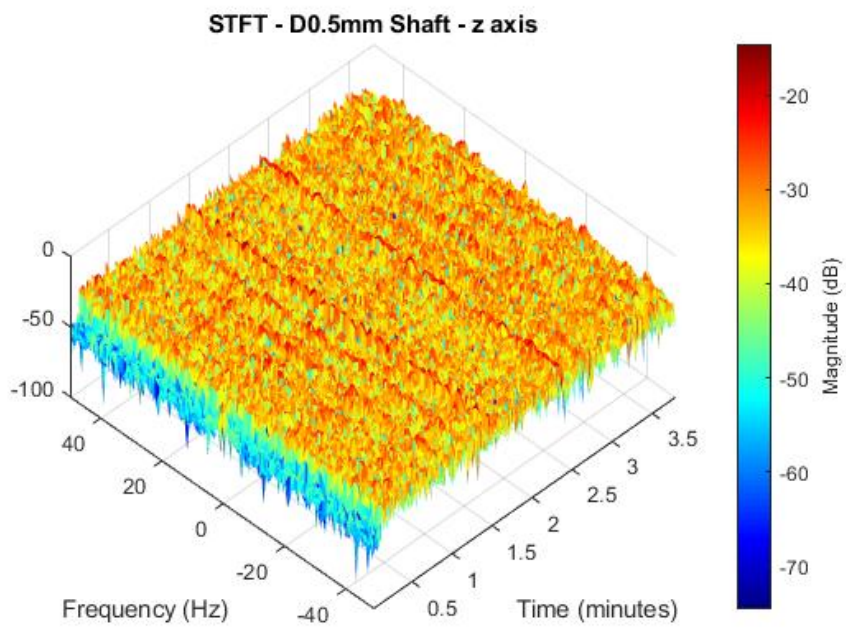
(c)

(d)

Figure K.3: Short-Time Fourier Transform of Shaft Wear on the x-axis (cont.)
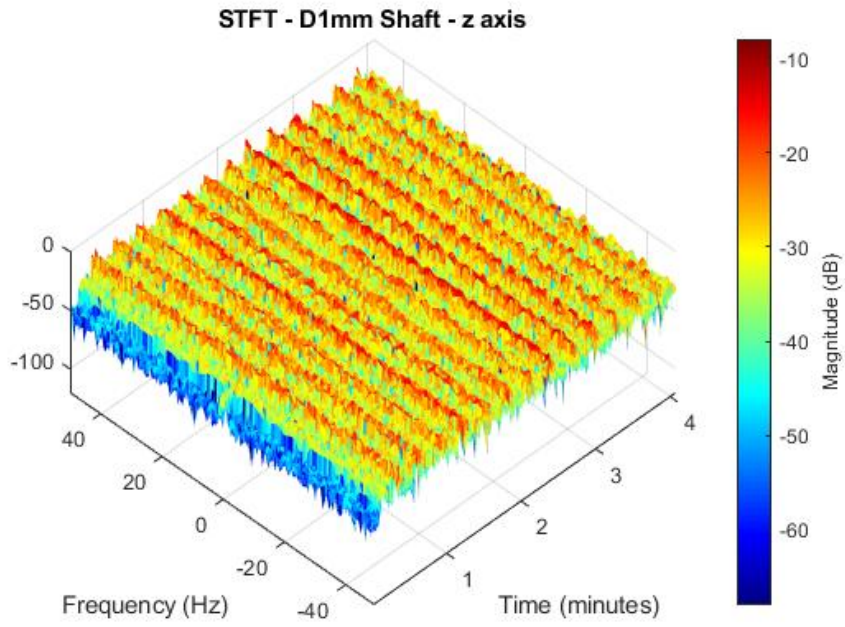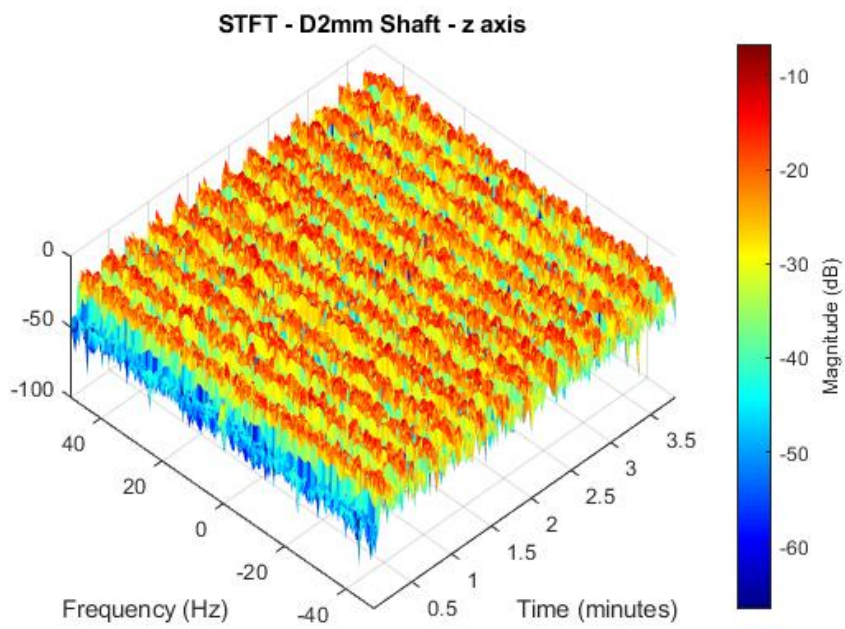
157

(a)

(b)

Figure K.4: Short-Time Fourier Transform of Shaft Wear on the z-axis

(c)

(d)

Figure K.4: Short-Time Fourier Transform of Shaft Wear on the z-axis (cont.)

159

Appendix L: Model Design Experience

Modelling should not just be simulated in the designing software such as Solidworks or Matlab. For the full understanding of the working mechanism of the phenomenon, it is important to bring the model to life. A physical model can be used to conduct experiments such as dynamics and kinematics validation and fault diagnosis. The process from the design to manufacturing and to construction, however, is not a straight path involving various extra considerations. Those extra thoughts summarized below are not standards but come from the personal journey of the design of a scale cable shovel model. The considerations and personal design experiences can be applied to numerous experiments involving design and manufacturing. The reminders and experience obtained from this experiment are categorized by three stages of the project: design of a model, material ordering and designed parts machines and solid model assembly.

L.1 Stage 1: Design of a Model

L.1.1 Design Concepts

The concepts should be created as what the needs requests. With the same functionality, the part can be designed in different ways in various materials. Sometimes, due to the limitations of the manufacturing methods and material properties designs have to compromise. First of all, a large and complicated part should be avoided in the design and can always break into small and easy-to-make pieces. The iterative designing cycle with the results captured has inherent limitations; design can be produced that cannot be manufactured[108]. Therefore, the fabrication method and limitation factor ought be considered in the design process.

Secondly, the assembly process should also be pondered in advance. As mentioned before, simple and small pieces can be assembled to a desired functional part; there are several ways to combine these pieces together including common fasteners, welding, zip tie and so on. Compared to welding, the use of fasteners is recommended since it is more economical, easy to maintain and has good disassembly performance. Overall, a well-designed model requires the expected functionality, easy-to-create buildability and good assemble and disassemble performance.

L.1.2 Choice of Units

It is essential to use reasonable units in the design and engineering drawings. Metric unit is very common in Canadian educational institutions and manufacturing. On the other hand, the imperial unit should not be neglected. Most of the time, when manufacturing in Canada, materials are bought from the US where is applying the imperial unit in its products. Therefore, it would be convenient to use the imperial unit in some dimensions. Take sheet metal for example, the imperial measurement is commonly used in the thickness scale. The desired length can always be tailored afterwards no matter in the imperial and metric units. The thickness, however, is hard or even impossible to make a change. The model is invented due to designers' expectations but also ought to be designed according to the material in the market. Common material manufacturers and dealers such as McMaster Carr are located in America. Hence, the dual dimension (dimensions by using the combination of imperial and metric units) is highly recommended in the model design and engineering drawings. The use of the dual dimension technique can help the creator to choose the suitable material and assist machine shop technicians to fabricate the proper parts as the engineer requires.

L.1.3 Downloaded Components Insertion

When designing a complex machinery with multi components, it is not necessary to create all the components in the model. Some can be easily downloaded from the manufacturer and dealer website, e.g., McMaster Carr and Misumi. Those companies provide a 3D model of the component and the engineer can insert them directly into the design.

Besides, commonly-used 3D modelling software such as SolidWorks offers toolbox libraries so that the designers can drag the needed parts including gears, fasteners, bearings, keys, etc directly into the 3D model. In addition, those parts from the toolbox can also be easily customized according to the designers' needs. As mentioned earlier, all the designs ought to be created based on the existing material and components in the market. The toolbox parts customization function is not meant to be abused: it can only be used when the desired components exist in the market and the dealer or manufacturer may not provide the 3D model. In a word, the parts usage and creation are summarized in the flowchart L.1.
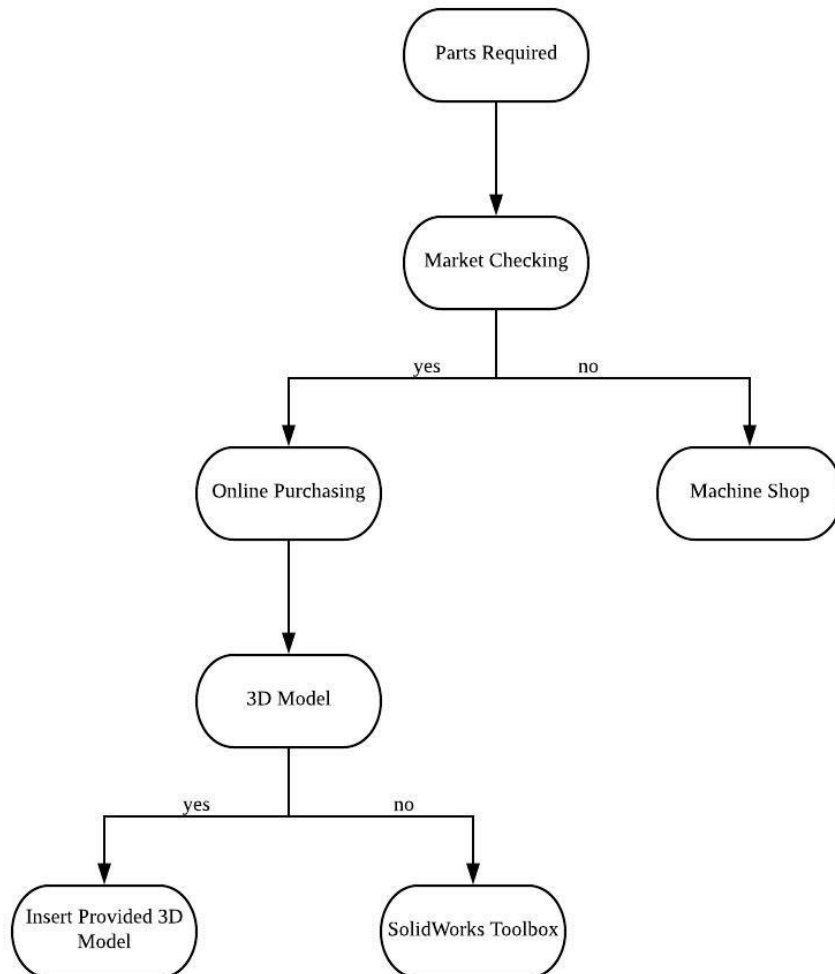

Figure L.1: Parts Usage or Creation Flowchart

L.2 Stage 2: Parts Ordering and Designed Parts Machining

The parts in the design either be purchased from online or machined in the machine shop. During the design, it would be best if the parts could be bought from online as more as possible since it is relatively economical and time-efficient compared to the machine shop. However, there are always some complicated and difficult-to-buy parts requiring manufacturing in the machine shop. However, is there an order about the material ordering and complex parts machining: should make online order first and then have parts machined or the opposite or those can be done at the same time?

Well, always talk to the machine shop technician first before ordering the parts. As a junior engineer, with a lack of experience in designing and manufacturing, the technician will provide constructive advice on the design. Some machined parts may need to be modified due to the material and fabrication constraints. As a result, the parts required to be purchased online may be altered. Sometimes, the technician needs the purchased parts in advance as a reference such as tolerance and width to create the machined parts. In a word, always ask the technician for advice first and order the parts as he requires.

L.3 Solid Model Assembly

The last step of creating a solid model is to assemble the parts. This process is the most labour intensive, physically demanding and dangerous but there is no doubt that it is the most enjoyable process when compared to the previous two. The reminders from common sense and personal experience are summarized below:

- *Safety and Potential Risks*: The first and always the most important step of solid model assembly is to keep a safe environment in the lab. Before assembling models, have a list of the tools which are needed to be used and identify the potential risks;

- *Assembly Plan:* from bottom to top and from subsystems to the whole model;

- *Never Fasten a Bolt too Tight:* understand each part's material limit and do

not get too close to the limit and never go over it;

- *Think and Ask Before Action:* there are always problems coming along. Google the problems or ask professionals before using a hammer;

- *Organize and Clean Working Area:* After finishing the assembly, remember to put it back in place. This can ease one's mind when the tool is wanted next time and also a good way when sharing with others in the lab.